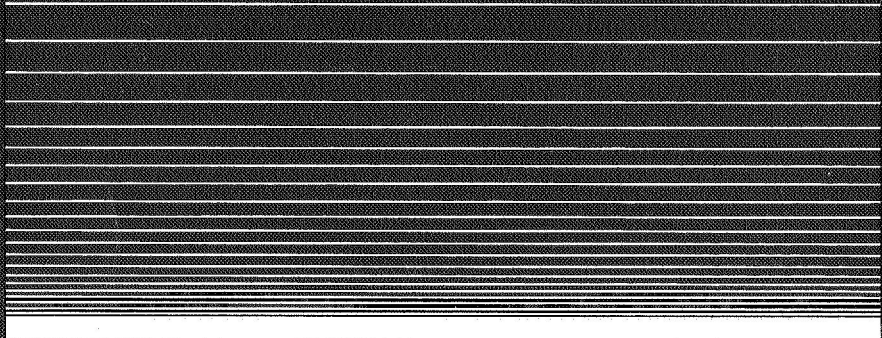


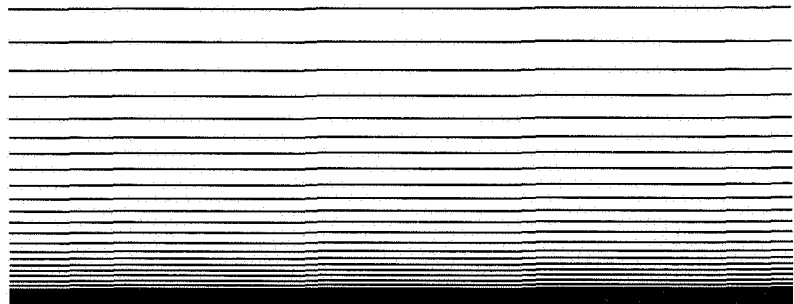
MOUNT ST. HELENS ERUPTIONS OF 1980



Atmospheric Effects and Potential Climatic Impact

National Aeronautics and Space Administration

MOUNT ST. HELENS ERUPTIONS OF 1980



Atmospheric Effects and Potential Climatic Impact

Report of Workshop on
MOUNT ST. HELENS ERUPTION: ITS ATMOSPHERIC EFFECTS
AND POTENTIAL CLIMATIC IMPACT
Washington, DC
20-21 November 1980

Sponsored by
NASA-Office of Space and Terrestrial Applications
Washington, DC 20546

Organized by
Institute for Atmospheric Optics and Remote Sensing (IAFORS)
P.O. Box P, Hampton, Virginia 23666, under NASA Contract
NAS1-16454

NASA SP-458

MOUNT ST. HELENS ERUPTIONS OF 1980

Atmospheric Effects and Potential Climatic Impact

A Workshop Report

Edited by

Reginald E. Newell

Massachusetts Institute of Technology
Cambridge, Massachusetts

Adarsh Deepak

Institute for Atmospheric Optics and Remote Sensing
Hampton, Virginia



Scientific and Technical Information Branch 1982
National Aeronautics and Space Administration
Washington, DC

Library of Congress Cataloging in Publication Data:

Workshop on Mount St. Helens Eruption: Its
Atmospheric Effects and Potential Climatic Impact
(1980 : Washington, D.C.)
Mount St. Helens eruptions of 1980.

(NASA SP ; 458)

“Report of Workshop on Mount St. Helens
Eruption: Its Atmospheric Effects and Potential
Climatic Impact, Washington, DC, 20-21 November
1980”; p.

Includes bibliographies and index.

1. Saint Helens, Mount (Wash.)—Region—Climate.
2. Saint Helens, Mount (Wash.)—Eruption, 1980. I.
Newell, Reginald E., 1931- . II. Deepak, Adarsh. III.
Title. IV. Series.

QC984.W2M68 1982 551.69797'84 82-8005

TABLE OF CONTENTS

	Page
<i>FOREWORD</i>	<i>vii</i>
<i>PREFACE</i>	<i>ix</i>
<i>WORKSHOP PARTICIPANTS</i>	<i>xi</i>
<i>COLOR ILLUSTRATIONS (C.1-C.4)</i>	<i>xv</i>
EXECUTIVE SUMMARY	<i>xxi</i>
1 VOLCANOLOGICAL DESCRIPTION OF THE 18 MAY 1980	
ERUPTION OF MOUNT ST. HELENS.....	1
1.1 Introduction	1
1.2 Activity of the Volcano.....	1
1.3 Solid Products of the 18 May Eruption.....	10
1.4 Volcanic Gases.....	21
1.5 A Comparison of the 18 May Mount St. Helens Eruption with Other Explosive Eruptions.....	27
1.6 Conclusions	32
1.7 References	33
2 TRANSPORT AND DISPERSION	37
2.1 Introduction	37
2.2 Observations and Results.....	37
2.3 Conclusions	45
2.4 Reference	46
3 CHEMICAL AND PHYSICAL MEASUREMENTS	
OF THE VOLCANIC CLOUD MADE <i>IN SITU</i>	47
3.1 Introduction	47
3.2 Purpose	47
3.3 Measurement Methods.....	48
3.4 Results	51
3.5 Discussions	55
3.6 Conclusions	58
3.7 Recommendations	59
3.8 References	60
4 REMOTE MEASUREMENTS OF MOUNT ST. HELENS	
EFFLUENT	63
4.1 Introduction	63
4.2 Measurement Methods and Results.....	63

4.3 Conclusions	82
4.4 Recommendations	83
4.5 References	85
5 CHEMISTRY OF MOUNT ST. HELENS EFFLUENT.....	89
5.1 Introduction	89
5.2 Early Composition and Development of the Eruption Clouds.....	89
5.3 Climate Effects by Conversion of Sulfur Gases to Particles.....	93
5.4 Effects Upon Stratospheric Ozone.....	95
5.5 Mount St. Helens Volcano and Acid Rain.....	95
5.6 Chemistry and Climate Effects.....	96
5.7 Overview of Chemically Generated Effects.....	97
5.8 Conclusions	99
5.9 Recommendations	99
5.10 References	100
6 INFLUENCE OF MOUNT ST. HELENS AND OTHER VOLCANOES ON CLIMATE AND WEATHER.....	103
6.1 Role of Volcanic Aerosols in Radiative Transfer and Energy Budget.....	103
6.2 Climatological Evidence from Past Volcanoes.....	104
6.3 Modeling Climatic Effects of Past Volcanoes.....	106
6.4 Relevance of Mount St. Helens to Interpretation of Volcanic Effects on Climate.....	107
6.5 Problems for Future Research.....	108
6.6 Conclusions	110
6.7 Recommendations	111
6.8 References	113
INDEX	115

FOREWORD

The study of atmospheric aerosols has emerged as an important topic of scientific research crucial to our understanding of the earth's radiation balance and climate. As part of NASA's role in the US National Climate Program, a "special study" was developed to exploit space technology in attempting to understand the basic physics and chemistry of aerosol particles, to monitor their global distributions, and to assess their role in heating and cooling the atmosphere.

Natural volcanic eruptions throughout history have long been thought to constitute the primary source of aerosols in the stratosphere. It was not until recently, however, that the instrumentation and observing platforms were available to go to the source of such volcanic emissions, measure their properties, and monitor their global spread. The May 1980 eruption of Mount St. Helens, while tragic with respect to its impact on human life and property, was, because of its location, an unprecedented scientific opportunity to provide new insight into the atmospheric effects and potential climatic impact of such phenomena. In the months that followed the eruption, NASA aircraft and research satellites acquired vast amounts of data. Together with the data collected by the other agencies, universities, and research institutions, these constitute a new body of knowledge which will aid in broad research by both atmospheric scientists and volcanologists.

The workshop reported in this document is an attempt to provide a definitive statement of what we believe that we have learned to date concerning the effects of Mount St. Helens on the atmosphere and climate.

Robert A. Schiffer
National Aeronautics and Space
Administration

PREFACE

This volume presents the technical results, including the recommendations, of the Workshop on Mount St. Helens: Its Atmospheric Effects and Potential Climatic Impact, held in Washington, DC, 20-21 November 1980. Thirty-eight invited scientists from universities, nonprofit institutions, research laboratories, and government agencies in the United States, England, and Italy participated in the workshop.

The 2-day workshop followed a 2-day symposium (18-19 November 1980) on the same topic at the same location. The purpose of the workshop was to bring together a small group of experts to assess and summarize the state of knowledge of the various atmospheric and climatic aspects of the 1980 eruptions of Mount St. Helens, and recommend research areas in which new or further efforts are needed. The purpose of the symposium was to present a tutorial program consisting of invited papers on different aspects of the eruption to all interested participants. Dr. Reginald E. Newell, Massachusetts Institute of Technology (MIT), was the workshop technical chairman; Dr. James P. Friend, Drexel University, was the symposium technical chairman; and Dr. Adarsh Deepak, Institute for Atmospheric Optics and Remote Sensing (IAFORS), was the symposium and workshop organizing chairman.

The workshop format consisted of organizing the participants into the following six working groups, which were chaired by the indicated scientists: Volcanological Description of the 18 May 1980 Eruption of Mount St. Helens (Dr. William I. Rose); Transport and Dispersion (Dr. Edwin F. Danielsen); Chemical and Physical Measurements of the Volcanic Cloud Made *In Situ* (Dr. Jarvis L. Moyers); Remote Sensing of Mount St. Helens Effluent (Dr. M. Patrick McCormick); Chemistry of the Mount St. Helens Effluent (Dr. James P. Friend); and Influence of Mount St. Helens and Other Volcanoes on Climate and Weather (Dr. James E. Hansen).

The participants were asked to address the following subjects in their specialty topics: summarize the measurements and techniques used in collecting the data; determine the missing gaps in data; assess models in the light of these data; and make recommendations for near-term and long-term research plans. The assessments and recommendations of each working group are summarized in a separate section of this workshop report. These working group reports were edited to present a cogent writeup of the workshop deliberations.

The workshop was sponsored by NASA Headquarters, Office of Space and Terrestrial Applications, on behalf of the US National Climate Program, and organized by IAFORS.

In order to ensure that the major disciplines involved were properly represented, a scientific program committee composed of the following scientists was set up: Drs. Adarsh Deepak, IFAORS; E. F. Nielsen, NASA-Ames Research Center; J. J. DeLisi, NOAA-Environmental Research Laboratory; J. P. Friend, Drexel U.; M. P. McCormick, NASA-Langley Research Center; R. E. Newell, MIT; J. B. Pollack, NASA-Ames Research Center; R. A. Schiffer, NASA Headquarters; W. A. Sprigg, National Climate Program Office; N. Sundararaman, FAA Headquarters; and W. E. Wilson, EPA-Environmental Sciences Research Laboratory.

The editors wish to acknowledge the enthusiastic support and cooperation of the working group chairmen, workshop participants, and workshop program committee members, for making this a successful and stimulating workshop. It is a pleasure to acknowledge the staff of IFAORS and Spectrum Press for organizing the workshop and preparing this manuscript for publication. Thanks are due the other members of the organizing committee, Drs. R. A. Schiffer, M. P. McCormick, and J. P. Friend, whose active assistance in the various aspects of the workshop assured its success.

It is, perhaps, the first time that atmospheric and potential climatic aspects of a volcanic eruption have been studied with such scientific thoroughness as are presented in this publication. It is hoped that this workshop report will serve as a reference volume for several years to come.

*Reginald E. Newell
Adarsh Deepak*

WORKSHOP PARTICIPANTS

WORKSHOP TECHNICAL CHAIRMAN:

Professor Reginald E. Newell, Massachusetts Institute of Technology, Department of Meteorology and Physical Oceanography, 54-1520, Cambridge, MA 02139

WORKING GROUP I: VOLCANOLOGICAL DESCRIPTION OF THE 18 MAY 1980 ERUPTION OF MOUNT ST. HELENS

Dr. William I. Rose, Department of Geology, Michigan Technological University, Houghton, MI 49931 (*Chairman*)

Mr. David M. Harris, US Geological Society, 959 National Center, Reston, VA 22092

Dr. Grant Heiken, Los Alamos National Laboratory, MS 575, P. O. Box 1663, Los Alamos, NM 87545

Dr. Andrei Sarna-Wojcicki, US Geological Survey, 345 Middlefield Road, Menlo Park, CA 94025

Dr. Stephen Self, Geology Department, Arizona State University, Tempe, AZ 85281

WORKING GROUP II: TRANSPORT AND DISPERSION

Dr. Edwin F. Daniels, NASA-Ames Research Center, MS 234-3, Moffett Field, CA 94035 (*Chairman*)

Dr. Marvin A. Geller, NASA-Goddard Space Flight Center, Code 964, Greenbelt, MD 20771

Dr. James D. Laver, National Weather Service, NMC, World Weather Building, Room 201, Washington, DC 20233

Dr. Kendall R. Peterson, Lawrence Livermore National Laboratory, Mail Code L-262, P. O. Box 808, Livermore, CA 94550

WORKING GROUP III: CHEMICAL AND PHYSICAL MEASUREMENTS OF THE VOLCANIC CLOUD MADE *IN SITU*

Dr. Jarvis L. Moyers, Chemistry Department, University of Arizona, Tucson, AZ 85721 (*Chairman*)

Dr. Robert J. Charlson, FC-05, University of Washington, Seattle, Washington 98195

Dr. Neil H. Farlow, NASA-Ames Research Center, Moffett Field, CA 94035

Dr. Edward C. Y. Inn, NASA-Ames Research Center, MS 245-5, Moffett Field, CA 94035

Dr. Robert Leifer, Environmental Measurements Laboratory, US Department of Energy, 376 Hudson Street, New York, NY 10014

Dr. James M. Rosen, Department of Physics and Astronomy, University of Wyoming, P. O. Box 3095, University Station, Laramie, WY 82071

WORKING GROUP IV: REMOTE SENSING OF MOUNT ST. HELENS EFFLUENT

Dr. M. P. McCormick, NASA-Langley Research Center, MS 234, Hampton, VA 23665 (*Chairman*)

Dr. John DeLuisi, NOAA-ERL-ARL-GMCC, 325 Broadway R329, Boulder, CO 80303

Dr. Geoffrey S. Kent, Institute for Atmospheric Optics and Remote Sensing, P. O. Box P, Hampton, VA 23666

Dr. G. M. Lerdal, NOAA/ERL, 325 Broadway, Boulder, CO 80303

Dr. David G. Murcray, Department of Physics and Astronomy, University Park, Denver, CO 80210

Dr. Larry L. Stowe, NOAA/NESS, 5200 Auth Road, World Weather Building, Washington, DC 20233

Dr. T. J. Swissler, Systems and Applied Sciences Corporation, 17 Research Drive, Hampton, VA 23666

WORKING GROUP V: CHEMISTRY OF THE MOUNT ST. HELENS EFFLUENT

Dr. James P. Friend, Department of Chemistry, Drexel University, Philadelphia, PA 19104 (*Chairman*)

Dr. Richard D. Cadle, 4415 Chippewa Drive, Boulder, CO 80303

Dr. Thomas E. Graedel, Bell Laboratories, Room 1D-349, Murray Hill, NJ 07974

Dr. Alan L. Lazarus, National Center for Atmospheric Research, P. O. Box 3000, Boulder, CO 80307

Dr. Richard P. Turco, R/D Associates, P. O. Box 9695, Marina del Rey, CA 90291

WORKING GROUP VI: INFLUENCE OF MOUNT ST. HELENS AND OTHER VOLCANOES ON CLIMATE AND WEATHER

Dr. James E. Hansen, NASA-Goddard Institute for Space Studies, 2880 Broadway, New York, NY 10025 (*Chairman*)

Dr. Reid A. Bryson, University of Wisconsin, 1225 West Dayton Street, Madison, WI 53706

Dr. Howard J. Critchfield, Office of the State Climatologist, Western Washington University, Bellingham, WA 98225

Dr. Giorgio Fiocco, Universita, Instituto di Fisica, Roma, Italy

Dr. P. M. Kelly, Climatic Research Unit, University of East Anglia, Norwich NR4 7TJ, United Kingdom

Dr. J. Murray Mitchell, Jr., NOAA/EDIS/DX6, Room 615, Gramax Building, 8060 Thirteenth Street, Silver Spring, MD 20910

Dr. Reginald E. Newell, Massachusetts Institute of Technology, Department of Meteorology and Physical Oceanography, 54-1520, Cambridge, MA 02139

Dr. Owen B. Toon, NASA-Ames Research Center, MS 245-3, Moffett Field, CA 94035

WORKSHOP ORGANIZING CHARMEN

Dr. Adarsh Deepak, Institute for Atmospheric Optics and Remote Sensing, P. O. Box P, Hampton, VA 23666 (*Chairman*)

Dr. Robert A. Schiffer, EE-8, NASA Headquarters, Washington, D.C. 20546 (*Associate Chairman*)

COLOR ILLUSTRATIONS

A century ago, scientists interested in studying volcanic phenomena relied on restricted ground-based measurements and visual observations. Today, scientists can employ a large array of sophisticated instrumentation—aircraft, balloons, and Earth-orbiting satellites—to study volcanic eruptions from an entirely new perspective. The crayon sketches of the 1883 Krakatoa eruption's twilight effects near London (Illustration C.1) cannot match the technical quality and colors of the photographs of the 1980 Arizona sunset caused by the Mount St. Helens' eruption cloud (Illustration C.2). These are both ground-based observations. The photographs of the Earth's limb (Illustration C.3), taken from a high-altitude balloon, confirm the altitude and stratification of the 1980 volcanic cloud. The immensity of an eruption cloud like that of Mount St. Helens, and its potential for affecting the atmosphere, is easily appreciated from the satellite infrared image (Illustration C.4). The technological advances of the past century have expanded not only our vantage points for research but also our scientific and environmental concerns. We have pushed our understanding of volcanic eruptions much further, to the question of how they influence climate.

TWILIGHT AND AFTERGLOW EFFECTS AT CHELSEA, LONDON
NOV. 26th 1883



No. 1. ABOUT 4.10 P.M.

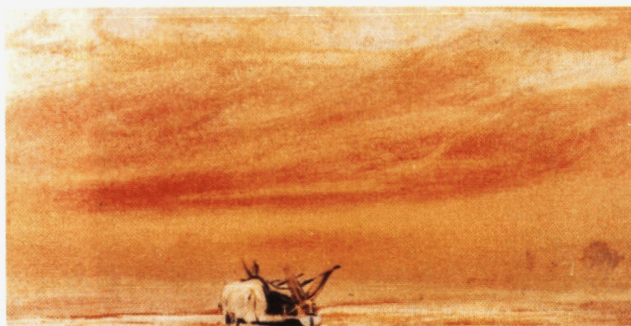


No. 2. ABOUT 4.20 P.M.



No. 3. ABOUT 4.30 P.M.

Illustration C.1 Reproduction of a series of crayon sketches made on the Thames, a little west of London, on the evening of 26 November 1883 by Mr. W. Ashcroft of Chelsea, London, 3 months after the Krakatoa eruption. Reproduced from the G.J. Symons report on the Eruption of Krakatoa and Subsequent Phenomena referred to in the Executive Summary and Chapter 1.

TWILIGHT AND AFTERGLOW EFFECTS AT CHELSEA, LONDON
NOV. 26th 1883

No. 4. ABOUT 4.40 P.M.



No. 5. ABOUT 5 P.M.



No. 6. ABOUT 5.15 P.M.



Illustration C.2 Twilight photographs taken on 27 and 28 August at Tucson, Arizona, by Aden and Marjorie Meinel of the Optical Sciences Department of the University of Arizona and kindly provided for this report.

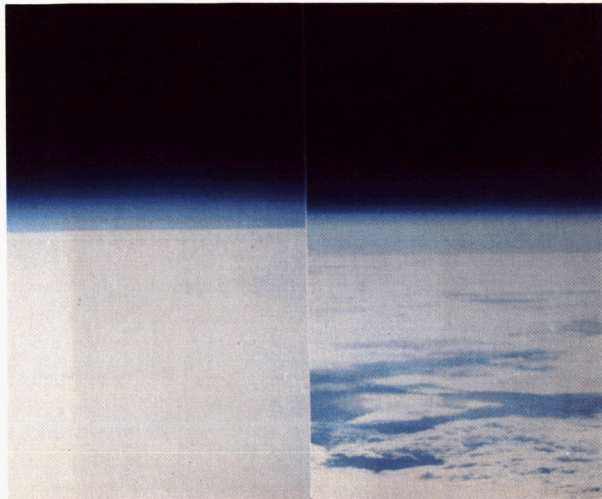


Illustration C.3 Photographs of the earth's limb taken from high altitude balloon at 35 km altitude on 5 June 1980, and at 37.5 km altitude on 15 October 1980, and kindly provided for the report by Dr. M. Ackerman of Institute D'Aeronomie Spatiale de Belgique. (See Ackerman et al., 1980 in Chapter 4.)

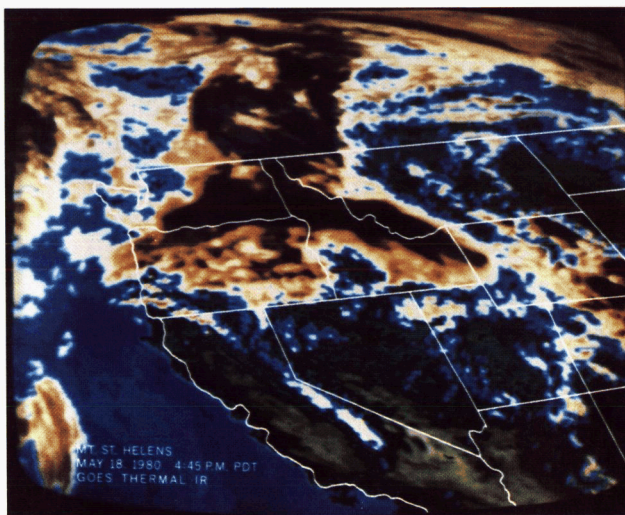


Illustration C.4 Computer-enhanced GOES satellite image of the Mount St. Helens eruption cloud taken on 18 May 1980 at 4:45 p.m. Pacific Daylight Time (PDT). Kindly provided by Michael Matson of the NOAA National Earth Satellite Service.

EXECUTIVE SUMMARY

The purpose of this Workshop, held in Washington, DC, in November 1980, was to examine the information available about the eruption of Mount St. Helens on 18 May 1980 and to try to assess whether the eruption and subsequent associated phenomena had any significant effects on the atmosphere and any potential climatic impact. Material from this massive eruption was observed at many places in the northern hemisphere from satellites, from aircraft, from balloons, and from ground-based instruments. Study of an event on this scale and of this complexity requires expertise from many disciplines: chemistry, geology, engineering, meteorology, and physics.

The assemblage of scientists and engineers was divided into six groups, each of which concentrated on a particular aspect of the phenomenon. A group of geologists, led by William I. Rose, examined what happened in the immediate region of Mount St. Helens and how it was related to previous eruptions there. A group of meteorologists, chaired by Edwin F. Daniels, looked at the evidence for the movement and dispersal of the cloud and tried to relate cloud properties to atmospheric structure. Measurements in the cloud and its surroundings, mostly from aircraft, were surveyed by a group of atmospheric chemists chaired by Jarvis L. Moyers. The movement and evolution of the cloud, as determined from remote sounding by satellites, aircraft, and ground-based systems, was the topic reviewed by M. P. McCormick and his colleagues. The chemistry of the possible processes governing the evolution of the gases and particles injected by the eruption, and the possible influence of the ambient atmospheric concentrations of certain minor constituents, was explored by J. P. Friend and his fellow atmospheric chemists. The sixth group, chaired by J. Hansen, considered the possible atmospheric effects and potential climatic impact of the eruption.

It is worth noting that Mount St. Helens is the first major volcanic eruption that has been measured from the ground, from the air, and from space. Aircraft sampling of this event *in situ* was made possible by the availability of satellite data collected by the National Oceanic and Atmospheric Administration (NOAA) and by the trajectory information developed by NOAA and the National Aeronautics and Space Administration (NASA). This cooperative effort enabled the NASA U-2 aircraft to penetrate the cloud 1 day after the eruption and the Department of Energy (DOE) WB-57F aircraft a day later. Many years of effort have gone into the background work on trajectory analysis. The NOAA data set were also used to vector the NASA P-3 aircraft and its lidar system into the proper position for a series of flights over

parts of the eastern one-third of the United States. The remote sensing of the cloud from space also represents the culmination of many years of work with the NASA satellite system known as SAGE (Stratospheric Aerosol and Gas Experiment). This system, which is based on solar occultation, was making measurements over northern Canada on 18 May and on subsequent days the latitude of measurement moved southward so that it was almost perfectly placed to sense the cloud from Mount St. Helens early in its lifetime.

The major findings and recommendations of the Workshop follow.

CONCLUSIONS

1. The volume of magma erupted at Mount St. Helens on 18 May was in the range from 0.3 to 0.6 km³. Eruptions of comparable volume occur on an average of once every 8 to 10 years.

2. The ash was very fine grained with the majority in the form of particles whose diameter was less than 200 μm .

3. Ash produces local atmospheric effects, chiefly the reduction of solar radiation at the ground. The NOAA-6 satellite measurements showed that the cloud over Montana and Wyoming on 19 May increased the albedo by a factor of two. On 20 May ground-based optical depths as high as 0.48 at 0.875 μm were recorded at Boulder, Colorado; a typical clear atmospheric value is 0.053.

4. Potential global climate effects depend on the ash and sulfur ejected into the stratosphere. The gaseous sulfur evolves into an aerosol which has a stratospheric residence (e-folding) time of about 1 year. More than 2×10^8 kg of sulfur was erupted on 18 May, but the amount entering the stratosphere is not known. This sulfur mass is relatively low, partly because the magma was poor in sulfur, and this demonstrates that explosivity alone is a poor criterion for judging the global atmospheric impact.

5. At about 12 km, the plume moved rapidly eastward, then turned to the southeast and later northeast, passed the United States east coast about 3 days after the eruption, and circuited the globe in about 16 days. At 23 km the debris moved toward the west with an average speed of about 8 m sec⁻¹, corresponding to a circuit time of about 56 days.

6. Trajectory analysis was used to predict the portion of the cloud in the early stages and was so successful that aircraft were able to penetrate the cloud in a day or two after the eruption.

7. The aircraft measurements showed sulfuric acid in the stratospheric portions of the plume, as well as gaseous sulfur in the form of SO_2 , OCS, and CS_2 . H_2S was the dominant sulfur species in the troposphere.

8. Water concentrations in the plume on 19 May were found to be 10 or more times the background water concentration. Enhanced levels of oxidized nitrogen compounds (NO , N_2O , and HNO_3) were also found.

9. This volcanic plume is among the first that has been monitored by satellites specifically designed to measure global stratospheric aerosols (SAGE).

10. Monitoring was also carried out by ground-based lidars in the northern hemisphere which yielded the detailed vertical structure of the clouds and the time for the upper westward-moving plumes to circuit the globe

11. Lidar scattering ratios for the material near 14 km were as large as 100 at $0.6943 \mu\text{m}$ (background ratios are approximately 1.1 at this wavelength). Extinction coefficients as high as 0.01 km^{-1} were measured at $1.0 \mu\text{m}$.

12. Stratospheric optical depths measured from SAGE for the northern hemisphere in August ranged from 0.001 to greater than 0.005 at $1.0 \mu\text{m}$.

13. From the single location lidar measurements at NASA-LaRC estimates of the increase in stratospheric aerosol mass were from 3 to $7 \times 10^8 \text{ kg}$, while the global SAGE data yielded about $3 \times 10^8 \text{ kg}$. This represents a 100% increase over the northern hemisphere background value. If a 4-km thick layer is assumed, the equivalent average mass density for the northern hemisphere is about $0.3 \mu\text{g m}^{-3}$, about four times higher than pre-erupted values.

14. The physical and optical properties of the Mount St. Helens aerosols were found to be such as to lead to an increase in the planetary albedo and to cause a warming of the lower stratosphere and a cooling of the troposphere (albedo for single scattering > 0.98).

15. Based on the observed rather small optical depths for the stratosphere, it is expected that the magnitudes of the long-term radiative effects will be small in comparison to the normal variability of the atmosphere.

16. It can be concluded, on the basis of findings from Mount St. Helens and prior research, that past single and multiple eruptions have caused significant climatic effects.

RECOMMENDATIONS

1. Sampling aircraft need to be maintained so that composition measurements can be made in a volcanic plume as soon as possible after an eruption (probably within 12 hours) and as often as is logically practical during the first few days after the eruption. Contingency plans should be available to cover possible eruptions from tropical America to Alaska. This kind of effort demands close cooperation and coordination by all experimenters under one agency, group, or person.
2. A capability to compute three-dimensional trajectories in real time should be developed and be readily available for use in making aircraft flight plans.
3. Measurements of gaseous sulfur compounds, sulfuric acid, and sulfate should be made at different times in the same region of the plume, as far as possible, to try to assess gas-to-particle conversion rates.
4. During the next few sets of Airstream flights, the sulfur and nitrogen species should be measured to try to assess conversion rates on a longer time rate.
5. Measurements with SAM II and SAGE should continue so that a global climatology of stratospheric aerosol may be established. Similar satellites with improved capabilities should be launched to replace these two. Shuttle lidar flights may provide a valuable complement to these observations.
6. A study of the feasibility of satellite SO₂ measurements should be made.
7. Lidar should continue to be used to monitor atmospheric aerosol and stations should be established in the southern hemisphere and at equatorial and high latitudes.
8. Radiation in and below a volcanic plume should be measured as a function of wavelength from an aircraft platform to establish which wavelengths are absorbed.

9. In order to monitor volcanic activity over the globe on a long-term basis, a network of well calibrated ground-based sensors capable of measuring diffuse and direct solar radiation is required. With the new data available from SAM II and SAGE, the present two global networks, the turbidity network of the World Meteorological Organization and the NOAA Geophysical-Monitoring for Climatic Change Network, should be carefully examined to see if any modifications are desirable.

10. In order to see what effects volcanoes had on past climate, improved reconstructions of global scale surface temperature and precipitation are required.

11. To assess historical variations of atmospheric volcanic aerosol loading, more ice core studies are required, including ice cores from more than one ice sheet to minimize the effects of local weather and circulation.

12. The effect of volcanic aerosols on regional climate should be studied with the aid of three-dimensional models.

13. The new data on precursor gases and aerosols from Mount St. Helens should be used as input to improve photochemical models of aerosol formation, growth, and decay. Eventually, such models may be used for scaling aerosol properties to volcanoes of different sizes and types.

14. The detailed justification for these conclusions, together with further findings and recommendations, will be found in reports of the various groups which follow.

It is worth noting that there is a precedent for the examination of the eruption of one volcano by a group of scientists from several disciplines. The Krakatoa Committee of the Royal Society of London produced a report in 1888, edited by G. J. Symons, entitled *The Eruption of Krakatoa and Subsequent Phenomena*. The first chapter of that report was devoted to the geological aspects of the eruption of 26-27 August 1883. The second chapter covered meteorological aspects including the atmospheric pressure waves and the third covered twilight effects. The fourth chapter dealt with the effects on the ocean, particularly waves, and the fifth terrestrial magnetism and electricity. It is of interest to see how the emphasis has changed during the past century. There is still much stress of course on the geological aspects and the twilight effects. All measurements a century ago were from the ground whereas now aircraft sampling and observations from satellites play a major role in contributing information. There were arguments then about what happened; for example, how did the material get moved about the earth? Now it

seems this aspect is understood but still the details of how and why the aerosol forms and how it may influence climate are not known. Climate has come to the fore as a topic of major concern and the question of how volcanoes influence climate is one of the most challenging of modern-day meteorology. It must be answered before the prospect for climatic forecasting can be assessed.

Reginald E. Newell
Workshop Technical Chairman

CHAPTER 1

VOLCANOLOGICAL DESCRIPTION OF THE 18 MAY 1980 ERUPTION OF MOUNT ST. HELENS

1.1 INTRODUCTION

This chapter gives a general volcanological background to the 18 May 1980 eruption of Mount St. Helens for the reader primarily concerned with volcano-atmosphere and volcano-climate interactions. It is not a comprehensive summary of geologic work on the eruption. The volcanologic observations and data are emphasized that are believed to be pertinent to the atmosphere and climate. Also this eruption is compared with historic eruptions to illustrate its size in a geologic perspective and to identify its typical and atypical aspects. For additional geological data on the eruption the reader should see the report compiled by Lipman and Mullineaux (1981).

1.1.1 Definitions

Because some of the volcanologic terms in this chapter may be unfamiliar to atmospheric scientists, a few definitions have been included.

Tephra—fragmental material of any size that is ejected from a volcano.

Magma—a molten rock under the earth's surface and at the point of eruption.

Pyroclast—individual particles of any size ejected by an explosive volcanic eruption.

Phreatic eruptions—eruptions that result from the interaction of ground water with hot rock surrounding a magma body.

Phreatomagmatic eruptions—eruptions that result in part from the interaction of ground water with magma.

Pumice—rock froth, usually of a light color and high silica content.

Magmatic eruptions—eruptions that result primarily from the escape of volcanic gas from magma.

Plinian eruptions—gas-rich sustained explosive eruptions with exceptionally high (> 10 km) eruption columns: named by Pliny the Younger who described the AD 79 Vesuvius eruption.

1.2 ACTIVITY OF THE VOLCANO

1.2.1 Previous Eruptive Activity of Mount St. Helens

There has been intermittent volcanic activity from Mount St. Helens for 40,000 years, and four periods of sustained activity with durations from 400 to 900 years have occurred since about 2500 BC, when the present cone formed

(Crandell et al., 1975; Crandell and Mullineaux, 1978). The last of these was from 1300 AD to 1857 (Fig. 1.1). The 1831-1857 activity of Mount St. Helens was recorded by eyewitness accounts (Harris, 1976). This eruptive activity has been exceptionally variable in both character and composition of material erupted which includes pyroclastic flows, lava flows, mudflows, domes, and tephra falls ranging from basaltic to dacitic compositions. Typical repose periods between eruptions were a few centuries or less, a timing which suggested that an eruption was likely "perhaps even before the end of this century" (Crandell et al., 1975; Crandell and Mullineaux, 1978). During the past 4000 years, at least five major episodes of explosive eruptions produced silicic magma, that exceeded the volume and mass of material produced in the 18 May 1980 eruption by a factor of at least two. One of these eruptions, which occurred about 3000 to 4000 years ago and produced a tephra layer, Y_n , was estimated to be 4.5 to 5 times larger than that of 18 May (Table 1.1).

TABLE 1.1. Estimate of Minimum Total Mass and Volume of Deposits from Eruptions during the Current Episode of Volcanic Activity, and Comparison with Estimates for Previous Historic and Prehistoric Eruptions of Mount St. Helens (Sarna-Wojcicki et al., 1981a).

	1980 activity					Prehistoric	
	Early phreatic ¹ 22 July 25 May 15 June 18 May ⁴					Layer T (ca. 1800 A.D.)	Layer Y_n (ca. 4000 b.p.)
Mass ($\times 10^{14}$ g)	0.0080	0.040	0.42	0.45	4.9	10.0	22.5
Volume ² (km^3)	0.0004	0.002	0.02	0.02	0.2	0.4	0.9
Volume ³ (km^3)	0.0020	0.010	0.12	0.12	1.1	2.2	5.0

¹Phreatic eruptions, 27 March to 17 May 1980.

²Calculated for a solid-rock density of 2.6 g/cm³.

³Calculated for a bulk density of 0.45 g/cm³.

⁴Airfall tephra only. Does not include basal lithic pyroclastic surge deposit, debris avalanche deposits, mudflow deposits, and pyroclastic avalanche deposits.

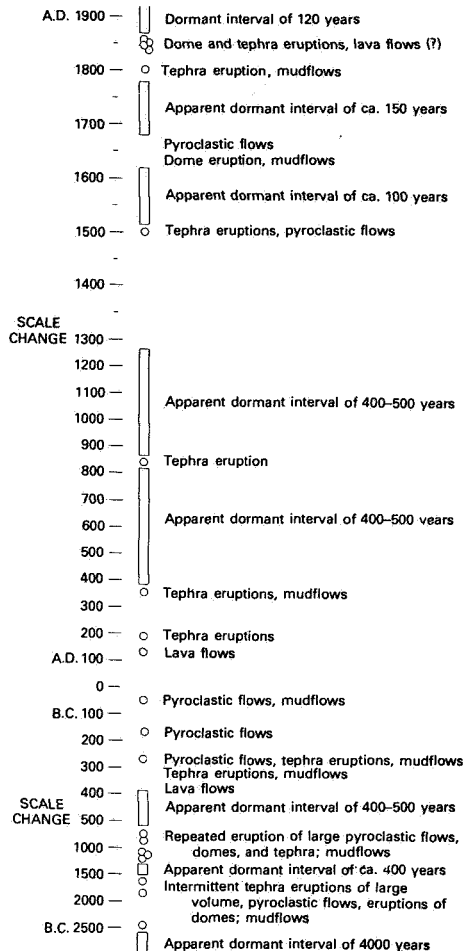


FIGURE 1.1 Eruptions and dormant intervals at Mount St. Helens since 2500 BC. The circles represent specific eruptions that have been dated or closely bracketed; the vertical boxes represent dormant intervals. The known eruptions at Mount St. Helens can be roughly grouped into four periods: 2500 to 1600 BC, 1200 to 800 BC, 400 BC to AD 400, and AD 1300 through about the middle of the 19th century. Dormant intervals have typically lasted no more than a few centuries, and the recent behavior of the volcano has been variable. From Crandell and Mullineaux, 1978.

1.2.2 Observations of the 18 May Eruption

For 2 months before the eruption of 18 May, geodetic monitoring at Mount St. Helens indicated that the north flank of the volcano was bulging away from the summit crater, apparently in response to emplacement of magma at shallow depths. This intrusion steepened and destabilized the north flank of the volcano.

Descriptions of the 18 May eruption are aided by excellent photographic records of the first few minutes (Christianson, 1980). At 0832 PDT a large earthquake (Richter mag. 5.1) triggered a massive slide on the north slope of the Mount St. Helens cone. More than 2 km³ of the cone was removed in a landslide that formed a 15 km long hummocky debris flow in the North Fork of the Toutle River. Phreatic eruptions, similar to those which began on 27 March, then began from the summit crater. A strong, northward lateral blast (pyroclastic surge) followed almost immediately, overtaking the moving debris avalanche and devastating about 500 km² of forest as far as about 30 km to the north of the cone. The surge deposit contains mainly material from the old Mount St. Helens cone, but it also contains dacitic rock which represents new magma. This blast was one of the most violent historical examples of pyroclastic surge (Rosenbaum and Waitt, 1981). After the surge, about 4 minutes after the earthquake, a vertical plinian eruption column rose to a height of more than 24 km. The ash ejected in this phase of the eruption was preserved as hot pyroclastic flow deposits, restricted to the northern slopes of Mount St. Helens itself, and as an extensive pyroclastic fall deposit which is found east of the volcano (Sarna-Wojcicki et al., 1980, 1981a,b). Elutriation of material from the hot pyroclastic flows contributed to the air fall deposit.

1.2.3 Downwind Progress of the Airborne Ash Plume

The prevailing westerly winds on 18 May swept the ash plume toward the northeast and east-northeast. A sequence of National Oceanographic and Atmospheric Administration (NOAA) satellite photos provide an excellent record of the progress of the ash plume as it moved eastward. An isochron map was compiled for the leading edge of the ash plume from the NOAA satellite photos, which were taken from a geosynchronous orbit at half-hour intervals from 0845 to 1816 PDT on 18 May (Fig. 1.2). By 0945 the widening ash front had passed over Yakima, Washington. The ash front reached Spokane, Washington, about 1215, about 3.5 hours after the start of the eruption. By about 1500 the front of the ash plume had passed over Missoula, Montana, and the northwesterly winds there began to swing the front of the plume to the southeast. By dusk, about 1800, the plume front had passed southeast into northwestern Wyoming. After dark the progress of the plume could not be monitored with photos in the visible spectrum, and infrared photo imagery did not have sufficient resolution to define plume boundaries.

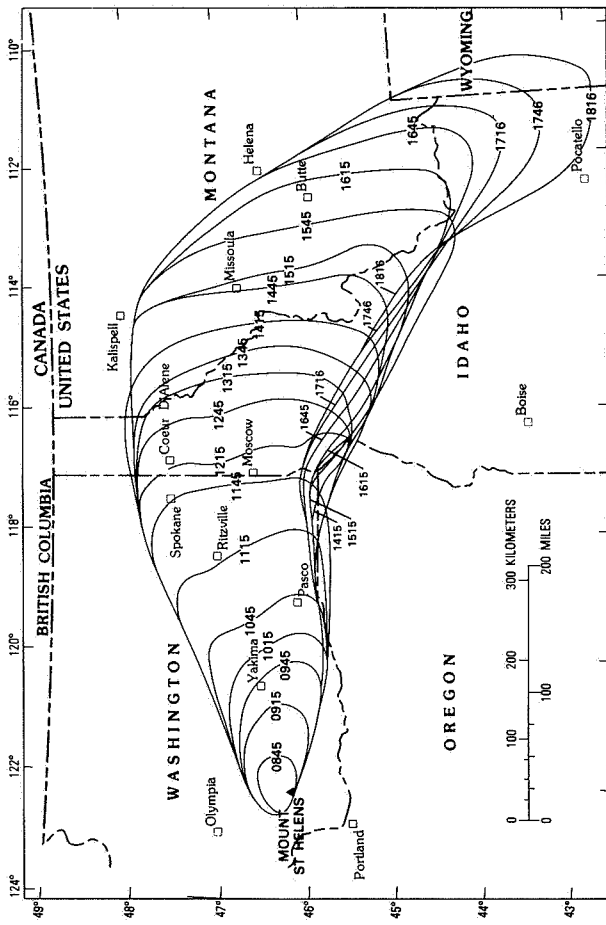


FIGURE 1.2. Isochron map of extent of airborne ash plume erupted from Mount St. Helens on 18 May 1980. Map shows maximum downwind extent of ash carried in fastest wind layer for any given time as observed in satellite photos. Appreciable darkening at many distal sites was not noted by ground observers for as much as 2 or more hours later than times shown, and ash-fall was not observed till even later (see text). Map is compiled from NOAA satellite photos (sector KB7 and SA40) taken at half-hour intervals between 0845 and 1816 Pacific Daylight Time (PDT), or between 1545 18 May and 0116 19 May Greenwich Mean Time. Plot of plume position relative to ground was visually corrected for zenith angle. Probable errors in position of plume boundaries are ± 10 km in the north-south direction, and ± 5 km in the east-west direction. From Sarna-Wojcicki et al., 1981a.

The advancing front of the airborne plume was defined by the ash carried in the fastest moving wind layer, at an altitude of about 10 to 12 km traveling with an average velocity of about 100 km/hr over the first 1000 km downwind. The front part of the cloud became more diffuse at greater distances downwind. The cloud darkened and ash began to fall sometime after the airborne plume front passed. At Spokane, Washington, for example, a ground observer noted only a "halo" around the sun at the time of the passage of the plume front overhead, an appreciably darker cloud about 2.5 hours later, and ash fall, about 3 hours later. A somewhat shorter lag, about 2 hours, before the first ash fall was observed at Pullman, Washington (Sarna-Wojcicki et al., 1981a).

1.2.4 Radar Observations

The 18 May 1980 eruption of Mount St. Helens was observed on the National Weather Service (NWS) radar system at Portland, Oregon. Additional radar coverage of the 18 May eruption was provided by the Auburn (Washington) NWS office which integrated data from radar systems, at Seattle and Spokane. The Portland radar data documents the height of the eruption column as a function of time. The maximum column heights and durations of ash emission at various elevations in the atmosphere are obtained directly (Fig. 1.3). The Seattle radar system was used on 18 May 1980 from 0940 PDT to 2240 PDT to track the ash cloud trajectories from Mount St. Helens to the Idaho panhandle (Fig. 1.4). The radar observations (Harris et al., 1981a) show four relative maxima in the column height and peak reflectivities between 0832 and 1800 PDT. The first relative maximum occurred between 0840 and 0900 when column height was in excess of 24.4 km. The top of the ash could not be measured by the Portland radar because the top exceeded the mechanical limit for the vertical angle of the antenna beam axis. Later maxima in column height and reflectivity during the 18 May 1980 eruption occurred at 1200-1230 (17.3 km), 1330-1500 (14.6 km), and at 1700 (19.2 km). The radar-detectable column height over the volcano exceeded 13.7 km (ASL) for more than 8 hours (0845 to 1700 PDT). The rate of ash emission during the eruption can be estimated using the column height information and the theory of Wilson et al. (1978). The calculations (Table 1.2) show that the eruption rate varied by an order of magnitude during the 9 hours.

Satellite observations of the 18 May eruption permit us to infer the velocity of column rise. Between 0832 and 0900 PDT, or 7.6 km and 22.9 km, respectively, the updraft velocity was approximately constant at 44 m/s (160 km/hr). During the 7 August eruption, radar height measurements made every 20 seconds during the rise from 7.0 km to 13.4 km indicated an updraft velocity of 43 m/s (155 km/hr). The velocity of column rise may be an important factor in modeling entrainment of tropospheric air and the dynamics of interaction between the column and the stratosphere.

TABLE 1.2. Estimates of Magma Eruption Rates on 18 May 1980 using Radar Measurements of Plinian Column Heights (From Harris et al., 1981a).

Measurement PDT	Column height above vent H (km)	Eruption rate of dense dacite \dot{V} ($m^3 s^{-1}$)
0845	22	23.00×10^3
0915	12	2.00×10^3
0938	12	2.00×10^3
1100	13	2.80×10^3
1158	15	5.00×10^3
1255	11	1.50×10^3
1330	13	2.80×10^3
1500	13	2.80×10^3
1605	14	3.80×10^3
1705	17	8.30×10^3
1800	5	0.06×10^3

Calculations based upon the formulae, $H = 8.2 \times Q^{0.25}$, and $Q = \sigma \dot{V} s (\theta - \theta_A) F$, of Wilson and others (1978), where H = measured column height above vent, Q = steady state release of thermal energy, σ = density of dacite (2500 $kg m^{-3}$), S = specific heat of dacite ($1.1 \times 10^{-3} J kg^{-1} deg^{-1}$), θ = magmatic temperature of dacite (1200°K), and θ_A = air temperature (300°K) and $F = 0.9$ (an efficiency factor).

Later eruptions (25 May, 12 June, 22 July, 7 August, and 16-18 October 1980) were observed on NWS radar at Portland; the maximum height, the duration of ash emission, and the relative amounts of stratospheric injection of materials in the plinian column of 18 May 1980 greatly exceeded those of later eruptions.

1.2.5 Activity at Mount St. Helens after the 18 May 1980 Eruption

Five smaller, mainly magmatic eruptions have occurred at Mount St. Helens in the 6 months following 18 May. In total, the additional magma erupted is less than 15% of the volume of the 18 May eruption. These events all had eruption columns 12 km high or more, and generally lasted less than 1 hour. On the basis of past activity and analogy with other volcanoes, this kind of activity could continue for some years to come, and the eruptive activity may change to extrusion of domes or blocky lava flows. Considering previous activity at Mount St. Helens, a very broad range of possibilities exists. Similar eruptions have occurred at other composite andesitic-dacitic stratovolcanoes, in recent times: the 1956 Bezymianny eruption (Gorshov, 1961), the 1951 Mount Lamington eruption (Taylor, 1958), and the 1964 Shiveluch eruption (Fedotov, personal communication) all involved "blasts" and destruction of

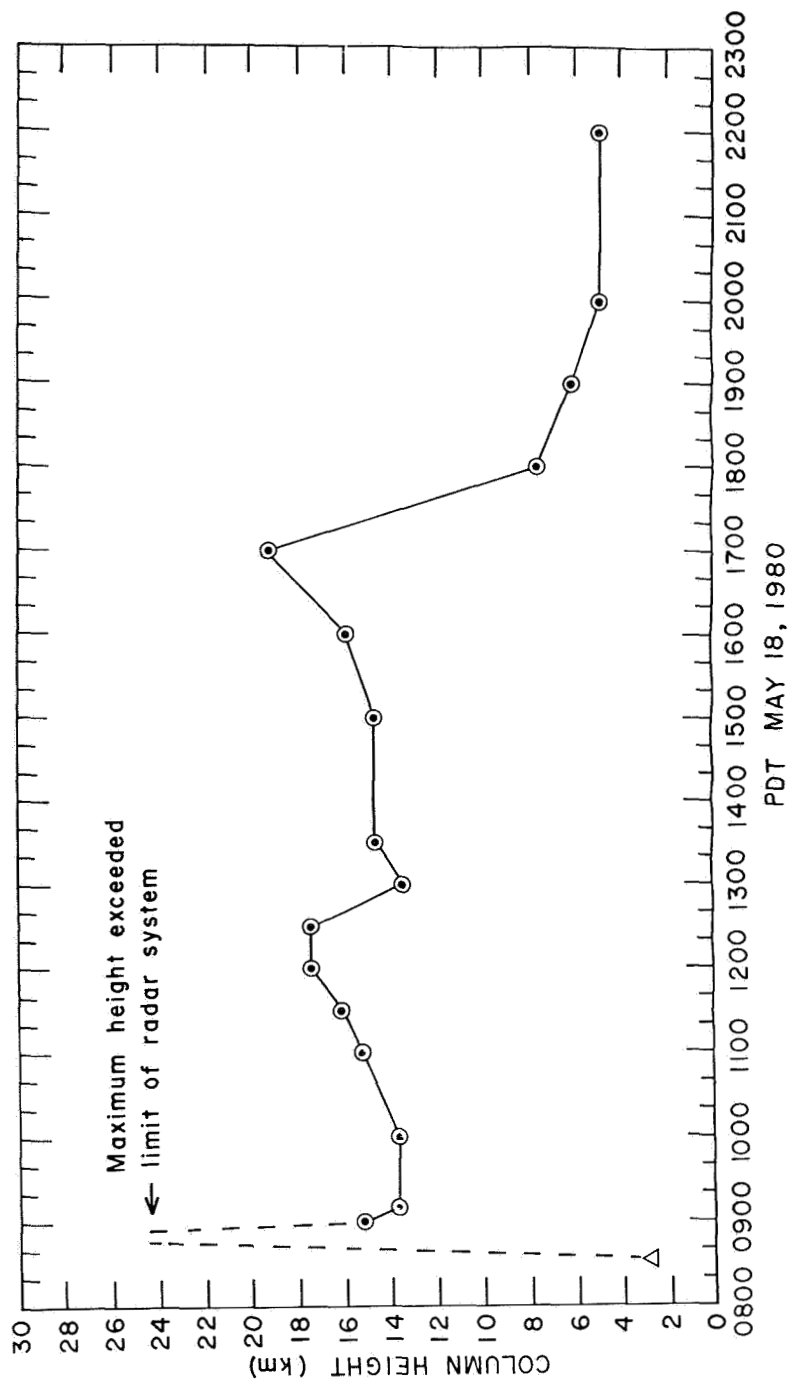


FIGURE 1.3. Height of the 18 May 1980 Plinian eruption column near Mount St. Helens, as determined by Portland NWS radar. Triangle represents elevation of Mount St. Helens vent at the onset of eruption. Heights are relative to sea level. From Harris *et al.*, 1981a.

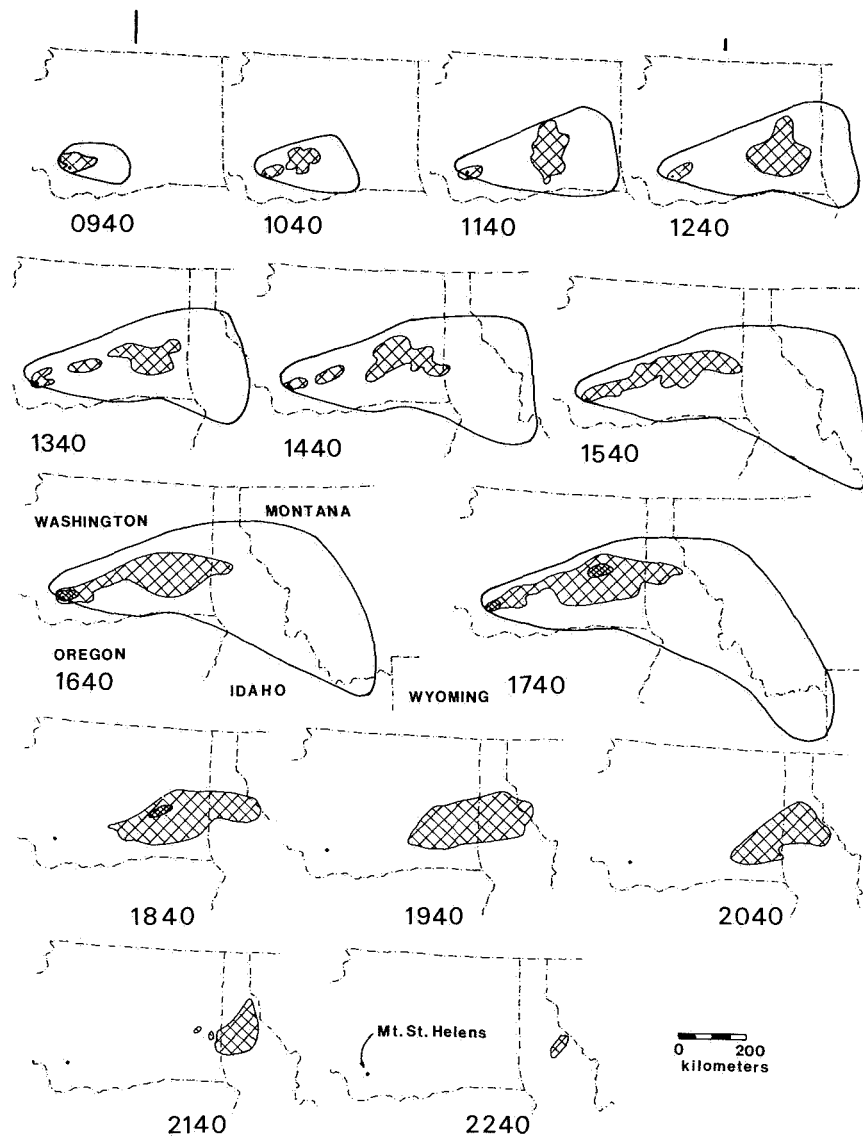


FIGURE 1.4. Shape and structure of the 18 May 1980 eruption cloud from Mount St. Helens, as depicted by Seattle and Spokane radar systems and NOAA weather satellite. Hourly tracings (PDT) of radar reflections of "Level 1" are shown as cross-hatched areas. "Level 2" reflections are shown by denser cross-hatching. The solid lines outline the whole ash cloud, as seen in the satellite images, at the same times, from 0940 to 1740 PDT. From Harris et al., 1981a.

the top of the volcano. All, incidentally, ended their eruptive phases by dome extrusion and produced volumes of ejecta similar to that produced by Mount St. Helens.

1.3 SOLID PRODUCTS OF THE 18 MAY ERUPTION

1.3.1 Introduction

The material erupted from Mount St. Helens on 18 May consisted of four kinds of particles. These are (a) *lithic fragments*, particles of the rock which made up the summit of the volcano prior to eruption; (b) *pumice*, a rock froth formed by the rapid quenching of magma, composed of volcanic glass, crystals of several different minerals, and gas bubble voids; (c) *crystals and crystal fragments* of several different minerals, which were derived from lithic fragments as well as from the crystallizing magma; and (d) *shards of volcanic glass*, broken from the frothy magma.

Particles range in size from large blocks and bombs many centimeters in diameter, to very fine dust, a fraction of a micrometer in diameter. The proportions of the particles and size ranges erupted on 18 May varied with time, and particles were erupted to different altitudes above the volcano at different times (Table 1.3). Consequently, the fine particles of the erupted material (i.e., the volcanic ash) are a complex mixture of crystals, crystal fragments, shards of volcanic glass, and lithic fragments (Fig. 1.5).

TABLE 1.3. Maximum Heights of Eruption Columns at Mount St. Helens from Radar Observations, 1980.¹

<i>Date of eruption</i>	<i>Maximum column heights (km)</i>	<i>Duration of ash emission at elevations above 12 km</i>
18 May	>24.4, 17.3, 14.6, 19.2	about 9 hours
25 May	12.2	less than 30 minutes
12 June	15.2, 10.7, 9.8, 10.7	about 30 minutes
22 July	13.7, 14.5, 13.7	25 minutes
7 August	13.4, 10.0, 6.1, 7.6, 6.1, 5.2	2 to 5 minutes
16 October	12.8	less than 5 minutes
17 October	14.3, 13.7	less than 5 minutes
18 October	5.2, 7.9	less than 5 minutes

¹From Harris *et al.*, 1981a.

1.3.2 Crystal Pyroclasts

The crystal component of the tephra (both coarse ejecta and finer ash) consisted of the following minerals, in order of abundance: plagioclase

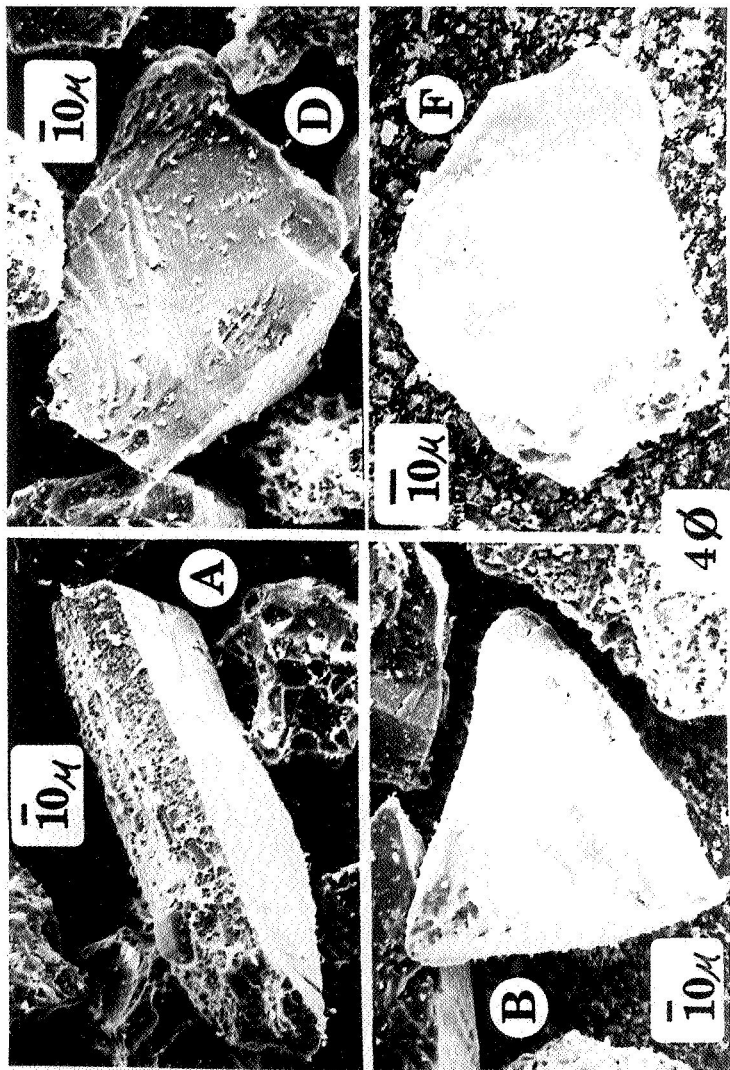


FIGURE 1.5. Individual particles of the 4 (100 μ m) split of Spokane ash, identified by energy dispersive x-ray analysis. Most are crystal pyroclasts. A is a hornblende crystal, with a glass jacket. It is probably magmatic, and shows that crystals from the magma are also found in the 4 material. B and D are fragmented plagioclase crystals. F is a titaniferous magnetite grain. Many vesicular glass particles occur in this size fraction also. From Rose and Hoffman, 1980.

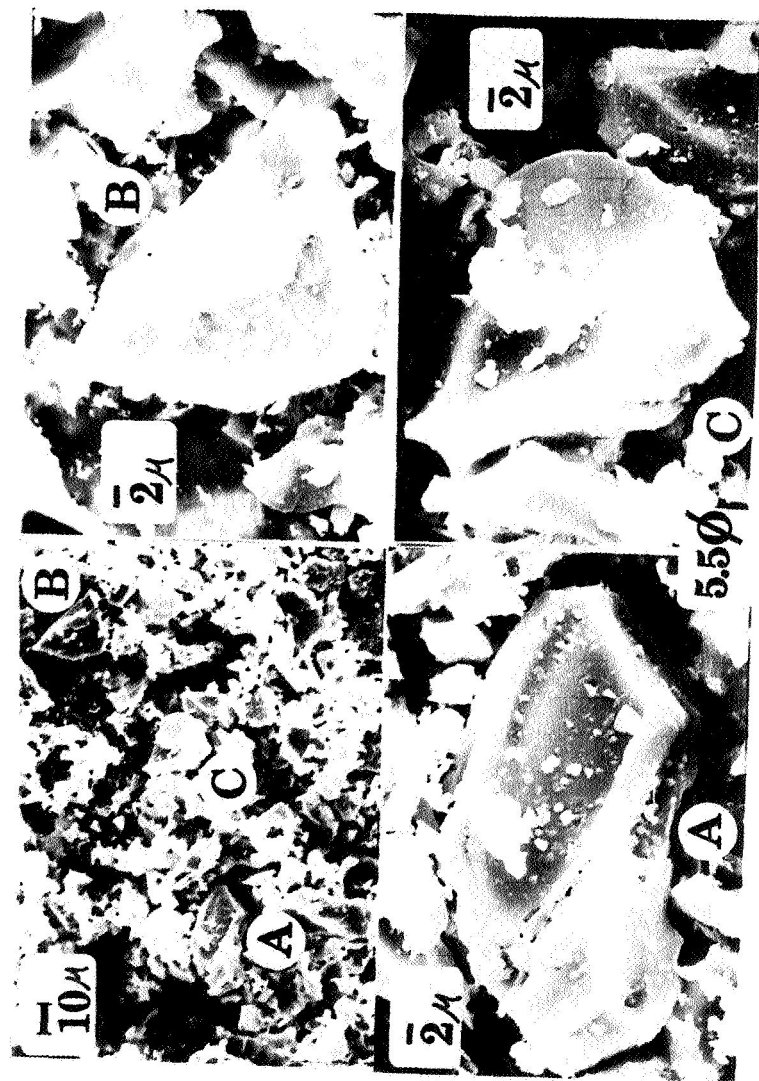


FIGURE 1.6. SEM images of the 5.5 ($\approx 25 \mu\text{m}$) split of Spokane ash. This material is chiefly glass pyroclasts. A and C are glasses with compositions of 70% SiO_2 , 5% K_2O . B is a composite grain, with the left side glass and the right side titaniferous magnetite. The bulk composition of this size fraction reflects glass enrichment. From Rose and Hoffman, 1980.

feldspar, hypersthene, hornblende, titanomagnetite, and minor ilmenite, apatite, and augite. These minerals are found in pumice, in lithic fragments, and as loose crystals and crystal fragments in the airfall ash. Typical chemical compositions of some of these minerals are given in Table 1.4. In addition to these minerals, quartz, cristobalite, chlorite, and sericite also have been identified. Some formed before eruption through hydrothermal activity in the volcanic vents.

TABLE 1.4 *Chemical Composition of Some Coarse Crystalline Minerals in Downwind Volcanic Ash (all data reported as weight percent)*¹.

Component	1	2	3	4
<i>SiO₂</i>	52.9	55.7	--	45.7
<i>TiO₂</i>	0.1	--	7.8	2.3
<i>Al₂O₃</i>	0.5	27.6	0.9	10.1
<i>FeO</i>	0.7	0.2	87.4*	13.8
<i>CaO</i>	0.9	10.3	--	12.1
<i>MgO</i>	0.5	--	0.9	13.4
<i>Na₂O</i>	0.3	5.8	--	2.5
<i>K₂O</i>	3.9	0.2	--	0.4
<i>Total</i>	100.8	99.8	97.4	100.3

¹L. L. Ames, written communication, 1980.

1. Hypersthene, Yakima, Washington.

2. Plagioclase feldspar (labradorite), Yakima, Washington.

3. Titaniferous magnetite, Yakima, Washington.

4. Augite, Rosalia, Washington.

*As Fe_3O_4 .

1.3.3 Glassy Pyroclasts

The tephra from the 18 May eruption consists mostly of glassy pyroclasts: pumice and shards (Fig. 1.6). Pumice forms when magma bearing gas in solution is decompressed or quickly quenched; the magma solidifies and the gas comes out of solution to form bubbles (vesicles) surrounded by thin walls of glass. Pumice lumps may be entrained in an eruption column or in pyroclastic flows, or they may be shattered in the eruption. Glass shards are fragments of the vesicle walls and are generally small, angular, and irregularly shaped. Glassy pyroclasts range in size from pumice blocks more than 10 cm across near the vent or in pyroclastic flows to shards less than 5 μm in diameter in airfall deposits.

Pumice, then, generally consists of three components: vesicles, thin glass vesicle walls, and generally minor fractions of crystalline minerals. Vesicles are variable in both shape and size; they range from simple ovoids to elongate tubes and from a few micrometers to more than 100 μm long. Vesicle walls are glassy and quite thin, from one half to a few tens of micrometers thick. Pumice pyroclasts are generally 60% to 80% glass; the remainder is crystals or crystal fragments largely of plagioclase feldspar with lesser amounts of magnetite, ilmenite, orthopyroxene, and hornblende (Sarna-Wojcicki et al., 1981b; Melson et al., 1980; Hooper et al., 1980), as shown in Table 1.5.

TABLE 1.5 Mineralogical Composition of Pumice and Ash from Eruption of 18 May 1980 (not counting vesicle volume) in Volume Percent.

	<i>Glass</i>	<i>Plagioclase</i>	<i>Hornblende and orthopyroxene</i>	<i>Magnetite</i>
1	64	26	10	2.2
2	82	11	8	1.7

1. Bulk pumice (Wozniak et al., 1980).

2. Missoula ash (Rose and Hoffman, 1980).

The glass of 18 May is rhyolitic in composition (Table 1.6). The bulk composition of the rhyolitic glass with the crystalline phases is that of a dacite; the compositions are very similar to those reported for products of other historic eruptions of Mount St. Helens.

The glassy tephra are particularly important for plume studies because the large surface areas of pumice and shards scavenge liquid aerosol particles in the eruption cloud.

1.3.4 Lithic Pyroclasts

Lithic fragments consist of finely comminuted fragments of older lavas and pyroclastic rocks from the conduit and crater of Mount St. Helens. These were particularly important in the early phases of the eruption, although they probably were not a large component of stratospheric plumes.

Most lithic pyroclasts are angular, blocky fragments of dacite and andesite. Two common types are (a) dark brown glass with abundant microlites (crystals with grain sizes smaller than 10 μm), and (b) coarser-grained lavas in which lithic pyroclasts are a composite of plagioclase phenocrysts and glass (Hooper et al., 1980). During the phreatic activity preceding the 18 May eruption, all of the tephra consisted of lithic and mineral fragments produced by fragmentation of the older lavas and pyroclastic deposits that made up the summit area.

TABLE 1.6. Composition of Rhyolitic Glass Phases and Dacitic Ash ("Pale Ash").

Component	Weight percent		
	Glass composition	Dacitic ash from Missoula	
SiO_2	72.20	71.40	67.80
Al_2O_3	15.40	14.60	16.10
TiO_2	0.45	0.37	0.64
Fe_2O_3	2.51	2.40	4.50
FeO			
MnO	0.04	n.d.	n.d.
CaO	2.48	2.60	4.10
MgO	0.98	0.53	1.50
K_2O	1.99	2.00	1.70
Na_2O	3.88	4.30	4.60
P_2O_5	n.d.	0.99	0.13
Source:	1	2	3

1. Hooper *et al.*, 1980—analysis by electron microprobe.

2. Melson *et al.*, 1980—analysis by electron microprobe.

3. Rose and Hoffman, 1980—X-ray fluorescence analysis.

n.d. = not determined.

It is difficult to determine an *average* chemical composition for these pyroclasts because a large variety of rock types are represented. However, bulk compositions of ashfall deposits made of largely lithic pyroclasts are available (Table 1.7).

1.3.5 Downwind Airfall Ash Distribution

Figure 1.7 shows the downwind distribution of the airfall ash from the eruption of 18 May. The greatest thickness of ash fell in the vicinity of the volcano and to the northeast thickness decreased downwind to a minimum at a location 40 km northeast of Yakima. A secondary maximum ashfall thickness formed in the vicinity of Moses Lake and Ritzville, with thicknesses decreasing with distance downwind toward the east-northeast. Maximum thicknesses along the dispersal axis various distances downwind were 100 mm (40 km), 20 mm (130 km), 50 mm (320 km), 20 mm (420 km), and about 5 mm (600 km). Thickness measurements varied considerably depending on when the measurements were made and especially where rainfall had compacted the ash. Consequently, combining thickness and area measurements does not give a reliable estimate for the volume of ash erupted. Figure 1.8 is an isomass map, based on ash collected from measured areas. The total mass of ash within the

TABLE 1.7. Composition of "Dark Ash" in Weight Percent.

Component	1	2
SiO_2	64.21	58.50
Al_2O_3	17.20	18.30
TiO_2	0.70	0.83
Fe_2O_3	2.21	5.80*
FeO	2.53	
MnO	0.07	n.d. **
CaO	5.07	5.40
MgO	1.85	2.60
K_2O	1.52	1.30
Na_2O	4.47	4.60
P_2O_5	0.19	0.16

1. Dark ash, fell at Pullman, Washington, Hooper et al., 1980.

2. Dark ash, fell at Richland, Washington, 1300-1400 PDT, Rose and Hoffman, 1980.

*Total Fe as Fe_2O_3

**n.d. = not determined

studied area was calculated from Fig. 1.8 to be between 4.9 and 5.5×10^{14} g. The total volume of airfall ash within the isopach map area is about 1.1 km^3 , approximately equal to a dense rock volume of 0.2 to 0.25 km^3 . Both mass and volume estimates are *minima*, and may represent as little as one-half of the total airborne mass and volume. The remainder of the ash was either deposited in areas outside the sampled area, or remained suspended in the atmosphere.

1.3.6 Proximal and Distal Stratigraphy of the 18 May Ash

There are four units of airfall ash and coarser ejecta near the volcano that reflect distinct eruptive stages (Waitt and Dzurisin, 1981; Sarna-Wojcicki et al., 1981a). The basal unit (A) consists of a thin, fine-grained lithic and vitric-crystal ash, and probably represents the disintegrated summit and north flank of the volcano together with some pumice from the magma. Above it is a thick, coarser gray unit (B) composed of coarse lithic fragments, crystal grains, and pumice lapilli. The basal part of the unit contains coarse lithic lapilli and finer pumice lapilli (unit B1). Upward in unit B, pumice lapilli increase in size and in abundance relative to the other components. Abundant pumice in unit B marks the first major appearance of juvenile material. Unit B is inferred to have been derived from the major (plinian) eruption column after the initial blast. Above unit B is a thinner layer (unit C) of tan ash composed of fine pumice lapilli, lithic fragments, crystals, and volcanic glass inferred to be the finer particles from unit B, together with fine elutriated ash from phreatic eruptions at Spirit Lake and the pyroclastic ash flows (units B4 and C). The

uppermost unit (D) is composed of fine, gray, vitric-lithic-crystal ash similar in appearance to basal unit A. This unit is found only close to the volcano in the downwind areas, and marks the waning period of the 18 May eruption.

The stratigraphy of airfall ash is progressively simpler downwind. At Yakima, about 135 km downwind, a thin basal, dark-colored fine silty unit correlates with unit A. Overlying the A unit is a thin, somewhat coarser, fine sandy unit that correlates with unit B1. This in turn is overlain by a thicker, light-colored vitric unit that correlates with units B2-B4, together with finer ash winnowed from C and borne by wind away from the volcano, as well as possible late-settling fine-grained debris from the other units. The middle unit lenses-out or merges with the uppermost between Yakima and Moses Lake, some 250 km downwind to the southeast. Only the two layers, the basal (A) and upper (B2-B4), can be traced downwind to the vicinity of Moscow, Idaho, and some undetermined distance beyond. At Missoula, Montana, only a single, thin light-gray vitric layer can be distinguished, and most likely represents mixed material combined from both the lower and upper distal units.

1.3.7 Distribution of Fallout

The thickness of the ashfall deposits downwind did not decrease monotonically with distance, as can be seen from the isopach map (Fig. 1.7). The thick secondary accumulation of ash near Moses Lake and Ritzville in eastern Washington is a feature which has not been well described for previous volcanic eruptions. It may be a relatively common feature of downwind volcanic ash distribution patterns because the 18 May eruption and four of the later eruptions (25 May, 12 June, 7 August, and 16-18 October) of Mount St. Helens have also produced similar maxima and they have been described for eruptions of Cerro Azul (Quizapu), Chile (Larrson, 1937), and Taupo, New Zealand (Walker, 1980). Mechanisms of formation for these secondary maxima are poorly understood.

1.3.8 Accretionary Particles

At the end of the first eruptive phase (represented by unit A) there were numerous *accretionary lapilli* deposited near the volcano. *Accretionary lapilli* are agglomerations of fine particles that are arranged in concentric layers and are held together by moisture, and are common in deposits from eruptions that produced large volumes of water and steam (Self and Sparks, 1978). The accretionary lapilli, which are several mm in diameter, attract very fine-grained tephra; each aggregate is made up of several thousand to several million individual pyroclasts (Self and Sparks, 1978).

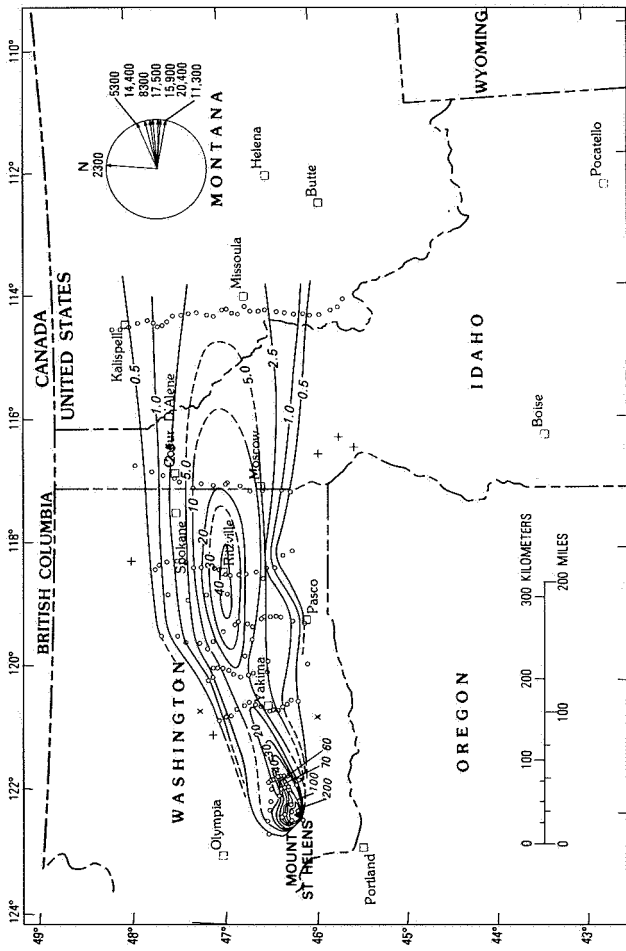


FIGURE 1.7. Isopach map of ash erupted from Mount St. Helens on 18 May 1980. Isopach lines represented uncompacted thickness, in millimeters. Open circles represent observation stations. Dashed line represents an approximate zero thickness isopach. Thicknesses along north-south traverse through Ritzville and at four observation sites about 30 to 50 km to the west have been corrected for post depositional compaction by rain. Most thicknesses along the north-south traverse through Missoula were too thin to measure directly, and have been calculated from mass per unit area, using thickness and associated mass per unit area measured near Missoula as conversion factors. From Sarna-Wojcicki *et al.*, 1981a.

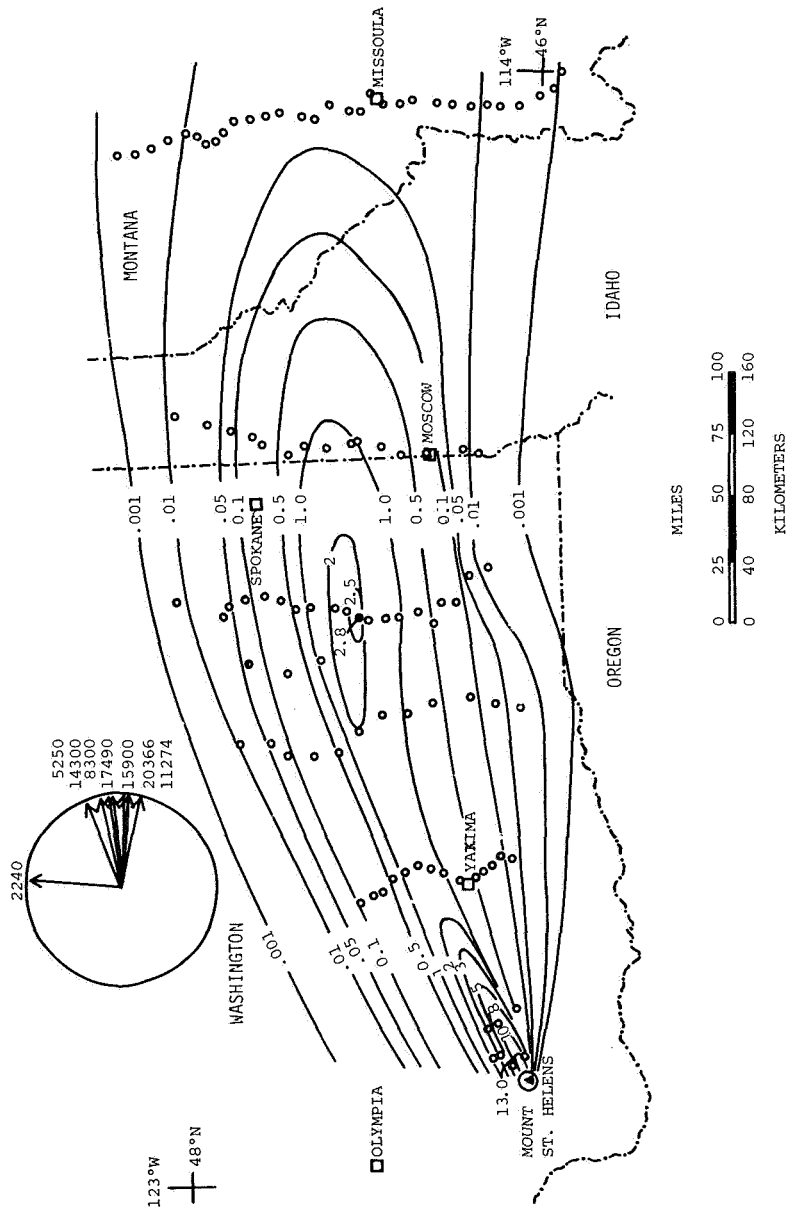


FIGURE 1.8. Isomass map of ash erupted from Mount St. Helens on 18 May 1980. Contours represent mass of ash per unit area, in g/cm^2 . Open circles represent observation stations. Samples of ash were collected from measured, essentially horizontal surfaces, oven dried at 60°C for 12 hours, and weighed. From Sarna-Wojcicki *et al.*, 1981a.

Other pyroclasts that accrete fine-grained tephra are the larger ($> 20 \mu\text{m}$) pumice fragments (Figure 1.9). Nearly all of these particles, with their complex surfaces and large surface areas, are at least partly (or, in some cases, completely) coated with $0.5 \mu\text{m}$ to $10 \mu\text{m}$ pyroclasts. The mechanism for cohesion of particles may be moisture or surface charges on the particles, or both. Whatever the mechanism, coalescence effectively removed some (unknown amount) of the finer-grained tephra produced in the eruption. Discussion of the accretion processes is given in Rose and Hoffman (1980). Similar agglomeration was reported for the Krakatoa ashes falling out as "clumps" at Jakarta. Also, ships in the Krakatoa dust experienced "St. Elmo's fire," a static electrical phenomena (Symons, 1888) that may reflect electrical charges on fine particles.

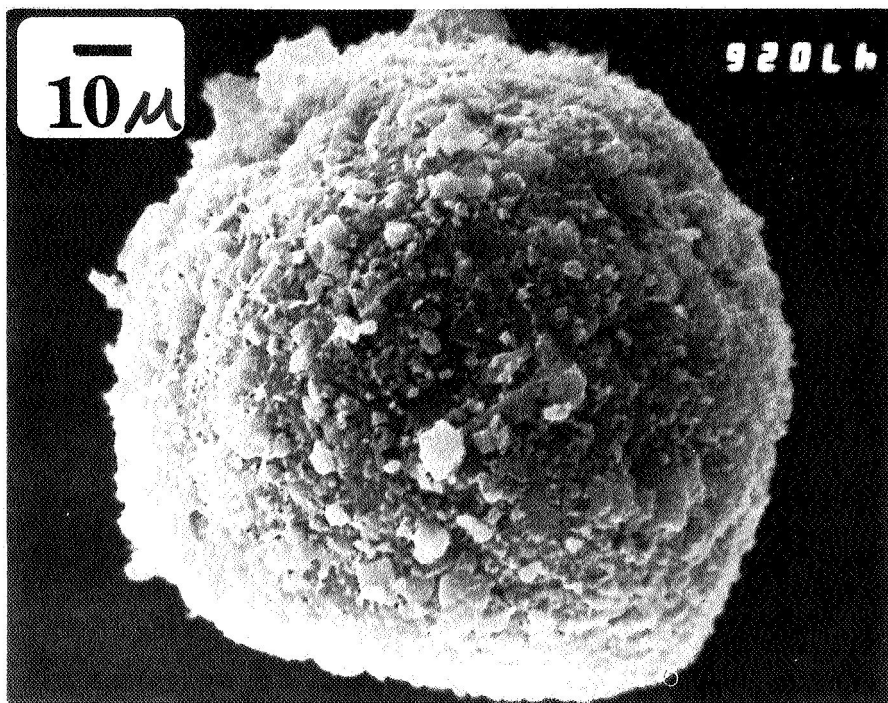


FIGURE 1.9. Electron micrograph of Mount St. Helens ash particle, either an aggregate of small particles or small particles adhering to a large spherical particle. This is from a lithic-rich ash which fell at Kennewick, Washington, on 18 May. Photo by T. Fillers and courtesy of D. Kreinsley and J. Marshall, Arizona State University.

1.3.9 Volume of Material Erupted

The volumes of various eruption units of the 18 May eruption are given in Table 1.8. The volume of rock missing from the cone is mostly accounted for by the massive debris flow which descended the North Fork of the Toutle River. Of the estimated total volume (minimum) for the 18 May eruption (0.3 km³ of dense rock), the airfall ash volume was equivalent to 0.2 to 0.25 km³ of dense rock; the airfall ash volume amount is important to the potential atmospheric effects of the eruption. However, because the eruption had such great dispersive power, the true volume of airfall ash probably exceeds this minimum which is the volume within the 2.5 mm isopach. A rough estimate of the volume of airfall ash, 0.48 km³ dense rock (Rose and Hoffman, 1980), is derived from the area-thickness relationships of the measured ash blanket.

1.3.10 An Estimate of the Mass of Small Silicate Particles Added to the Stratosphere

Fine ash particles (those less than 2 μm in diameter) have residence times in the atmosphere long enough for them to constitute an important addition to the atmosphere. It is therefore important to estimate the amounts of fine ash produced in the 18 May 1980 eruption. The overall proportion of fine particles in the most distal samples is about 1% to 2% (Fruchter et al., 1980; Rose and Hoffman, 1980). If we assume that 1% of the 0.48 km³ to be fine ash particles, then we calculate a volume of 0.0048 km³ or 1.2×10^{13} g. This figure represents the ash less than 2 μm in diameter which did fall out. The amount that remained in atmosphere is unknown.

1.4 VOLCANIC GASES

The plinian eruption column was the principal means for transporting particles and gases into the stratosphere during the 18 May 1980 eruption. The gases and nonsilicate aerosol particles contained in the plinian column have six possible sources:

1. tropospheric air entrained by the ascending column;
2. geothermal fluids near the magma body;
3. vaporization of ground water from melted snow, ice, and rain;
4. reaction of vegetation in a conifer forest with a cloud of hot ash and gas;
5. gases released explosively from the silicate liquid in the erupted magma; and
6. gases released explosively from the silicate liquid in the magma that was *not* erupted.

TABLE 1.8. *Volume Estimates of Eruptive Units of Mount St. Helens, 1980.*

Unit	Date	Dense rock volume km ³ ^a	Equivalent magma volume (dense rock), km ³
Debris flow	18 May	2.500 ^b	small
Surge deposit	18 May	0.190 ^c	0.048 ^c
Pyroclastic flow	18 May	0.060 ^d	0.060 ^d
Airfall	18 May	0.200 ^{ef}	0.160 ^f
		<i>Total 18 May</i>	0.268
<i>Missing volume of cone</i>	18 May	2.7-2.8	--
Airfall	25 May	0.007 ^f	0.007 ^f
Pyroclastic flow	25 May	0.001	0.001
Airfall	12 June	0.003	0.003
Pyroclastic flow	12 June	0.008	0.008
Dome	12 June	0.005	0.005
Airfall	22 July	0.004	0.004
Pyroclastic flow	22 July	0.001	0.001
Airfall	7 August	0.002	0.002
Pyroclastic flow	7 August	<0.001	<0.001
Dome	7 August	0.001	0.001
Airfall	16 October	0.004	0.004
Pyroclastic flow	16 October	0.001	0.001
Dome	16 October	0.002	0.002
		<i>Total post-May 18</i>	0.039

^aIncludes lithic material.^bK. M. Nolan, oral communication, 1980.^cJ. G. Moore, R. J. Janda, oral communication, 1981.^dP. W. Lipman, oral communication, 1980.^emin. volume (volume inside 0.25 cm isopach).^fA. M. Sarna-Wojcicki, oral communication, 1980.

1.4.1 Nonmagmatic Sources

The amount of tropospheric air entrained by the eruption column is not known at present. Wilson (1976) discussed the theory and observations concerning mixing of atmospheric air with plinian eruption columns. It may be possible to estimate the amounts of air (and, hence H₂O, CO₂, O₂, N₂, etc.)

entrained by the eruption column during the 18 May 1980 eruption. This is probably a significant source for H_2O , CO_2 , N_2 , O_2 and trace species (both natural and anthropogenic) found in the stratosphere following large plinian eruptions.

The phreatic eruptions at Mount St. Helens, which began 27 March 1980, probably involved interaction of nonmagmatic water (e.g., geothermal fluids, cold ground water) with the hot margins of a partly solidified magma body. The high temperatures of the geothermal fluids circulating near the magma body would have raised the solubilities of cations, such as Ca^{++} , Si^{+4} , K^+ , and of anions, such as Cl^- and $\text{SO}_4^{=}$, above those for cold ground water. A geothermal system at Mount St. Helens best explains the pre-May non-magmatic eruptions. The total volume of the geothermal system, the reservoir porosity, and the chemistry of the fluids are not known. Whether or not the fluids from such a geothermal reservoir contributed to the plinian column depends upon the location of the geothermal system with respect to the large region where massive slope failure occurred. Also, a geothermal system might make its greatest contribution of volatile substances to the plinian column in a period of time much shorter than the 8 hour duration of ash emission. The principal chemical contributions, if any, of geothermal fluids to the plinian column on 18 May 1980 are likely to have been H_2O , CO_2 , HCl , and reduced sulfur species (H_2S , H_2SO_4). This contribution is likely to be important in phreatic and phreatomagmatic eruptions, but of lesser significance for a purely magmatic eruption.

The volume of glacial ice and snow on Mount St. Helens decreased as a result of the 18 May eruption. Some of the ice may have been vaporized during the initial plinian eruption. The decrease in ice volume was about 0.1 km^3 (M. Brugman, oral communication). Although the distribution of glacial ice among the eruption products is not known, much ice was carried down the North Fork of the Toutle River in the debris flow--blocks more than 20 m in diameter were observed in the flow. Some ice may have been melted by the directed blast. The potential contribution of glacial ice to the eruption column is probably on the order of 0.005 to 0.02 km^3 of ice (density = 0.9 gm/cc)--5% to 20% of the total change in ice volume. The principal contribution to the column would have been H_2O vapor, with negligible amounts of CO_2 and other gases.

A forested area (500 km^2) within a 120° sector north of Mount St. Helens was devastated by the directed blast of the 18 May 1980 eruption. Some tree trunks within the devastated area show evidence of abrasion, drying of exposed wood surfaces, and possible distillation of volatiles. The thermal energy required could have been supplied by the large mass and moderate temperatures of the directed blast. The gas species distilled from the vegetation and the sizes of their potential contributions to the eruption column are not known. Reaction products would become mixed with the eruption column

through entrainment of air. Vegetation is probably a small source of materials injected into the stratosphere, but it may be an important source for some trace gases of otherwise unknown origin.

1.4.2 Magmatic Sources

It is widely agreed that the magma itself is a major source of gases and aerosols in the eruption column. The concentration and composition of gases dissolved in the magma just prior to eruption depend on the composition, confining pressure, temperature, and the amount of crystallization and vapor loss of the magma. The release of dissolved H_2O from magma at high pressure is believed to cause a rapid expansion in the volume and to be a major cause of explosive eruptions.

The amount and types of volatile species in a magma vary greatly as do magma types. In general, it may be that a basalt contains more S and less Cl than silicic magma, but this hypothesis has not yet been confirmed. Volatile contents of magmas must be inferred from microprobe analysis of glass inclusions trapped before eruption within crystalline phases because the majority of the glass erupted has lost most of its volatile content (Anderson, 1975). Comparison of the results of such tests show that the Mount St. Helens dacitic magma (Melson et al., 1980) contained less S and more Cl than the high-Al basalt of Fuego, in Guatemala, and was generally similar in composition to the dacitic magma of Augustine Volcano, in Alaska (Table 1.9).

1.4.3 Nature of the S Released from Magmas

Although studies of gas samples from basaltic volcanoes (Nordlie, 1971) have shown clearly that SO_2 is the dominant sulfur gas leaving mafic magmas, relatively little direct gas sampling at silicic volcanoes has been done. During the 18 May eruption aircraft sampling of the periphery of the plinian cloud showed that H_2S was the dominant sulfur species (Hobbs et al., 1981). Further gas samples taken on high temperature fumaroles of the lava dome at Mount St. Helens in September 1980 also were H_2S -rich (Casadevall and Greenland, 1981). These observations agree with thermodynamic calculations that show H_2S to be the dominant S species under the conditions of temperature and oxygen fugacity likely to prevail in a dacite magma (Gerlach, 1980). Thus H_2S is probably the main S gas leaving the Mount St. Helens dacite. Even so, this H_2S is apparently quickly oxidized by the atmosphere, especially when gas production rates are low and atmospheric mixing more efficient. Rapid oxidation explains both the high SO_2 emission rates measured in aircraft surveys (Casadevall et al., 1981) and the high SO_2/H_2S ratios measured at times of low level activity (Hobbs et al., 1981). The extent to which the (possible) phreatomagmatic component in 18 May eruption affected H_2S/SO_2 in the gaseous emissions is unknown, but possibly important.

TABLE 1.9. Concentrations of Volatiles in Glass Inclusions

	CO ₂ (ppm)	S (ppm)	Cl (ppm)	H ₂ O (wt. %)
<i>Kilauea basalt^a</i> (Harris, 1979a)	500 ± 200	1300	150	0.21 ± 0.04
<i>Fuego, 1974,^a</i> <i>High-Al basalt</i> (Harris, 1979b)	1300 ± 400	2500	820	1.60 ± 0.30
<i>Augustine, 1976^b</i> <i>dacite</i> (Johnston, 1978)	unknown	100- 500	3000- 6000	6.60 ± 1.50
<i>Mount St. Helens</i> (Melson et al., 1980)	unknown	<500	1000	5

^aH₂O and CO₂ values obtained by vacuum heating stage/gas analyzer; S and Cl by electron microprobe.

^bS and Cl values obtained by electron microprobe; H₂O estimated by electron microprobe analysis by difference.

1.4.4 Minimum S, Cl and H₂O Contribution of Mount St. Helens Eruption

The minimum volume of magma produced in the Mount St. Helens eruption and the pre-eruption volatile content can be used to calculate the mass of volatiles added to the atmosphere (Table 1.10). These calculations do not include the contribution of meteoric water in H₂O estimates and they do not consider scavenging of H₂O by ash. Cl estimates are poor because much or nearly all of the Cl is not degassed, but remains dissolved in the silicate glass. Also, the erupted ash contains water-soluble Cl that was scavenged from the eruption cloud during fallout of ash particles. S estimates also neglect scavenging; the degassing efficiency and the initial magmatic S content are not well-constrained. Nonetheless the estimates represent the best ones that are possible at the present time. The estimates reflect only contributions from magma that was erupted. Since the sulfur present as sulfate on ash surfaces is 100 to 2000 ppm (Taylor and Lichte, 1980; Rose and Hoffman, 1980), it is difficult to reconcile the estimates without contribution of S (and presumably Cl and H₂O) from magma in excess of the amounts that were erupted. Further studies of the Mount St. Helens tephra will consider these problems, and will undoubtedly produce better estimates.

TABLE 1.10. Estimate of Volatiles Released by the 18 May 1980 Eruption of Mount St. Helens.

Mass of magma erupted at Mount St. Helens (Table 1.8):	
18 May volume ^a	0.3 km ³
post-18 May volume	0.03 km ³
Total	0.33 km ³
Initial content ^b	
S	<500 ppm
Cl	1000 ppm
H ₂ O	5 wt. %
Minimum volatiles erupted:	
S	(0.33 km ³) (250 ppm) (2.4 g/cc) x 10 ¹⁵ = 2 x 10 ¹¹ g
Cl	(0.33 km ³) (1000 ppm) (2.4 g/cc) x 10 ¹⁵ = 0.8 x 10 ¹² g
H ₂ O	(0.33 km ³) (5%) (2.4 g/cc) x 10 ¹¹ = 4 x 10 ¹⁴ g

These values assume: (a) no meteoric, hydrothermal, or atmospheric water, (b) no scavenging, (c) complete degassing, and (d) no contribution from intrusive magma. Estimates of atmospheric impact will have to consider and evaluate these factors.

^aValue is uncertain, between 0.2 and 0.5 km³.

^bValues based on data of Melson et al. (1980). Note particularly the uncertainty for S.

These minimum erupted values can be compared to similarly obtained values for the Fuego 1974 eruption. These were 1.6 x 10¹² g S, 6 x 10¹¹ g Cl, and 9 x 10¹² g H₂O (Rose et al., 1981; Murrow et al., 1980). The Fuego eruption was considerably smaller in magma volume (~ 1/3) than the Mount St. Helens eruption. Evidence of participation of intrusive (but noneruptive) magma in the Fuego eruption was discussed by Rose et al. (1981).

1.4.5 Passive Emissions at Mount St. Helens Before and After 18 May

Measurements of passive gas emission rates of SO₂ were obtained by correlation spectrometer several times between 29 March and 14 May. These ranged from 10 to 50 tonnes/day. From 25 May to 10 October, the SO₂ emission rates changed from a low of 130 tonnes/day to a high of 3,400 tonnes/day. The total amount of SO₂ emitted during the noneruptive periods from 5 June to 10 October was 150,000 tonnes (Casadevall et al., 1981).

CO₂ emission from 6 July to 30 October, measured by infrared spectrometry ranged from a minimum of 2,000 tonnes/day to a maximum of

22,000 tonnes/day. The total amount of CO₂ emitted to the atmosphere during noneruptive periods from 5 July to 30 October was 9.1×10^{11} g (Harris et al., 1981b).

These gas emission data suggest that a large shallow magma body (comparable in size to the 18 May magma body) still exists below Mount St. Helens. Gas emissions during the small eruptions after 18 May are probably less than 20% of the amounts emitted passively through 30 October 1980.

1.5 A COMPARISON OF THE 18 MAY MOUNT ST. HELENS ERUPTION WITH OTHER EXPLOSIVE ERUPTIONS

1.5.1 Introduction

Eruptions can be compared with respect to characteristics of the eruption itself, their effects on the surrounding area, or their deposits (Table 1.11). Such comparison shows that the 18 May eruption was, in general, a modest one, but that its eruption column was uncommonly large. Other features of the eruption, which will be clearer after the comparison parameters are individually discussed, are quite distinctive.

1.5.2 Magnitude and Volume

Estimates of the volume of the airfall deposit from the 18 May eruption range from 0.16 to 0.48 km³ (see section on volume above). This is a modest volume as can be seen by reference to Table 1.12. However, as will be shown later, the deposit as a whole might be unusually fine-grained and a large proportion of this volume may have remained in the upper tropopause and lower stratosphere, where it was rapidly transported downwind at the 12 km altitude range. Tsuya (1955) used the volume erupted to compare the magnitude of eruptions: his logarithmic scale of 1 to 10 is based on an exponential (base 10) increase in volume. Hence, Mount St. Helens is 6 on Tsuya's scale (6 = 0.1 to 1.0 km³).

1.5.3 Intensity

The intensity of an eruption can be defined as the rate of release of thermal energy, which is related to the flux of magma and, because the eruption column is largely a convective phenomenon, to the column height. The relation between these three characteristics allows one to be inferred from another. Applying the formulae of Wilson et al. (1978), the maximum column height of 23 to 27 km, maintained less than 15 minutes on 18 May, indicates a maximum extrusion rate of 2.0×10^4 m³/s (Table 1.2). The average column height of 18 km, maintained for more than 8 hours, indicates an extrusion rate of 1.0×10^4 m³/s. An independent check on this figure can be gained by taking the airfall

TABLE 1.11. Comparison of the 18 May 1980 Eruption of Mount St. Helens with Other Eruptions.

	Mount St. Helens	Worldwide maximum past 250 years	Worldwide maximum all time
<i>Total magma volume erupted, (expressed as km³ of dense rock)</i>	0.5	75	>1000
<i>Eruption magnitude^a</i>	6	9	10
<i>Eruption column height, (km above volcano)</i>	23-27 maximum	18 average	28-35 ^d
<i>Duration of climax of eruption (hrs)</i>	9	38	48
<i>Volcanic explosivity index (VEI)^b</i>	5	7	8
<i>Area covered by isopach enclosing half volume of deposit (km²)</i>	1×10^5	6×10^4	10^6
<i>Area of complete devastation (km²)</i>	500	1000	5×10^4 ^c

^aTsuya (1955).

^bNewhall and Self (1982).

^cWalker (1980).

^d>40 km supposedly reached by Krakatoa, 1883, and Bezymianny, 1956; both inadequately substantiated.

TABLE 1.12. Volumes of Some Recent Airfall Deposits Given as Minimum and Maximum Estimates.

Volcanic eruption	Volume (km ³ of dense rock)
Mount St. Helens, 1980	0.2 - 0.48
Fuego, 1974	0.1
Agung, 1963	0.6 - 1.2 (March and May events)
Bezymianny, 1956	0.5 - 2.0
Hekla, 1947	0.3
Santa Maria, 1902	4 - 9
Krakatoa, 1883	5 - 10
Tambora, 1815	30 (very approximate)
Taupo, 160 AD	6 - 10

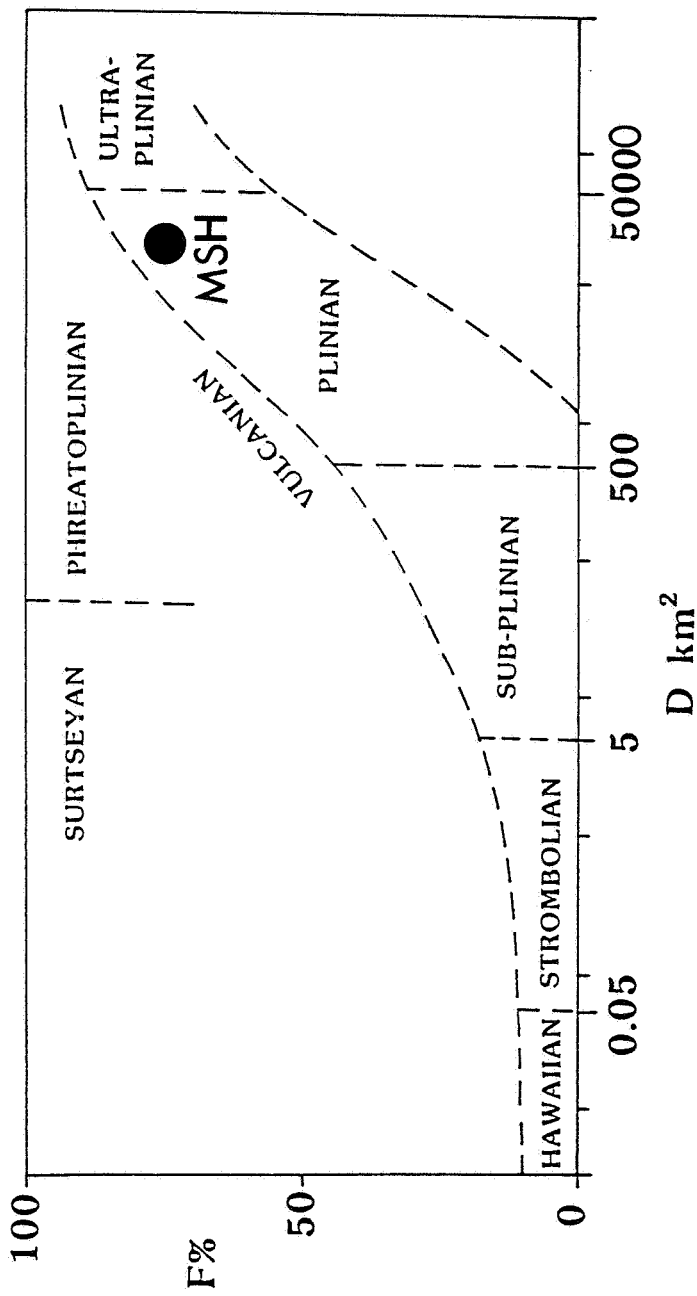


FIGURE 1.10. Plot of fragmentation index F (= wt % finer than 1 mm where 0.1 T max isopach crosses dispersal axis) against dispersal index D (= area enclosed by 0.01 T max isopach) for fall deposits. T max is the maximum thickness. Modified from Walker (1973), with revisions by Self and Sparks (1978) and Walker (1980). MSH is the region in which the 18 May airfall deposit boundaries are gradational.

deposit volume of 0.48 km^3 and dividing it by the duration of 9 hours: this gives $1.48 \times 10^4 \text{ m}^3/\text{s}$. Considering the variability of methods involved, these are in reasonable agreement. To put these rates in perspective, extrusion rates for other plinian eruptions are indicated in Table 1.13. It can be seen that extrusion rates vary from 10^3 to $10^6 \text{ m}^3/\text{s}$, although many plinian eruptions have peak extrusion rates of the order of $10^4 \text{ m}^3/\text{s}$. This represents mass rates of $2.6 \times 10^7 \text{ kg/s}$ to $2.6 \times 10^8 \text{ kg/s}$. The Mount St. Helens event is of moderate intensity ($2 \times 10^4 \text{ m}^3/\text{s}$) for a plinian eruption.

TABLE 1.13. *Eruption Rates and Column Heights of Some Recent Eruptions, Data from Self et al. (1981).*

Eruption	Maximum volume flux rate (m^3/s dense rock)	Maximum column height (km) above volcano ^a
Mount St. Helens, 1980	2×10^4	22 (o)
Hekla, 1947	2×10^4	24 (o), 21(c)
Agung, 1963	3×10^4	23(c)
Bezymianny, 1956	2×10^5	45(o), 42(c)
Santa Maria, 1902	4×10^4	34(c), 29(o)
Hekla, 1970	6×10^3	16(o), 15(c)
Ngauruhoe, 1975 ^b	2×10^3	10(o), 10(c)
Taupo, 160 AD	1×10^6	>50(c)

^ao = observed, c = calculated.

^bA vulcanian (less intense than plinian) eruption.

1.5.4 Dispersive Power

The dispersive power of an eruption, defined on the basis of a dispersal index (D) of the deposit (Walker, 1973), depends on the column height, the grain size and density of the ejecta (which control the terminal fall velocity), and the energy of the dispersing agent, generally wind. The dispersal index of a deposit is the area within the isopach 0.01 times the thickness of the deposit at its source (T max). Plotted against the fragmentation index (F), the weight percent of grains smaller than 1 mm in diameter where the dispersal axis crosses the isopach $0.1 \times T \text{ max}$, the dispersal index can be used to distinguish "fields" typical of specific types of eruptions (Fig. 1.10; Walker, 1973). Plinian eruptions are among the most widely dispersed; very widely dispersed, very fine-grained plinian deposits are called phreatoplhinian (Self and Sparks, 1978; Walker, 1980).

The Mount St. Helens deposit from the 18 May eruption, with $D = 23,000 \text{ km}^2$ ($T \text{ max} = 50 \text{ cm}$) and $F = 75\%$ falls within the plinian field of Walker (1973, 1980), near the ultraplhinian field (Fig. 1.10). Although

moderate compared to some eruptions, the dispersive power of the 18 May eruption was very high compared to historic eruptions. The dispersion of an airfall deposit is a useful guide to the atmospheric effects of the eruption because D is generally proportional to column height.

The 18 May airfall deposit also has an uncommonly high fragmentation index. The observed grain size of the deposit may reflect, in part, the opportunity to sample fine distal deposits before they were eroded; recent studies have shown that certain plinian deposits had a larger fine-grained component than previously realized, a component that fell far from the volcano (Walker, 1980). Even allowing for observational bias, however, the Mount St. Helens ashes seem extraordinarily fine-grained; the high fragmentation may reflect the postulated phreatomagmatic character of the eruption during (at least) the first hour or so. Phreatomagmatic eruptions are characterized by very-fine grain size (Self and Sparks, 1978).

1.5.5 Violence or Destructive Potential

The violence of an eruption is hard to estimate and perhaps of least importance to atmospheric studies. It can be quantitatively estimated as the rate of release of kinetic energy. The total kinetic energy for the initial blast of the 18 May eruption of Mount St. Helens using 100 m/s as the muzzle velocity (approximately 1/3 of the speed of sound in air at the altitude of Mount St. Helens) was about 5×10^{22} ergs. The kinetic energy per unit mass has been assumed by Kieffer (1980) to be 10^8 ergs/g. An energy budget for the 1974 Fuego eruption (Harris, 1981) suggests that the kinetic energy per unit mass was about $3.2-7.3 \times 10^8$ ergs/g. Many eruptions have estimated instantaneous releases of 10^{22} to 10^{24} ergs, but most of these estimates are imprecise.

Perhaps a better way to measure the violence of an eruption is by its destructiveness, or the area laid waste by the eruption. The totally devastated blast area totals 500 km²; the large area covered by the airfall deposit cannot be considered devastated. Devastation generally depends on the type of eruption: The Mount St. Helens plinian eruption was preceded by the horizontally-directed blast (a pyroclastic surge possibly driven by a phreatomagmatic explosion), which has seldom been recorded in historic eruptions or recognized in deposits from plinian eruptions. Hence, the violence of the Mount St. Helens eruption was apparently large compared to estimates inferred from deposits from other plinian eruptions. However, compared to ignimbrite-producing eruptions that cover areas of several thousands of km² with ash to depths of many tens of meters deep, a devastated area of 500 km² is small (Table 1.11).

1.5.6 Possible Characteristics of the Mount St. Helens Eruption

The importance of phreatomagmatic activity to the 18 May eruption is controversial and we disagree in our opinions of it. Most geologists agree that, whatever the extent of the phreatomagmatic component, it was most significant in the early stages of the eruption and declined thereafter. The post-18 May activity has been nearly completely magmatic.

Most of us believe that phreatomagmatism played a significant role in the 18 May eruption for a number of reasons:

1. Fine grain size ash is typical for phreatoplhinian ashes (Self and Sparks, 1978).
2. Phreatic activity before the eruption demonstrated the existence of an active hydrothermal system.
3. The abundance of lithic material in the lower layers of the fall deposit would be expected in a phreatomagmatic eruption.
4. The dispersive power and extensive surge of the eruption are characteristic of phreatomagmatic eruptions and, at least to some degree, anomalous in plinian eruptions.
5. The long repose period between eruptions and the high rainfall in the Cascades would encourage saturation of the hydrothermal system.
6. Accretionary lapilli in the ejecta record the presence of water in the eruption cloud.

If the eruption was phreatomagmatic, certain characteristics of its deposits and interaction with the atmosphere may be atypical for a plinian eruption. For example, it might contribute larger than usual concentrations of reduced gases, H_2O and possibly H_2SO_4 , to the atmosphere. Also, the abundance of H_2O in a phreatomagmatic eruption cloud might facilitate removal of fine ash from the cloud, so less fine ash would be suspended in the atmosphere than in other plinian eruptions. None of the evidence for the phreatomagmatic character of the 18 May eruption is conclusive; we mention it because of its possible atmospheric effects.

1.6 CONCLUSIONS

1. The volume of magma erupted at Mount St. Helens on 18 May is equivalent to 0.3 to 0.6 km^3 of dense dacite; 0.2 to 0.5 km^3 is related to the plinian phase of eruption—the part with most atmospheric relevance. Uncertainty in the volume estimate is due to the violence of the eruption, because a large fraction of the ash fell so far away from its source. Eruptions of comparable volume occur on average once every 8 to 10 years.

2. The ash is very fine-grained. A great majority of the mass is made up of $< 200 \mu m$ diameter particles. About 1% of the mass is $< 2 \mu m$. In spite of the fine grain size, however, the ash seemed to be removed from the air quickly; even the finest ash began falling out within a few hours.

3. More than 2×10^{11} g of S was erupted on 18 May. This is a poor estimate for atmospheric purposes because it is not known how much was released to the atmosphere, how much was removed from the ash fall, and how much additional S was contributed by intrusive (nonerupted) magma. The S mass is low, partly because the magma is S-poor. This shows that explosivity *alone* is a poor criterion for judging the atmospheric impact of an eruption.

4. The 18 May eruption may have had an unusually important phreatomagmatic component for a plinian eruption. This conclusion is not definite, but if a phreatomagmatic component was significant it may have had important chemical and physical effects on the atmosphere.

1.7 REFERENCES

Anderson, A. T., 1975: Some basaltic and andesitic gases. *Reviews of Geophysics and Space Physics*, 13, 37-55.

Ames, L. L., 1980: Preliminary mineralogical investigation of collected ash samples from the May 18, 1980, Mount St. Helens eruption. Report for Rockwell Hanford Operations, August 1980 (Richland, Washington). [Unpublished.]

Casadevall, T. J., and L. P. Greenland, 1981: The Chemistry of gases from Mount St. Helens. *US Geol. Surv. Prof. Paper 1250*, Washington, DC.

Casadevall, T. J., D. A. Johnston, D. M. Harris, W. I. Rose, Jr., L. L. Malinconico, R. E. Stoiber, T. J. Bornhorst, and S. N. Williams, 1981: SO₂ emission rates at Mount St. Helens, March 29-November 1, 1980. *US Geol. Survey Prof. Paper 1250*, Washington, DC.

Christianson, R. L., 1980: Eruption of Mount St. Helens: Volcanology. *Nature*, 285, 531-533.

Crandell, D. R., and D. R. Mullineaux, 1978: Potential hazards from future eruptions of Mount St. Helens volcano, Washington. *US Geol. Survey Bull. 1381-C*, Washington, DC, 26 p.

Crandell, D. R., D. R. Mullineaux, and M. Rubin, 1975: Mount St. Helens volcano: Recent and future behavior. *Science*, 187, 438-441.

Fruchter, J. S., et al., 1980: Mount St. Helens ash from the 18 May 1980 eruption: Chemical, physical, mineralogical, and biological properties. *Science*, 209, 1116-1125.

Gerlach, T. M., 1980: Chemical characteristics of the volcanic gases from Nyiragongo. *J. Volcanol. Geoth. Res.*, 8, 177-190.

Gorshkov, G. S., 1961: Gigantic eruption of the volcano Bezymianny. *Bull. Volc.*, 25, 77-108.

Harris, D. M., 1979a: Geobarometry and geothermometry of individual crystals using H₂O, CO₂, S and major element concentrations in silicate melt inclusions: The 1959 eruption of Kilauea, Hawaii. *GSA Abst. with Prog.*, 11, 439.

Harris, D. M., 1979b: Pre-eruption variations of H₂O, S, and Cl in a subduction zone basalt. *Trans. A.G.U.*, **60**, 968.

Harris, D. M., 1981: The concentrations of H₂O, CO₂, S and Cl during pre-eruption crystallization of some mantle derived magmas: Implications for magma genesis and eruption mechanisms, Ph.D. thesis, University of Chicago, University Microfiche, Ann Arbor, Michigan, 235 pp.

Harris, D. M., W. I. Rose, Jr., R. Roe, and M. L. Thompson, 1981a: Radar observations of ash eruptions at Mount St. Helens, Washington. *US Geol. Surv. Prof. Paper 1250*, Washington, DC.

Harris, D. M., M. Sato, T. J. Casadevall, W. I. Rose, Jr., and T. J. Bornhorst, 1981b: Emission rates of CO₂, *US Geol. Surv. Prof. Paper 1250*, Washington, DC.

Harris, S. L., 1976: *Fire and Ice: The Cascade Volcanoes*. Pacific Search Press Seattle, Washington, 320 pp.

Hobbs, P. V., L. F. Radke, M. W. Eltgroth, and D. A. Hegg, 1981: Airborne studies of the emissions from the volcanic eruptions of Mount St. Helens. *Science*, **211**, 816-818.

Hooper, P. R., I. W. Herrick, E. R. Laskowski, and C. R. Knowles, 1980: Composition of the Mount St. Helens ashfall in the Moscow-Pullman area on 18 May 1980. *Science*, **209**, 1125-1126.

Johnston, D. A., 1978: Volatiles, magma mixing and the mechanism of eruption at Augustine volcano, Alaska. Ph.D. Dissertation, University of Washington, 177 p., University Microfiche, Ann Arbor, Michigan.

Kieffer, S. W., 1980: The May 18 lateral "blast" of Mt. St. Helens: Preliminary mapping of effects of the devastated area and a model for multiphase fluid flow. *EOS*, **61**, 1135.

Larrson, W., 1937: Vulkanische Asche von Ausbruch de chilenisen Vulkans Quizapu (1932) in Argentian gessmelt. *Uppsala Bull. Geol. Inst.* **26**, 27-52.

Lipman, P. W., and D. R. Mullineaux, eds., 1981: The 1980 eruptions of Mount St. Helens, Washington. *US Geol. Surv. Prof. Paper 1250*, Washington, DC.

Melson, W. G., C. A. Hopson, and C. F. Kienle, 1980: Petrology of tephra from the 1980 eruption of Mount St. Helens (abs.). *Geol. Soc. Amer. Abst. with Prog.*, **12**, 482.

Murrow, P. J., W. I. Rose, and S. Self, 1980: Total grain size distribution in a vulcanian eruption column and its implications to stratospheric aerosol perturbation. *Geophysical Res. Lett.*, **7**, 893-896.

Newhall, C. G., and S. Self, 1982: The volcanic explosivity index (VEI): An estimate of explosive magnitude of historic eruptions. *J. Geol. Res.*, **87**, 1231-1238.

Nordlie, B. E., 1971: The composition of the magmatic gas of Kilauea and its behavior in the near surface environment. *Amer. Jour. Sci.*, **271**, 417-463.

Rose, W. I., R. E. Stoiber, and L. L. Malinconico, 1981: Eruptive gas compositions and fluxes of explosive volcanoes: Problems, techniques and initial data. In *Orogenic Andesites and Related Rocks*, R. S. Thorpe (ed.). Wiley and Sons, New York.

Rose, W. I., Jr., and M. F. Hoffman, 1980: The May 18, 1980 eruption of Mount St. Helens: The nature of the eruption with an atmospheric perspective. Paper presented at NASA Workshop on Mount St. Helens Eruption: Its Atmospheric Effects and Potential Climatic Impact (Washington, D.C.), November 18-19.

Rosenbaum, J. G., and R. B. Waitt, 1981: Eyewitness accounts of the May 18, 1980, eruption of Mount St. Helens. *US Geol. Surv. Prof. Paper 1250*, Washington, DC.

Sarna-Wojcicki, A. M., S. Shipley, R. B. Waitt, D. Dzurisin, W. H. Hays, J. O. Davis, S. H. Wood, and T. Bateridge, 1980: Area distribution, thickness, and volume of downwind ash from the May 18, 1980, eruption of Mount St. Helens. *US Geol. Surv. Open-File Rpt. No. 80-1078*, Washington, DC.

Sarna-Wojcicki, A. M., and R. B. Waitt, 1980: Area distribution, thickness and composition of volcanic ash erupted from Mount St. Helens on May 18, 1980. *Geol. Soc. Amer. Abst. with Programs*, 12, 515.

Sarna-Wojcicki, A. M., S. Shipley, R. B. Waitt, Jr., D. Dzurisin and S. H. Wood, 1981a: Aerial distribution, thickness, mass, volume and grain size of airfall ash from the six major eruptions of 1980. *US Geol. Surv. Prof. Paper 1250*, Washington, DC.

Sarna-Wojcicki, A. M., C. E. Meyer, M. J. Woodward and P. J. Lamothe, 1981b: Composition of air-fall ash erupted on May 18, May 25, June 12, July 22 and August 7. *US Geol. Surv. Prof. Paper 1250*, Washington, DC.

Self, S., and R. S. J. Sparks, 1978: Characteristics of widespread pyroclastic deposits formed by the interaction of silicic magma and water. *Bull. Volcanologique*, 41, 1-7.

Self, S., M. R. Rampino, and J. J. Barbera, 1981: The possible effects of large nineteenth and twentieth century volcanic eruptions on zonal and hemispheric surface temperatures. *J. Volcanology and Geothermal Research*, 11, 41-60.

Symons, G. J., 1888: The eruption of Krakatoa and subsequent phenomena. Report of the Krakatoa Committee of the Royal Society London, 494 p.

Taylor, G. A., 1958: The 1951 eruption of Mt. Lamington, Papua, Australia. *Dep. Nat. Dev. Bur. Min. Res. Bull.*, 38, 117 p.

Taylor, H. E., and F. E. Lichte, 1980: Chemical composition of Mount St. Helens volcanic ash. *Geophys. Res. Lett.*, 7, 949-952.

Tsuya, H., 1955: Geological and petrological studies of Volcano Fuji: Vol. 5 of the 1707 eruption of Volcano Fuji. *Bull. Earthquake Res. Int.*, 33, 341-383.

Waitt, R. B., and Dzurisin, D., 1981: Proximal airfall deposits from 18 May 1980 eruption. *US Geol. Surv. Prof. Paper 1250*, Washington, DC.

Walker, G. P. L., 1971: Grain size characteristics of pyroclastic deposits. *J. Geol.*, 79, 696-714.

Walker, G. P. L., 1973: Explosive volcanic eruptions: A new classification scheme. *Geol. Rund.*, 62, 431-446.

Walker, G. P. L., 1980: The Taupo pumice: Product of the most powerful known (ultraplinian) eruption. *J. Volcanol. Geothermal Res.*, 8, 69-94.

Wilson, L., 1976: Explosive volcanic eruptions: III. Plinian eruption columns. *Geophys. J. Royal. Astr. Soc.*, 45, 543-556.

Wilson, L., R. S. J. Sparks, T. C. Huang, and N. D. Watkins, 1978: The control of volcanic column heights by eruption energetics and dynamics. *J. Geophys. Res.*, 83, 1829-1836.

Wozniak, K. C., S. S. Hughes, and E. M. Taylor, 1980: Unpublished chemical analyses (June 4, 1980). Personal communication, Oregon State University.

CHAPTER 2

TRANSPORT AND DISPERSION

2.1 INTRODUCTION

On Sunday morning, 18 May, a weak, upper level trough was moving eastward over the Washington coast. Cirrus clouds in advance of the trough were passing over Mount St. Helens when the major eruption began. The eruption cloud penetrated this layer of cirrus clouds, forming a massive anvil in the stratosphere whose evolution could be observed and studied by both visible and infrared photographs from geosynchronous (GOES) and orbiting (TIROS) satellites. The eruption continued with varying intensity for approximately 8 hours (1532 to 2330 UT) and subsided just as the trough and the clear sky to its west were approaching the volcano. The presence of the natural cirrus cloud offers possible confusion for determining the boundaries of the eruption cloud, but it also provides a reference level for height and temperature determination.

2.2 OBSERVATIONS AND RESULTS

It is fortunate that there is a very representative rawinsonde observation to specify the environmental temperature, moisture, and wind velocity profiles for the erupting cloud which allows interpretation of the unique satellite observations. These profiles, measured at Salem, Oregon, upwind from the volcano approximately 3 hours prior to the initial eruption, are shown in Fig. 2.1. Temperatures decrease quasilinearly in the troposphere to a sharp minimum of -63.5°C at the tropopause (194 mb or 12 km). The cirrus clouds are colder than -25°C and probably extend to the tropopause. The absence of stable layers in the troposphere and the near-normal tropopause height for this latitude and season indicate that the eruption plume would not encounter significant buoyant resistance to its upward progress until it passed the 12 km level.

On the basis of independent measurements, both direct and remote, it is known that the eruption cloud penetrated another 9 to 10 km into the stratosphere, where the increased resistance produced a massive anvil > 80 km in diameter. The wind profiles, at the right in Fig. 2.1 imply that this tall eruption cloud would be increasingly distorted by the environmental wind shears, the midlevels of the cloud moving eastward much more rapidly than the upper and

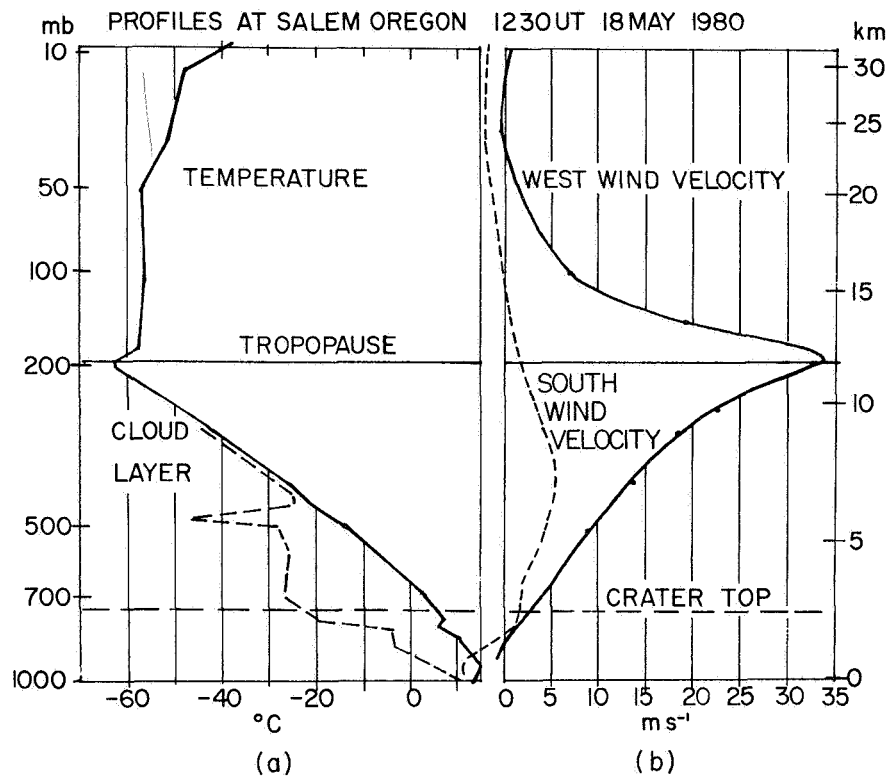


FIGURE 2.1. Profiles measured at Salem, Oregon, 1230 UT, 18 May 1980. (a) Temperature and dew point (dashed) profiles. (b) West wind and south wind (dashed) velocity profiles.

lower portions. In particular, the stratospheric portion would rotate toward the horizontal and be drawn out into a thinner and thinner lamina, as shown schematically in Fig. 2.2(a).

This conversion of a vertical cloud to a thin inclined lamina is extremely important to an understanding of the subsequent transport and dispersion of the cloud. Furthermore, when viewed from the satellite, this conversion process is not at all obvious. Instead, one has the impression of an expanding conical plume from a large smoke stack. However, when the plume is viewed in the infrared (enhanced to reveal the temperature structure), there is evidence that the coldest temperatures, highest elevations of the cloud, are lagging well behind the leading edge of the plume [see Fig. 2.2(b)].

The curvature of the plume over southwestern Montana implies that the leading edge has passed a ridge in the flow. This implication is confirmed by the standard, constant pressure, meteorological analysis and by specially prepared constant-entropy analyses (see Fig. 2.3). The latter charts, which permit a reasonable resolution of the three-dimensional trajectories, indicate that the air descends after passing the ridge. Compressional warming during descent would then evaporate the ice crystals in the cloud and leave only the volcanic ash to be detected by the satellite. In fact, this change in opacity is confirmed by the photographs. The plume appears to change from a solid grey tone to a wispy veil.

Although the descent is not large, from 200 mb to the 260 mb level, compressional warming of $\sim 18^\circ\text{C}$ is more than that required to evaporate the cloud's ice crystals and/or water droplets. With the rapid decrease in opacity, the thin lamina that represents the eruption plume becomes increasingly difficult to detect. However, video tapes or film loops, where time continuity can be followed, permit further detectability. In general, the movements are consistent with those derived from meteorological analyses.

Although the satellite photographs are excellent for studying the lower stratospheric and upper tropospheric portions of the eruption plume, the more attenuated, higher stratospheric portions cannot be resolved. To study these higher portions it is necessary to compute trajectories. Due to the much slower speeds (see Fig. 2.1) at 100, 70, and 50 mb, which imply weak pressure patterns, the uncertainty in computed trajectories increases and the results are more dependent on the trajectory computational method. For example, use of predicted rather than observed pressure fields and of geostrophic rather than ageostrophic winds tends to underestimate negative curvatures and anticyclonic loops in the trajectories and, therefore, to underestimate dispersion. For a review of trajectory methods plus a discussion of their probable errors, see Daniels (1974).

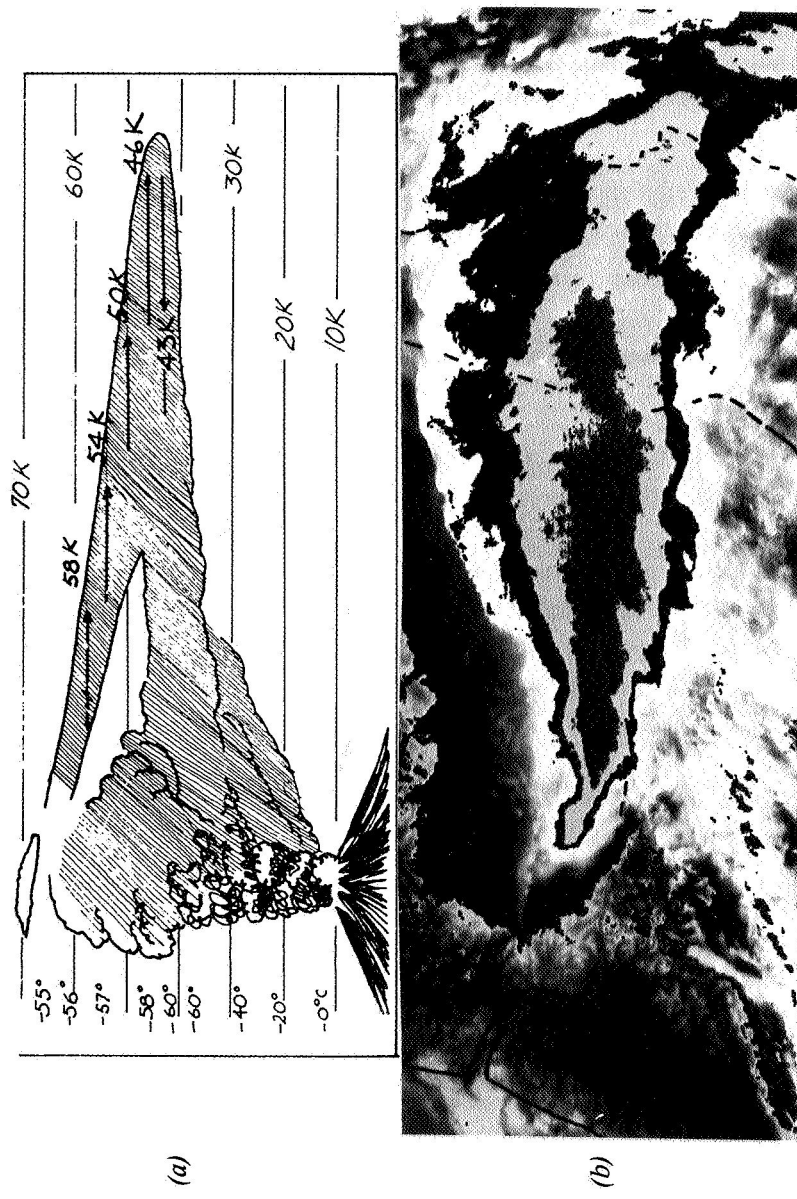


FIGURE 2.2. (a) Schematic cross section of plume distortion caused by wind shears. Heights are expressed in thousands of feet for convenience of pilot. (b) Enhanced infrared photograph from the TIROS satellite taken at 0238 UT, 18 May 1980.

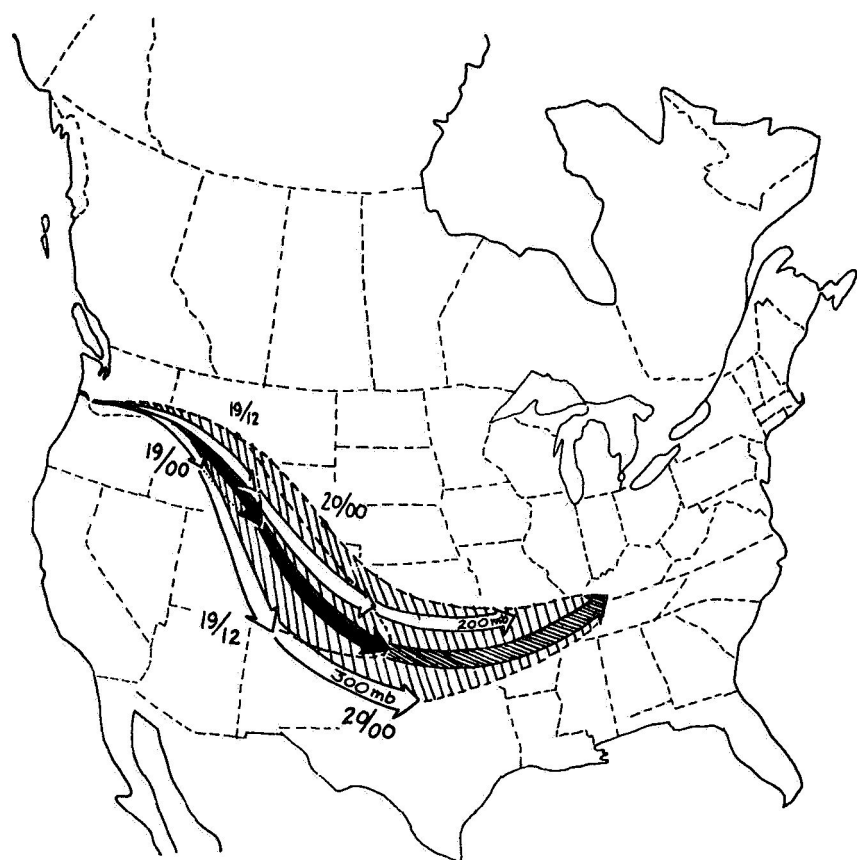


FIGURE 2.3. Trajectories of 18 May 1980 eruption for the 300-mb and 200-mb levels, plus black arrow depicting path of isentropic trajectory starting at 200 mb. Days and hours, in Universal Time, are appended.

As shown in Fig. 2.4, the trajectories from the eruption of 18 May meander, loop and diverge in a diffusive manner. Where the trajectories diverge, a small error in the analyzed gradients or in position can lead to dissimilar trajectories. This result is interesting because it implies considerable meridional diffusion with light winds. Conversely, where the winds and patterns are strong, as in a jet stream, the uncertainty and sensitivity of the computed trajectories to different methods is reduced. Furthermore, since convergence normal to a jet is required to maintain it against small-scale diffusion, this convergence counteracts the lateral spreading of a trace substance. Therefore, in the lower stratosphere the diffusion is predominantly zonal rather than meridional.

In either case, inhomogeneities in the debris from a volcano, or other discrete sources, tend to be maintained much longer than generally perceived. Trajectory analyses suggest that debris from the 18 May eruption maintains horizontal structure and remains thin vertically for periods of 5 to 6 months before it begins to smooth out zonally and vertically. Similar periods are implied by lidar and SAGE satellite measurements.

The extremely thin layers or laminar structure of the Mount St. Helens debris confirmed by lidar and aircraft observations is caused, of course, by the vertical shear of the horizontal wind. The lower stratospheric (12 to 15 km) debris being advected eastward, at the jet level, circles the earth in an undulating manner every 15 to 16 days, at an average zonal speed of approximately 25 m s^{-1} (see Fig. 2.5). The upper stratospheric debris (18 to 23 km) slowly drifts westward and spreads meridionally in the nonsteady transition region to the summer easterlies.

The proponents of one- and two-dimensional models are cautioned to consider a time lag of ~ 0.5 years before attempting simulations that require smooth Gaussian distributions for the computations.

This discussion applies to volcanic emissions of gases and of those particles small enough to remain suspended by the small-scale turbulent motions. To a first approximation they act as passive constituents and are transported by the three-dimensional motions of the air. Of course, they are not completely passive; by absorbing and emitting radiation, they are thermodynamically active, but their effects oscillate diurnally, accumulate slowly, and can be ignored for periods of several weeks.

The situation is very different and much more complicated for the entire range of larger particles—those whose terminal velocities preclude suspension and exert a significant drag force on the air. Spatial inhomogeneities in the magnitude of this drag force initiate convection, that is, negative vertical velocities.

Descending air warms by compression and develops a positive buoyancy to act against the drag force. However, if the ash cloud also contains ice crystals or water drops, as did the Mount St. Helens eruption cloud, much of

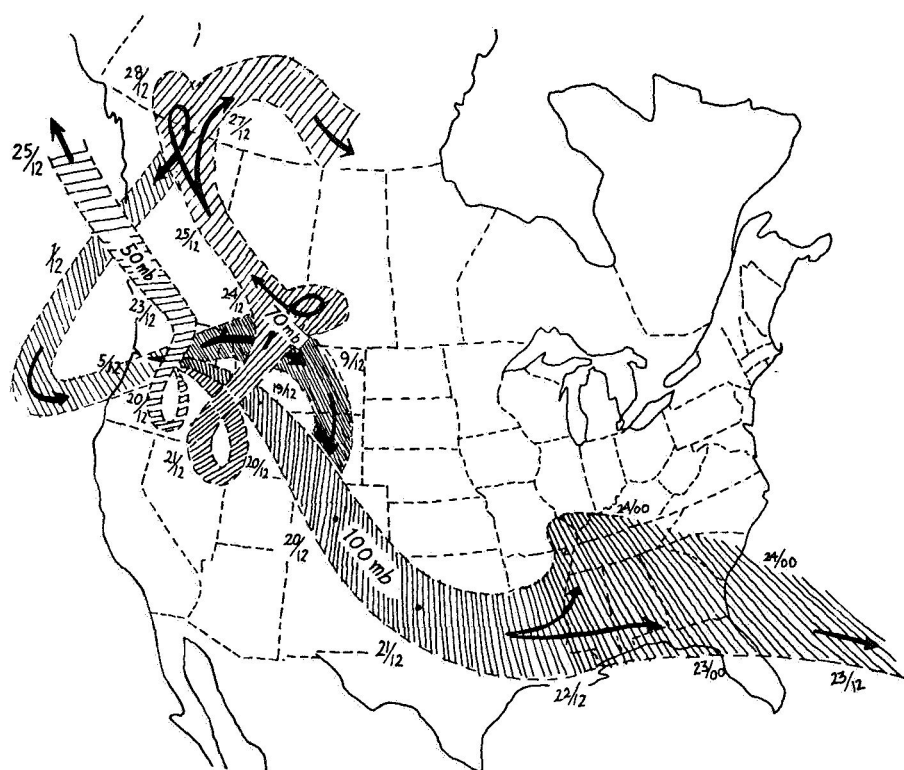


FIGURE 2.4. Trajectories of 18 May eruption for the 100-, 70-, and 50-mb levels.

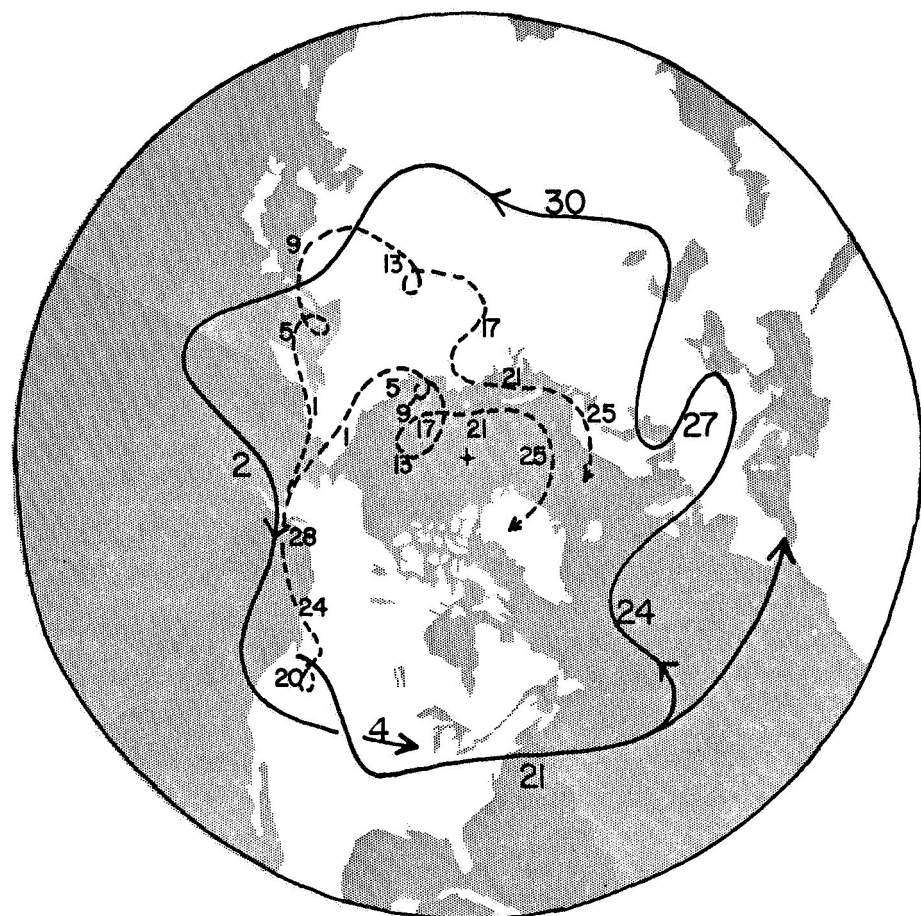


FIGURE 2.5. Estimated global trajectories of 18 May eruption at 200 mb (continuous line) and at 50 mb (broken lines). Days in May and June are appended.

the heat of compression is used to evaporate the hydrometeors and the downward accelerations increase. The resulting cloud form, called mammatus, is essentially an inverted cumulus and is sustained by negative rather than positive buoyancy. It is known that this process was active in the Mount St. Helens plume because there are many excellent photographs of mammatus cloud forms along the undersurface of the plume, especially over the state of Washington, where the major ashfall occurred.

Mammatus clouds, due to their downward accelerations and vertical velocities, propel the larger particles downward and have a major influence on the distribution of ash fallout from the eruption cloud. They also act to mix the cloud vertically after it has acquired the horizontal velocities of the environment and is being extruded into an inclined lamina.

If one could neglect the shear-induced vortex motions in the ascending plume and the drag-induced vortex motions in the quasi-horizontal plume, the ash particles could be treated as projectiles rising and falling through the air while being transported horizontally by the air. Since the horizontal velocities vary with height, as shown in Fig. 2.1, the direction and distance of travel depends directly on the height to which the ash is projected and on its terminal velocity, which varies with size, shape, and density, because it determines travel time.

However, by neglecting the vortex motions, the travel time and, therefore, the travel distance would be seriously overestimated. Also, the fallout pattern would strongly reflect the wind shears, the heaviest particles falling out to the northeast of the volcano and the lighter particles falling more toward the east and much farther downwind. The effect of the vortex motions is to mix the momentum, to reduce the effects of the shear, and to concentrate the fallout both in range and in azimuth. Integrating the southerly and westerly momentum of Fig. 2.1 yields a mean vector toward the east-northeast, where the maximum fallout would be expected. The distribution transverse to this axis would be skewed to the north because any ash not carried into the stratosphere would move mostly toward the northeast. Indeed, the major tropospheric plume did move to the northeast across the northern United States and southern Canada.

2.3 CONCLUSIONS

The main conclusions derived from the observations are given as follows.

1. The generally good correspondence between *in situ* measurements and the predicted horizontal and vertical positions of the volcanic plume have demonstrated the capability for making important in-plume measurements by aircraft within a day or two following the eruption.
2. The importance of vertical shears of the horizontal wind to the generation of slightly inclined thin laminae is confirmed by aircraft and lidar

measurements. The thin vertical dimensions of the laminae clarify the need for an *in situ* sensor with direct read-out to the pilot to permit fine tuning of the aircraft's position to ensure representative sampling.

3. To study the dispersion of the stratospheric plume, a variety of observing techniques must be utilized during the various time periods following an eruption. Aircraft observations are the only practical means of sampling the plume in the period immediately following the eruption. Lidar and balloon measurements are valuable for determining the temporal variability and for reinitializing trajectory computations for aircraft sampling. Satellite measurements provide the best means for observing the spatial and temporal variability on the global scale.

4. Observations of the Mount St. Helens plume as well as atmospheric nuclear explosions indicate that the transported plume remains discrete in the horizontal and laminar in the vertical for a period of at least 5 months after stratospheric injections. Chemical modeling efforts utilizing large-scale diffusive transport are applicable only for times exceeding this period.

5. Three-dimensional trajectories of volcanic effluents should be calculated (for example, by isentropic analysis) instead of the commonly used two-dimensional constant-pressure analyses.

6. Confidence in trajectory calculations is greater when the wind speeds and their related pressure gradients are large. These conditions combined with an increase in the measurement errors with altitude lead to lesser confidence in the high-altitude trajectories relative to those at low altitudes. This trend is manifested in the increasing disagreement between the trajectory analyses by different groups at higher elevations.

7. Given an explosive injection of ash into the stratosphere, the subsequent ash transport distance from the volcano is dominated by stratospheric winds rather than those in the troposphere.

2.4 REFERENCE

Danielsen, E. F., 1974: Review of trajectory methods. In *Advances in Geophysics*, Vol. 18B. Academic Press (New York), 73-94.

CHAPTER 3

CHEMICAL AND PHYSICAL MEASUREMENTS OF THE VOLCANIC CLOUD MADE *IN SITU*

3.1 INTRODUCTION

The direct sampling and analysis of volcanic plumes to determine the amount and composition of effluents can provide important information about the volcanological process and its potential impact on chemical, physical, and climatic atmospheric processes. Continuous and integrated measurements of effluent species as a function of time and space can provide useful information for the geological and atmospheric sciences. In the Mount St. Helens eruptions of the past 6 months, it has not been possible to obtain detailed or representative measurements of the plume composition during the major eruptive phases. The violence and short-term nature of the Mount St. Helens eruptions have limited the scientific communities' ability to probe thoroughly and sample this type of plume (which is of primary interest). Limited measurements have been conducted from small fixed-wing aircraft during the first and subsequent major eruptive events. Only peripheral plume penetration has been possible in these studies. If the heterogeneity of both the eruption process and the plume are known, the "representativeness" of the data obtained from these investigations must be carefully considered. *In situ* plume measurements of several effluent species have been conducted during quiescent periods of Mount St. Helens. How the chemistry of the plume changes between quiet and active periods is not known. Thus, although these various tropospheric studies have provided very important information about plume chemistry, it is not possible at the present time to use these data to quantitatively describe the initial composition and concentration of plume material delivered to the stratosphere.

3.2 PURPOSE

Before describing the variety of *in situ* measurements that were made on the materials emitted from Mount St. Helens, it is useful to mention the reasons why these measurements were made. Among the main purposes of the *in situ* measurements was the desire to characterize volcanic emissions. Concentrations of gases such as H_2O , SO_2 , OCS, and CS_2 were wanted at several altitudes and locations, and particle compositions, concentration size distributions, optical properties, and radioactivity were also sought. Some

measurements had never been made before on volcanic plumes, and other simultaneous observations provided much needed intercomparisons. In some instances, data were to be acquired to estimate emission fluxes, and in others measurements were made to infer constituent burdens over local regions or over the northern hemisphere.

After their departure from the volcanic cone, emitted materials undergo chemical and physical changes before they are removed from the atmosphere. Gases such as SO_2 and H_2S are likely to be oxidized to SO_4^{2-} and hence are transformed from gaseous to particulate matter. The immediate sink for such gases may be mainly this aerosol. Of course, such gaseous and particulate matter can also be removed from the atmosphere by sedimentation, by incorporation into rain or snow, or through reactions with--or absorption by--the earth's surface. The physical process of coagulation acts as the primary sink for very small ($< 0.1 \mu\text{m}$) particles inasmuch as their usual fate is to collide with and stick to larger particles. Observations of these kinds of processes were looked for in the various studies.

In situ data were also needed for understanding some of the longer range effects of Mount St. Helens. Perhaps the chief target was the desire for a data base related to the influence of particles on visible and infrared radiation, and subsequent climate effects. Simultaneously, the presence in the upper atmosphere of materials from Mount St. Helens allowed studies of their transport over long distances.

Another family of effects produced by trace atmospheric material is its potential influence on photochemical processes. At the same time, the influences of radiation, latent heat release, direct heating, and water vapor injection by the volcano itself suggest that trace substance information may lend useful inputs for understanding the thermal and physical structure of the upper atmosphere.

Still another important reason to obtain detailed *in situ* chemical and physical data is to provide direct inputs for checking the internal consistency of the entire data set. Multiple measurements of related variables by different instruments were available for such intercomparisons.

Finally, both climate and chemical models require data on the presence of trace materials in air. A set of *in situ* experiments could provide an extensive, but perhaps incomplete, set of quantities for study via conceptual models.

3.3 MEASUREMENT METHODS

Many independent measurements within the Mount St. Helens plume have been obtained since the mountain became active in March of 1980. These studies have included both ground and airborne measurements of volcanic material in the boundary layer and the upper atmosphere. The extensive measurement capabilities provided by both modern air chemical and aerosol

technologies, along with the use of several research aircraft (WB-57F, U-2, B-23, P-3) and balloons, amount to an unequaled opportunity for observing volcanic activity. Some of the more complex aircraft and balloon programs that were involved with the Mount St. Helens eruption sampling are described briefly as follows.

3.3.1 WB-57 Aircraft

For the past decade, this Department of Energy airplane has participated in Project Airstream. Until 1974 these flights sampled at four altitudes between 12 km and 20 km, spanning from 51°S to 75°N latitude each January, April, July, and October. From 1974 to the present, the latitudinal coverage has been reduced to the equator to 75°N and the frequency has been reduced to each April, July, and October. In addition to the filter samples which have been analyzed for radioactivity, sulfate, ammonium, and total nitrogen, pressurized whole air samples have been collected for measurement of F-11, F-12, N₂O, CCl₄, and SF₆. Over some portions of the decade, various other instruments have also measured O₃, H₂O, Aitken nuclei, infrared spectra, ultraviolet spectra, NO_x, and particle sizes on these flights. Thus, an extended time history of variations in stratospheric trace species has been established. Of principal use in understanding stratospheric contributions from the Mount St. Helens eruption has been the history of sulfate aerosol concentrations distributed through the stratosphere. Detailed results are presented by Sedlacek et al. (1980) and are summarized later in this chapter.

3.3.2 U-2 Aircraft

The Aerosol Climate Effects (ACE) study at NASA Ames Research Center utilizes U-2 aircraft for its atmospheric research project. A number of instruments are used simultaneously for gathering information on interrelated upper atmosphere characteristics. These devices are managed by university, industry, and government researchers in a common effort to learn more about critical properties that might influence climate. One objective of the special study is to assess processes evolving from major volcanic eruptions. By good fortune, eruptions of Mount St. Helens were ideally suited for extensive sampling missions with the high-flying U-2 aircraft. Each of the three initial major eruptions was sampled with a variety of instruments, not always flown together, but usually with at least two simultaneously. Instruments that were flown one or more times on these flights were a cryogenic whole air sampler (NASA-ARC) for ion and gas chromatography, a sequential filter sampler (NCAR), a quartz crystal microbalance cascade impactor (NASA-LaRC), an opal glass impactor for optical measurements (University of Washington), and

a wire impactor device (NASA-ARC). Detailed results obtained by these devices were presented at the symposium; a summary of these data follows later in this chapter.

3.3.3 B-23 Aircraft

Low-altitude sampling of the plume for particles and gases around the periphery of the plume as the Mount St. Helens eruption occurred was carried out by using the University of Washington B-23 aircraft. This sampling provided some measure of the nature of the ejecta as the eruption proceeded. Filter samples were taken between the tropopause and 14 km altitudes on 20 days between 4 June and 8 August 1980. These samples were analyzed for ^{7}Be (as a stratospheric tracer), sulfate, nitrate, and trace elements. This sampling indicated the passage of the sulfate cloud at just above the tropopause on the 1st, 2nd, and 3rd circuit of the earth at approximately 12- and 14-day intervals.

Also in the B-23 aircraft, an integrating nephelometer was used to give the scattering component of extinction due to particles, whereas on both the U-2 and B-23 aircraft the absorption coefficient σ_{ab} was measured with the opal glass integrating plate method (IPM) (Ogren et al., 1981). The albedo for single scatter δ of the aerosol particles, defined by the ratio σ_{sc}/σ_{ext} , was thus estimated for the first time from *in situ* microphysical data.

3.3.4 P-3 Aircraft

Project RAVE (Research on Atmospheric Volcanic Emissions) is a joint university-NASA research effort. A Lockheed Orion P-3 four-engine turboprop aircraft was outfitted with active and passive instrumentation for monitoring and sampling gases and aerosols in volcanic plumes. The first field study in this project was performed on 22 September 1980 at the Mount St. Helens volcano. Measurements made in this study included remote sensing of SO_2 and aerosol burdens and fluxes; in-plume analysis of SO_2 , H_2S , NO , NO_2 , O_3 , and particle size distribution; and the filter collection of aerosols and reactive gases for subsequent laboratory analysis.

3.3.5 Balloons

Frequent aerosol profiles were obtained following the 18 May eruption by the University of Wyoming atmospheric physics group. These measurements were made with a balloon-borne photoelectric particle counter (dustsonde) capable of measuring the concentrations of particles greater than or equal to about $0.3 \mu\text{m}$ diameter. In many of the soundings, multiple instruments were flown and thus allowed for the simultaneous determination of other parameters such as volatility, condensation nuclei (CN) concentration, and

CN size. The instrumentation has previously been described by Hofmann et al. (1975) and has been in use for about 17 years. Highlights of the volcano dust measurements are presented.

3.4 RESULTS

The results of these measurements are summarized for each program separately as follows.

3.4.1 WB-57 Aircraft

Following the 18 May 1980 eruption of Mount St. Helens, two special sampling flights were flown on 20 May and 21 May to measure the aerosol and trace gas injected into the stratosphere by Mount St. Helens as the debris plume moved across the United States. The regular WB-57F sampling in late July to early August also contributed significant measurements relevant to the stratospheric contributions of aerosol and trace gases by Mount St. Helens. The samples were analyzed to give mass concentrations of sulfate, ash, radioactivity, elemental composition, aerosol morphology and mineralogy, and a few trace gases.

Another series of similar measurements in the northern hemisphere will be made in the spring of 1981 to follow the dispersion and removal of Mount St. Helens debris in the stratosphere.

WB-57F aerosol samples collected on 20 and 21 May contained concentrations of sulfate that were about 25 times higher in the plume than outside it at 15.24 km and 5 to 35 times higher in the plume at 18.29 km. These findings are consistent with similar samplings at Soufriere of St. Vincent on the day of the 17 April 1979 eruption when sulfate concentrations 3 to 5 times higher in the plume than outside the plume were measured.

The volcano cloud appeared to be inhomogeneous with respect to acid and ash. The initial samples collected on 20 and 21 May over the west central part of the United States showed considerable variation in the ratio of ash to sulfate sampled. Higher ratios of ash to acid occurred at lower altitudes, but even at the same sampling altitude, considerable variation in ratios and concentrations occurred as portions of the debris cloud associated with different parts of the rather extended 18 May 1980 eruption were encountered. One sample on 21 May even showed essentially no increase in sulfate above the pre-eruption ambient levels.

Microscopic examination of particles collected 3 days after the first eruption of Mount St. Helens on the WB-57F EML impactor indicates that the ash particles in the stratosphere provided surfaces for growth of sulfuric acid particles. In addition, extremely small (less than $0.06 \mu\text{m}$ radius) sulfate aerosols were detected in concentrations of 10^4 per cm^3 ; these concentrations exceed the pre-eruption concentrations by three orders of magnitude.

3.4.2 U-2 Aircraft

The first volcanic aerosol collections were made on the day following the first eruption of 18 May. These particles from two altitudes (14 km and 17 km) were dry and devoid of any evidence of fluid coatings. There was, however, a very small background of acid aerosol particles at the higher altitude. Distribution of these droplets was typical of that location before the eruption; apparently, it was undisturbed by the substantial dry ash intrusion. Mineralogically, the ash grains had variable compositions and were not similar at the different altitudes. This condition and subsequent mineral assessments after later eruptions suggest the cloud was inhomogeneous regarding the ash composition. Furthermore, the absence of any liquid associated with the ash in the first collections was contradicted by the presence of low marks in dust on the aircraft wings. Strong acid reactions with reagent papers pressed on the aircraft suggested the vehicle passed through liquid-contaminated zones in the eruption cloud. These inferential assessments implied the cloud was also inhomogeneous with respect to acid and ash content.

Subsequent flights through portions of the first eruption cloud 4 days and 16 days after the eruption revealed that all these volcanic collections were mixtures of liquid acid and ash that flooded the collecting wires. Samples of the second eruption cloud were obtained 2 days and 4 days afterward. These samples also were dense collections of liquid acid and ash. A sample collected less than a day after the third eruption also was a mix of fluid acid and ash. The concentrations of both, however, were smaller than those on previous occasions, but each discrete ash grain was coated with the liquid.

Following these initial surges of acid and ash and culminating with the third eruption sample on 13 June, no further ash samples were obtained. Rather, all subsequent collections contained only acid droplets; no obvious ash grains protruded from them. Acid drop concentrations peaked in mid-June over California at all altitudes from 12 km to 18 km and then decreased to a factor of two or three above pre-eruption background levels in August. By late October, based on one sounding from 12 km to 18 km, the acid concentrations were near normal.

Short expeditions were made with the U-2 aircraft to Fairbanks, Alaska, in mid-July, and thence from California, across Florida, to Panama for a 3-week expedition in September. Acid aerosol concentrations in Alaska were found to be higher by factors of four to six at lower altitudes (12 km) than were measured a year earlier. Concentrations at higher altitudes (15 km to 18 km) were perhaps slightly higher than those obtained previously.

Acid concentrations over Florida, both on the flights to and from Panama, also were significantly higher than those obtained 6 months earlier. Panama concentrations, however, were generally not higher, although on some days higher readings were observed, especially on the last day of the mission, when a very high concentration was seen.

The 18 May eruption was apparently dominated by SO_2 as shown by measurements made about 24 hours after the initial event. The plume concentration of SO_2 was enhanced by about 2000 times over that for prevolcanic conditions (Inn et al., 1981). Previous studies of eruption clouds of South American volcanoes have shown that SO_2 and OCS in the plume were found to be enhanced by about 2 to 3 times; however, the source of the enrichment may be either plume enrichment or entrainment of tropospheric air. Although plume measurements of the sulfur gases following the 25 May and 13 June eruptions show scatter in the concentrations, there is no indication of any enrichment of these constituents from those eruptions.

Measurements of other gases in the eruption plumes of Mount St. Helens (Inn et al., 1981) in the stratosphere have been reported and show significant enhancement compared with prevolcanic concentrations; CH_3Cl and NO_3^- (derived from NO_2 and/or HNO_3) were enhanced by 3 to 7 times and about 200 times, respectively, over concentrations typical of nonperturbed conditions in the stratosphere. The mixing ratio of HCl in the plume of the 18 May eruption was estimated to be about 10 ppbv to 50 ppbv which gives a ratio of $(\text{HCl}/\text{SO}_2) \cong 0.1$ to 0.5. Similar ratios were reported for the Fuego and the Guatemalan volcanoes (Lazarus et al., 1979). Whole air samples obtained in the plume 4 days after the 18 May eruption gave CO concentrations about 6×10^4 times greater than the prevolcanic stratospheric concentrations (Inn et al., 1980, private communication). ^{222}Rn was also measured from the cryogenically collected samples in the plume of the 18 May eruption. The measured radioactivity was 0.13 disintegrations per minute per liter (STP) which approximates that of ground level tropospheric air. Independent radioactivity measurements in the plume of ^{222}Rn with values ranging from 0.055 to 0.28 have also been reported by Leifer et al. (1980).

Water vapor concentrations in the plume of the 18 May eruption were estimated to be about 10- to 50-times that of the unperturbed stratosphere. Frost point hygrometer measurements on the same sampling experiment gave similar results (D. Murcray, private communication). Other gases measured were N_2O , CF_2Cl_2 , CFCl_3 , CO_2 , and CH_4 , which were all found to have concentrations in the plume very similar to those occurring in the unperturbed stratosphere.

In other sampling measurements of these gases on board the WB-57 aircraft, similar concentrations were found in the Mount St. Helens plume (Leifer et al., 1980). Current available information on nitrogen species (including NH_3) does not permit conclusions or speculations about their concentrations or distributions.

Before, during, and after the 18 May eruption, measurements were made to determine the integral optical properties of the aerosol related to radiative processes in the visible spectrum. The aerosol extinction coefficient σ_{ext} defined by the Beer law could only be determined from U-2 data by correlation with other microphysical variables, namely, the mass distribution with particle size. Alternatively, it was also inferred from SAGE which yielded almost identical values in the plume of 10^{-3} to 10^{-2} per km. Both in the troposphere (B-23 results) and stratosphere (U-2 results), the values of ω were very close to unity with values ranging from 0.98 to 0.995. The small absorption coefficient was due to small amounts of iron-containing minerals in the ash and the coefficient apparently decreased systematically with time following each major eruption. The stratospheric absorption coefficient was as high as $\approx 10^{-7} \text{ m}^{-1}$ and could contribute a small but finite amount of heating (about 0.1°C/day) due to absorption of sunlight. This result is consistent with studies of Mount Agung (Newell, 1970).

3.4.3 B-23 Aircraft

Initial measurements by Hobbs et al. (1981) of sulfur gases being emitted from Mount St. Helens on the day of the 18 May eruption suggest that hydrogen sulfide concentrations were significantly higher than the sulfur dioxide levels present in the tropospheric plume. The ratio of H_2S to SO_2 for this day was found to be about 10. However, after the 12 June eruption, the H_2S to SO_2 ratio had decreased to yield a value of approximately 0.1. It should be noted that the H_2S and SO_2 concentrations were not monitored simultaneously.

By contrast, R. A. Rasmussen, A. R. Dallugi, S. A. Penkett, and B. Jones (private communication, 1980) have analyzed Mount St. Helens ash from the ground for outgassing of various constituents. For the sulfur family they have found high concentrations of carbonyl sulfide and carbon disulfide and have suggested the possibility of other reduced sulfur gases being present.

3.4.4 P-3 Aircraft

A study of the quiescent tropospheric plume being emitted from Mount St. Helens on 22 September 1980 was made by a scientist on Project RAVE. Sulfur dioxide concentrations in the plume ranged from about 50 ppbv to 200 ppbv, which was in good agreement among three different measuring groups aboard the NASA P-3 (Friend et al., 1981). Simultaneous measurements were made of SO_2 , H_2S , CS_2 , and OCS with a real-time gas chromatographic system. The ratio of H_2S to SO_2 observed in this plume was 0.12; this result was significantly different from that seen on 18 May but was quite similar to what was determined for the 12 June eruption (Hobbs et al., 1981). The OCS and CS_2 concentrations during this RAVE flight were always below the lower

limit of detection of the gas chromatographic system and indicated that the OCS or CS_2 to SO_2 ratio was less than 0.05. Thus, during these measurements, the major sulfur gas constituent in the Mount St. Helens tropospheric plume was SO_2 .

3.4.5 Balloons

Two dustsonde measurements made on 19 May showed the presence of many layers between 10 km and 16 km with unusually large particles (diameter greater than or equal to about 1 μm). The following days, however, when more of the upper portion of the cloud was observed (16 km to 18 km), the layers were found to have a considerable amount of fine structure in that at some altitudes the particles were relatively small and at other slightly different altitudes, the particles were relatively much larger. The smaller particles observed are suggestive of acid droplets whereas the larger particles are perhaps the ash.

The dustsonde has been used to monitor the stratospheric aerosol concentration for about the last decade and these results were recently updated by Rosen and Hofmann (1980) in September 1980. The measurements show that by about August 1980, the number concentration had settled down to a value of about three times the typical pre-eruption values. However, the exact increase is somewhat obscured by the interference of other volcanic eruptions (Rosen and Hofmann, 1980).

The dustsonde was employed in a technique described elsewhere (Rosen, 1971) to measure the volatility of the volcanic aerosol in the stratosphere at 1 day and 39 days after the initial large eruption. The first sounding showed that the particles were relatively large (diameters greater than about 2 μm) and essentially nonvolatile. However, the possibility of a thin coating of volatile sulfuric acid on them cannot be excluded. In contrast, the second sounding showed that by this later time, most of the mass in the aerosol was highly volatile.

3.5 DISCUSSIONS

Discussions of the atmospheric species, based on the possible chemical and microphysical processes involved, are briefly given as follows.

3.5.1 Gases

Background tropospheric concentrations of sulfur dioxide, carbonyl sulfide, hydrogen sulfide, and carbon disulfide had been measured prior to the 18 May 1980 eruption of Mount St. Helens. Sulfur dioxide levels in the free troposphere were about 0.2 ppbv over continental areas and 0.09 ppbv over marine locations (Maroulis et al., 1980). Carbonyl sulfide concentrations were

found to be uniformly distributed throughout the troposphere at a concentration of 0.5 ppbv (Torres et al., 1980; Sandalls and Penkitt, 1977; Maroulis et al., 1977). Slatt et al. (1978) and Goldberg et al. (1981) have measured hydrogen sulfide to be about 0.020 ppbv in air masses which had spent time over open ocean. Boundary-layer measurements of carbon disulfide revealed concentrations of typically less than 0.030 ppbv in background air (Maroulis and Bandy, 1980).

Clearly a more detailed examination of these species is required in future studies. Direct measurement of oxides of nitrogen emissions from Mount St. Helens is very limited. Hobbs et al. (1981) suggested plume NO_x may be occasionally observed. Friend et al. (1981) estimated the NO concentration to be approximately 0.1% of the plume SO_2 during RAVE measurement of emissions during a quiescent period. U-2 sampling suggests a possible indication of a stratospheric NO_x anomaly at or near the volcanic cloud on 19 May and 14 June 1980 (Inn et al., 1981). Preliminary data from the 22 September RAVE mission suggests HNO_3 may have been present in the volcano plume at this time. Rasmussen et al. (personal communication, 1980) have made limited measurements of CH_3Cl , CF_2Cl_2 , CF_3Cl , and N_2O as well as additional gaseous species in Mount St. Helens emission. Available data are again limited and no conclusions can be made about plume concentrations of many gases.

3.5.2 Gas-to-Particle Conversion

Collection of a dry ash sample (low sulfate) on filters and high SO_2 concentrations 1 day after the first eruption compared with an acid-flooded ash sample (higher sulfate concentrations), together with low SO_2 concentrations 4 days after this eruption, suggests the possibility of rapid gas-to-particle conversion. There is evidence from the appearance of sulfur-containing droplets and liquid films on ash particles that suggests (1) coagulation of sulfuric acid embryos and/or aerosols with ash particles; (2) heterogeneous catalytic oxidation of SO_2 to form sulfuric acid on the surfaces of ash particles; or (3) homogeneous oxidation of SO_2 to form sulfuric acid embryos and subsequent growth. However, none of these mechanisms can be unambiguously identified. Reference to meteorological charts, however, shows the collections were probably not from the same cloud portion. Because of the inhomogeneity of the cloud, positive statements about particle formation and growth cannot yet be made. On the other hand, qualitative observations that reveal the presence of many small acid aerosol particles appearing in some collections about mid-June hint that nucleation and growth may, indeed, be occurring. But questions arise whether these samples are perhaps from cloud puffs still circling the earth more or less intact and do not represent the general background aerosol features.

Impactor samples collected on the WB-57F aircraft indicate the existence of large numbers of volatile submicron ($0.06 \mu\text{m}$ radius) particles in the plume.

It is impossible to tell, by using these impactor samples, whether gases were converted to particles during transport or whether the conversion occurred at the time of eruption.

The first profiles made with a modified dustsonde at about 45 days after the 18 May eruption show an unusually high concentration of particles ($\geq 300 \text{ cm}^{-3}$) in the 15 km to 20 km altitude range with an effective diffusion radius of about $0.01 \mu\text{m}$ to $0.02 \mu\text{m}$. This result is to be contrasted with the typical background concentration observed in the same altitude range of about 15 cm^{-3} and an effective radius of about $0.1 \mu\text{m}$. By carefully considering coagulation lifetimes through an approximate model, it may be possible to determine whether this high concentration is consistent with production occurring only at time of injection or whether subsequent production of new particles is required. This analysis has not yet been undertaken.

Measurements of sulfate concentrations and particle morphology made in the stratospheric plume of Mount St. Helens on 19, 20, 21, and 25 May by WB-57F and U-2 aircraft have all shown the presence of sulfuric acid droplets. Since no *in situ* stratospheric measurements were made on 18 May, the possibility that sulfuric acid was directly injected into the stratosphere by the 18 May eruption cannot be ruled out (Farlow et al., 1980).

3.5.3 Cloud Inhomogeneity

Filter samples collected on aircraft platforms and in different parts of the plume over a 4-day period showed large variations in the total ash content, sulfate concentration, and elemental compositions.

Impactor samples collected on the U-2 aircraft 1 day after the 18 May 1980 eruption showed no sulfuric acid associated with the ash particles, whereas later collections in different parts of the cloud showed large amounts. Spatial differences in the morphology of particles collected on the U-2 and WB-57F aircraft showed large differences.

Aerosol samples collected by the U-2 wire impactor at various times after the first three major eruptions qualitatively show considerable variability between the acid and ash proportions on each. First eruption samples, for example, show virtually no acid at lower altitudes despite evidence on the aircraft of considerable acid contamination. In later collections for all three eruptions, acid/ash variability was quite obvious visually. Not only does this variability suggest cloud inhomogeneity, but also mineralogical analyses show much variability of mineral and glass fragments in different parts of the clouds. Highly variable ash-to-sulfate ratios from filter and impactor measurements made in the stratosphere suggest that the ash and acid aerosols were inhomogeneously mixed. No consistent or unambiguous pattern of ash-to-sulfate ratios as a function of altitude or downwind distance has been observed (Sedlacek et al., 1980; Farlow et al., 1980).

3.5.4 Residual Aerosol Burden

A rough lower limit estimate of the mass of material that was injected ($\cong 1$ km 3 of the mountain) into the atmosphere and remained airborne for a significant period can be found by computing the known ash fall outside a 30-km radius from the volcano. An eyeball estimate of the data indicates a 12-mm average ash depth over an approximate 200 x 200 km area. This 12-mm depth will probably compress to 3 mm with a density of $\cong 2$. Then the total mass is $0.3 \text{ cm} \times 2 \text{ g cm}^{-3} \times 4 \times 10^{14} \text{ cm}^{-2} = 2.4 \times 10^{14} \text{ g}$ (240 megatons). Thus 240 megatons were airborne for a period on the order of hours.

Aircraft and balloon-borne observations (Sedlacek et al., 1980; Farlow et al., 1980; Rosen and Hofmann, 1980), however, all concur that most if not all the ash portion of the erupted material had fallen out of the stratosphere perhaps as early as mid-June and certainly by mid-August. A comparison of SAGE data (Kent, 1980; and Chapter 4), Project Airstream (Sedlacek et al., 1980), U-2 measurements, lidar data, and balloon-borne particle soundings all show that by August the quantity of acid aerosols in the stratosphere was about three times the pre-eruption amounts.

A crude estimate of the mass of this residual aerosol remaining in the stratosphere by late July and early August can be made from WB-57F measurements at four altitudes from the equator to 75°N. The total residual aerosol mass in a 4-km thick layer of the lower stratosphere was calculated to be $2.5 \times 10^{11} \text{ g}$ (0.25 megaton). For comparison, SAGE satellite data were used to calculate the aerosol masses in a 10-km thick layer of the lower stratosphere based on extinction; these values were $2.5 \times 5.0 \times 10^{11} \text{ g}$ (0.25 to 0.5 megaton). This residue, therefore, is only about 0.1% of the initial particulate mass. Of course, in this simplified assessment, no account is made of the quantity of gas products that may have converted to residual acid aerosols.

3.6 CONCLUSIONS

From the chemical and physical *in situ* measurements, the following conclusions are derived.

1. Sulfuric acid appeared in the stratospheric portions of the volcano plumes very early—perhaps on the same day as the eruptions or certainly within a few days. The acid may even have been part of the initial emissions from the crater.
2. The volcano cloud appeared to be inhomogeneous with respect to acid and ash.
3. The quantity of residual acid aerosol is very small compared with the initial mass of volcanic debris injected into the atmosphere.
4. By August the quantity of residual acid particles in the stratosphere was about three times the pre-eruption amounts.

5. Theory suggests gas-to-particle conversions should take place in volcano clouds in the stratosphere. At this time, interpretations of *in situ* measurements do not resolve questions about the extent of this process in Mount St. Helens eruptions.

6. Single scattering albedo has been derived for the first time from direct measurements in the stratospheric plumes of volcanic eruptions. This albedo now allows calculations of radiative climate effects resulting from the Mount St. Helens explosions.

7. The stratospheric aerosol burden inferred from direct *in situ* measurement of mass concentration agrees within a factor of two with the same quantities estimated optically from satellite determinations of extinction coefficient.

8. The absolute amount of gaseous sulfur injected into the stratosphere has not been directly measured. *In situ* measurements of the stratospheric cloud indicate that the primary gaseous sulfur species present 24 hours after the eruption was probably SO₂. No direct measurements of H₂S in the stratospheric cloud have been reported. OCS and CS₂ were apparently 1000 times less concentrated than SO₂ in the stratospheric plume.

9. Reported sulfur gas measurements of direct plume emissions suggest possible extreme variations in the sulfur composition. Such variations may have important implications to both volcanology and the atmospheric sciences. Subsequent to the 18 May eruption, the predominate sulfur gas was apparently SO₂.

10. Water concentrations in the stratospheric plume on 19 May were found to be ten or more times the background water concentration.

3.7 RECOMMENDATIONS

Efforts should be made to obtain more information about the chemistry and physics of the volcanic emissions. More measurements of aerosol size distribution, composition, physical, and chemical fractionation as well as optical properties need to be performed. Temporal and spatial distributions of sulfur and nitrogen gases in the plume need more extensive study as well as those for CO, CO₂, and H₂O.

These measurements need to be made in the plume as soon as possible (within 12 hours) after an eruption and as often as is logically practical during the first few days after the eruption. These measurements need to be made both in the troposphere and stratosphere. This kind of effort demands close cooperation and coordination by all experimenters under one agency, group, or person.

Interpretation of the data obtained from the kinds of measurements described would be enhanced by attempts to measure in a portion of the plume

that can be uniquely identified and revisited for subsequent measurements. Possible methods include improved trajectory forecasting in conjunction with plume tracer techniques.

3.8 REFERENCES

Cadle, R. D., A. L. Lazarus, B. J. Huebert, L. E. Heidt, W. I. Rose, Jr., D. C. Woods, R. L. Chuen, R. E. Stoiber, D. B. Smith, and R. A. Zielinski, 1979: Implications of studies of South American volcanic eruption clouds, *J. Geophys. Res.*, **84**, 6961-6968.

Farlow, N. H., G. V. Ferry, H. Y. Lem, and D. M. Hayes, 1979: Latitudinal variations of stratospheric aerosols, *J. Geophys. Res.*, **84**, 733-743.

Farlow, N. H., K. A. Snetsinger, V. R. Oberbeck, G. V. Ferry, G. Polkowski, and D. M. Hays, 1980: Time variations of aerosols in the stratosphere following Mount St. Helens eruptions. Paper presented at NASA Workshop on Mount St. Helens Eruption: Its Atmospheric Effects and Potential Climatic Impact (Washington, D.C.), November 18-19.

Farlow, N. H., V. R. Oberbeck, K. G. Snetsinger, G. V. Ferry, G. Polkowski, and D. M. Hayes, 1981: Size distributions and mineralogy of stratospheric ash particles from Mount St. Helens, *Science*, **211**, 832.

Ferry, G. V., and H. Y. Lem, 1974: Aerosols in the stratosphere, *Proceedings of the Second International Conference on the Environmental Impact of Aerospace Operations in the High Atmosphere*, American Meteorological Society (Boston, Massachusetts).

Friend, J. P., A. R. Bandy, P. J. Maroulis, L. Wilner, M. A. Hart, J. L. Moyers, W. H. Zoller, J. M. Phelan, D. Finnegan, A. Torres, R. E. Stoiber, J. Wells, M. P. McCormick, D. C. Woods, and W. I. Rose, Jr., 1981: Research on atmospheric volcanic emissions: An overview. [Available from first author, Drexel University, Philadelphia, Pennsylvania.]

Goldberg, A. B., P. J. Maroulis, L. A. Wilner, and A. R. Bandy, 1981: Studies of H₂S emissions from a salt water marsh, *Atmos. Environ.*, **15**, 11.

Hobbs, P. V., L. F. Radke, M. W. Eltgroth, and D. A. Hegg, 1981: Preliminary analysis of particles and gases from the Mount St. Helens volcanic emissions of 1980, *Science*, **211**, 819.

Hofmann, D. J., J. M. Rosen, and T. J. Pexin, 1975: Stratospheric aerosol measurements: I. Time variations at northern mid-latitudes, *J. Atmos. Sci.*, **32**, 1446-1456.

Inn, E. C. Y., J. F. Vedder, E. P. Condon, and D. O'Hara, 1981: Gaseous constituents in the plume of Mount St. Helens, *Science*, **211**, 821-823.

Kent, G. S., 1980: SAGE measurements of Mount St. Helens volcanic aerosols. Paper presented at NASA Workshop on Mount St. Helens Eruption: Its Atmospheric Effects and Potential Climatic Impact (Washington, D.C.), November 18-19.

Lazarus, A. L., R. D. Cadle, B. W. Gandrud, J. P. Greenberg, B. J. Huebert, and W. I. Rose, Jr., 1980: Sulfur and halogen chemistry of the stratosphere and volcanic eruption plumes, *J. Geophys. Res.*, **84**, 7869-7875.

Leifer, R., K. G. Sommers, S. F. Guggenheim, and I. Fisenne, 1980: Recent developments in high altitude aircraft sampling: Mount St. Helens and Stratospheric gases, IEEE Nuclear Science Symposium (Orlando, Florida), 5-7 November 1980.

Maroulis, P. J., and A. R. Bandy, 1980: Measurements of atmospheric concentrations of CS_2 in the eastern United States, *Geophys. Res. Lett.*, **7**, 681.

Maroulis, P. J., A. L. Torres, and A. R. Bandy, 1977: Atmospheric concentration of carbonyl sulfide in the southwestern and eastern United States, *Geophys. Res. Lett.*, **4**, 510.

Maroulis, P. J., A. L. Torres, A. B. Goldberg, and A. R. Bandy, 1980: Atmospheric SO_2 measurements on project GAMETAG, *J. Geophys. Res.*, **85**, 7345.

Newell, R. E., 1970: Modification of stratospheric properties by trace constituent changes, *Nature*, **227**, 697-699.

Ogren, J. A., R. J. Charlson, L. F. Radke, and S. K. Domonkos, 1981: Absorption of visible radiation by aerosols in the volcanic plume of Mount St. Helens, *Science*, **211**, 834-836.

Rosen, J. M., 1971: The boiling point of stratospheric aerosols, *J. Appl. Meteorol.*, **10**, 1044-1046.

Rosen, J. M., and D. J. Hofmann, 1980: Dustsonde measurements of the Mount St. Helens volcanic cloud over Wyoming. Paper presented at NASA Workshop on Mount St. Helens Eruption: Its Atmospheric Effects and Potential Climatic Impact (Washington, D.C.), November 18-19.

Rosen, J. M., and D. J. Hofmann, 1980: A stratospheric aerosol increase, *Geophys. Res. Lett.*, **9**, 669-672.

Sandalls, F. J., and S. A. Penkitt, 1977: Measurements of CS_2 and OCS in the atmosphere, *Atmos. Environ.*, **11**, 197.

Sedlacek, W. A., G. H. Heiken, E. J. Mroz, E. S. Gladney, D. R. Perrin, R. Fisenne, L. Hinchliffe, and R. L. Chuan, 1980: Physical and chemical characteristics of Mount St. Helens airborne debris. Paper presented at NASA Workshop on Mount St. Helens Eruption: Its Atmospheric Effects and Potential Climatic Impact (Washington, D.C.), November 18-19.

Slatt, B. J., D. F. S. Natusch, J. M. Prosperos, and D. L. Savoie, 1978: Hydrogen sulfide in the atmosphere of the northern equatorial Atlantic Ocean and its relation to the global sulfur cycle, *Atmos. Environ.*, **12**, 1981.

Torres, A. L., P. J. Maroulis, A. B. Goldberg, and A. R. Bandy, 1980: Atmospheric OCS measurements on project GAMETAG, *J. Geophys. Res.*, **85**, 7357.

CHAPTER 4

REMOTE MEASUREMENTS OF MOUNT ST. HELENS EFFLUENT

4.1 INTRODUCTION

This chapter describes observations of the Mount St. Helens effluent made with various remote sensors. These sensor techniques include radar, lidar, radiometry, limb extinction and total atmospheric extinction sun photometry, photography, and correlation spectrometry. In addition to being ground-based, the platforms include balloons, aircraft, and spacecraft. Brief descriptions of the techniques are given, but the majority of material deals with data and its synthesis. Where available, as in the case of lidar and the Stratospheric Aerosol and Gas Experiment (SAGE), a more "global" description is attempted. The ground-based radar data give an early look at the height, time, and duration of the eruption columns. A more detailed description of these data was given earlier, but a portion will be presented here for completeness. The correlation spectrometer (COSPEC) instrument has been used primarily to get a time history of the SO_2 flux put into the troposphere. No remotely sensed data, however, exists for the stratospheric SO_2 flux nor was any data taken nearby the volcano during the 18 May eruption.

It will be shown that the remotely sensed data presented herein represent a self-consistent set, in the sense that the arrival times of the volcanic material at various altitudes and locations appear to be consistent with each other, and reasonably consistent with the air mass movements deduced from geostationary satellite photographs, soon after the 18 May eruption, and predicted by trajectory analysis. Measured heights for the stratospheric injection also agree; that is, SAGE, lidar, and radar each indicate that material from the 18 May eruption reached to between 23 and 25 km above the earth's surface. The movement of material in the upper troposphere and lower-to-middle stratosphere are described vis-a-vis these data sets. Finally, agreement is shown between mass loading estimates from SAGE and lidar data for the stratospheric injection.

4.2 MEASUREMENT METHODS AND RESULTS

The measurement methods and programs that were involved in, or could be used for, performing remote sensing measurements of the optical, physical, and chemical properties of volcanic effluents are described as follows.

4.2.1 Satellite Measurements

NASA has launched two satellite instruments, the Stratospheric Aerosol Measurement II (SAM II) aboard Nimbus 7 on 24 October 1978, and the Stratospheric Aerosol and Gas Experiment (SAGE) aboard the Applications Explorer Mission 2 (AEM-2) satellite on 18 February 1979. These are designed specifically to measure stratospheric aerosol extinction and gas concentrations (McCormick et al., 1979). The SAGE satellite system has a geographic coverage of latitudes primarily between about 72°N and 72°S and has been well situated to observe enhanced stratospheric extinction produced by the Mount St. Helens eruption. SAM II is in an orbit that provides coverage of just the polar regions.

SAGE has four spectral channels, with the one at 1.0 μm designed principally for aerosol measurement. The instrument measures solar intensity profiles during each spacecraft sunrise and sunset as the satellite orbits the earth. Since the orbital period is about 90 minutes, approximately 30 measurements can be made each day (during 1980, because of AEM-2 power supply problems, measurements were confined to sunsets only). The position on the earth's surface of these measurements, moves in a regular manner from one extreme of latitude to the other in about 1 month. Following the 18 May Mount St. Helens eruption, SAGE was conveniently located to make measurements over the northern hemisphere. This was repeated again in August. Data for the period after that have not been analyzed at this time and, therefore, are not part of this report.

Transmission data from SAGE are inverted to give a profile of extinction as a function of altitude for each event. The vertical resolution is 1 km and the extinction values (at 1.0 μm) have a root mean square error of about $5 \times 10^{-6} \text{ m}^{-1}$. These profiles are integrated to give optical depth above any given altitude in the stratosphere. Typical extinction profiles obtained for a normal and volcanically enhanced stratosphere are shown in Fig. 4.1. Figure 4.1a shows a normal stratospheric background with a peak extinction of about 10^{-4} m^{-1} . Figure 4.1b shows an example with a volcanic enhancement. It shows a peak value of greater than 10^{-3} m^{-1} . In fact during this period immediately after the eruption, values as high as 10^{-1} m^{-1} were observed at various altitudes and locations.

On 18 May, SAGE was making measurements over northern Canada. The latitude of these measurements moved southward in subsequent days, crossing the latitude of Mount St. Helens on 25 May, and reaching 30°N on 30 May. Significant stratospheric enhancements were seen on approximately 20 occasions, ranging in latitude from 55°N to 25°N and in longitude between 10°W and 140°W. This area covered the western and northern United States with a

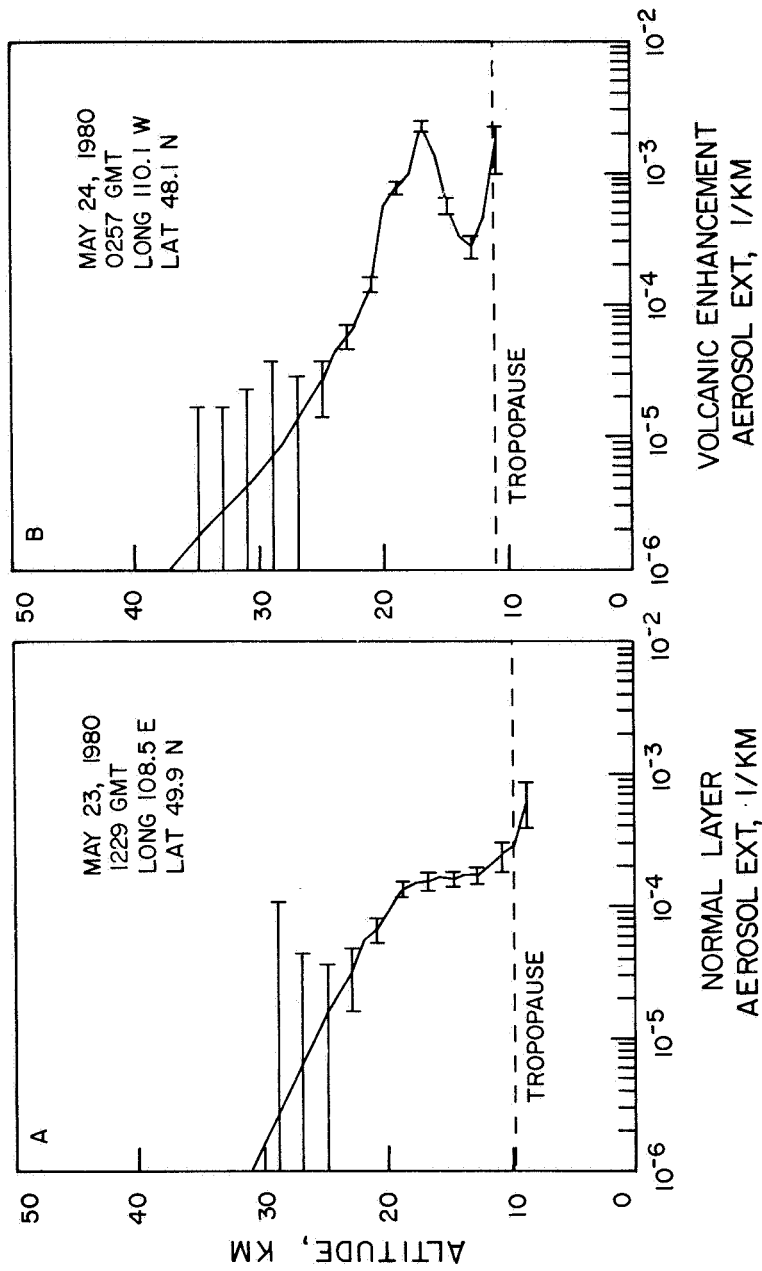


FIGURE 4.1. Stratospheric aerosol extinction profiles obtained by SAGE at a wavelength of 1 μ m. (a) Normal profile unaffected by volcanic effluents. (b) Profile showing an enhancement caused by Mount St. Helens of about a factor of 10 near the layer peak.

tongue of material extending over the Atlantic Ocean from the South Carolina coast almost to West Africa (diagrammatically shown in Fig. 4.2). Considerable vertical shearing had occurred, with the highest altitude material between 20 and 23 km observed off the coast of Washington and the lowest stratospheric material (below 16 km) over the eastern USA and the Atlantic Ocean. As observed by SAGE, apparent sharp vertical layers were detected, with thicknesses of 1 or 2 km, as well as thick layers reaching down into the troposphere. Figure 4.3 shows a preliminary analysis of SAGE observations made in August. The measurements were made between the dashed lines and it can be seen that the aerosol was spread longitudinally around the globe at this time. Inhomogeneities of continental and smaller sizes were still present, and the highest concentrations of stratospheric material were seen to the north of 50°N latitude. This effect is shown most clearly in Fig. 4.4, where the zonally averaged data are displayed as a function of height and latitude. Measured values of optical depth for the northern hemisphere varied from the typical pre-eruption value (for a 1.000 μm wavelength) of 1.0×10^{-3} to highs of greater than five times this value. The average optical depth for the northern hemisphere in August was greater than that observed immediately after the eruption. This condition probably indicates that a significant gas-to-particle conversion has already taken place. Vertical shearing was still very evident and movement of the upper layers (above 20 km) since the eruption could be traced and compared with that expected from high-altitude air movements. These movements have been discussed in much more detail in chapter 2.

The August optical depth map (Fig. 4.3) has been used to estimate the mass of aerosol produced by the volcano in the stratosphere at that time. This calculation involves certain assumptions concerning the amount of background aerosol present at the time of the eruption and the nature of the volcanic aerosol. The background aerosol has been estimated from earlier SAGE data and it has been assumed that the new aerosol is a sulfuric acid/water/ammonium sulfate mixture in the approximate proportions 9:3:4 (Russell et al., 1981). The particle size distribution has been modeled using available dustsonde measurements made since the eruption (Rosen and Hofmann, 1980). Calculations indicate a prevolcanic stratospheric aerosol loading in the northern hemisphere of approximately 0.3×10^6 tonnes (metric ton) and a stratospheric volcanic injection of about 0.3×10^6 tonnes. Corresponding average aerosol mass densities in the stratosphere are $0.1 \mu\text{g m}^{-3}$ for the background (10 km layer thickness) and about $0.3 \mu\text{g m}^{-3}$ for the new volcanically enhanced stratospheric aerosol (4 km layer thickness). This mass estimate is compared with those from other recent eruptions in Table 4.1.

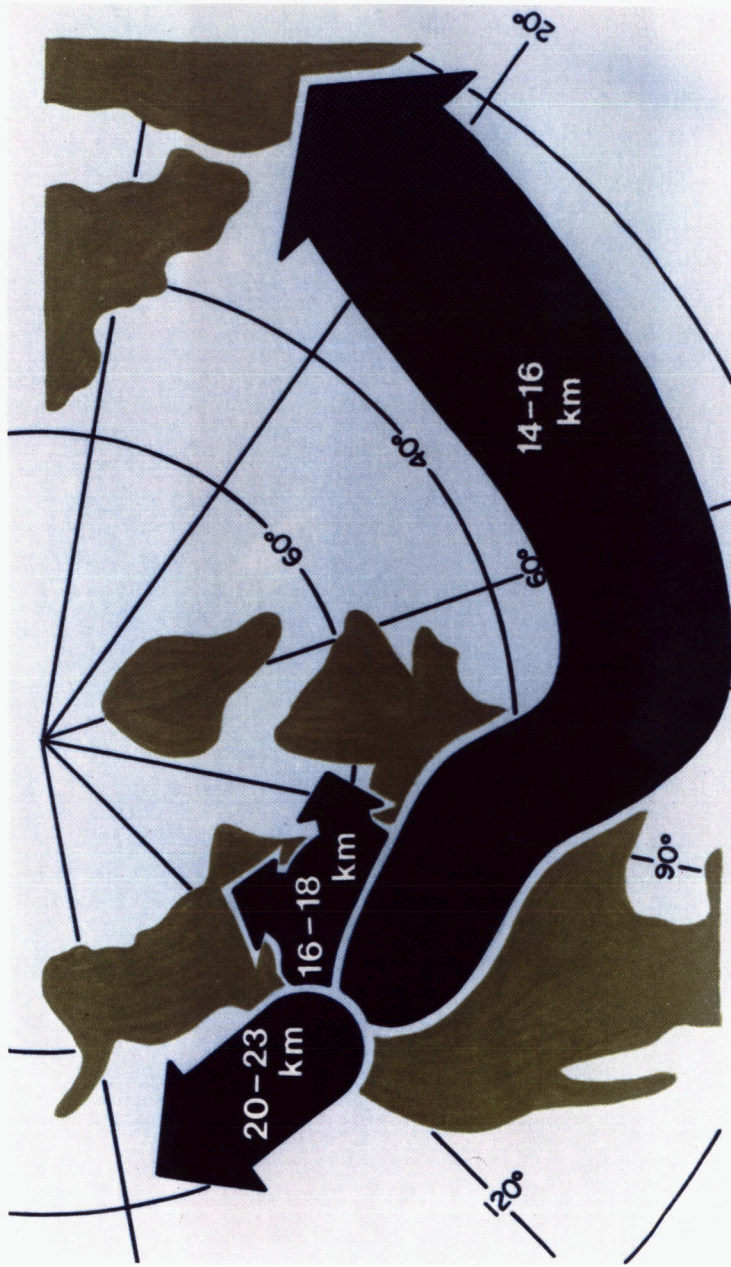


FIGURE 4.2 SAGE map of the stratospheric aerosol distribution for 23-29 May 1980. The differential motion of material at separate altitudes is very apparent.

SAGE MEASUREMENTS OF OPTICAL DEPTH
ABOVE MODEL TROPOAUSE + 2 KM
JULY 21 - AUGUST 26, 1980

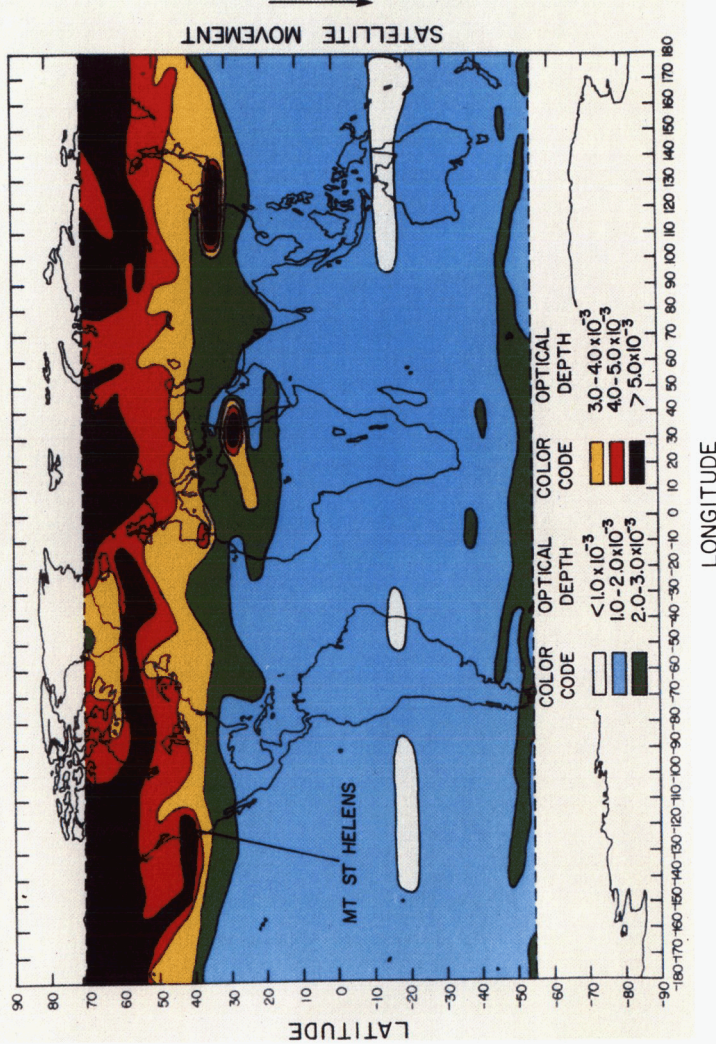


FIGURE 4.3 SAGE map of the stratospheric optical depth, 21 July to 26 August 1980. SAGE observations are confined to the regions between the dashed lines. Note the heavy concentration of the material toward the north.

SAGE MEASUREMENTS OF ZONAL MEAN EXTINCTION
 JULY 21-AUGUST 26, 1980
 SHOWN AS A FUNCTION OF HEIGHT AND LATITUDE

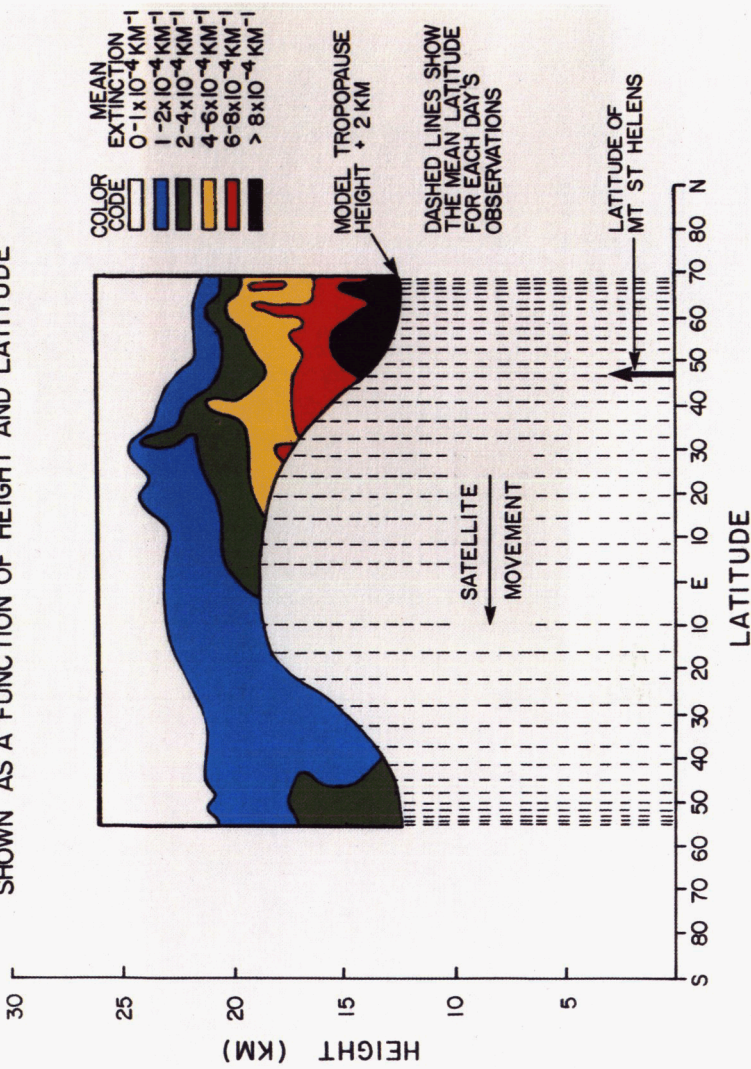


FIGURE 4.4 SAGE measurements of zonal mean extinction, 21 July to 26 August 1980, shown as a function of height and latitude. The heaviest concentrations of material occur north of latitude 40°N and just above the tropopause.

TABLE 4.1 Estimates of Stratospheric Aerosol Mass Loading for Recent Volcanic Eruptions

Date	Volcano	Added stratospheric aerosol (megatonnes)	Reference
March 1963	Agung	≈30	1,2
October 1974	Fuego	≈ 6	1,2
		3	3
January 1976	St. Augustine	≤ 0.6	2
April 1979	Soufriere	≤ 0.003	4
May 1980	St. Helens	0.3	This study

1. Cadle, R. D., C. S. Kiang, and J. F. Louis (1976).
2. Cadle, R. D., F. G. Fernald, and C. L. Frush (1977).
3. Lazarus, A. L., R. D. Cadle, B. W. Gandrud, J. P. Greenberg, B. J. Huebert, and W. I. Rose, Jr. (1979).
4. McCormick, M. P., G. S. Kent, G. K. Yue, and D. M. Cunnold (1981)

SAGE is continuing to make global measurements of stratospheric extinction. As further data sets from SAGE, and those from SAM II, become available for analysis, it will become possible to perform a number of interesting studies. For example, studies of the length of time for the gas-to-particle conversion processes to produce a maximum aerosol content and then be offset by the various cleansing mechanisms; to delineate the movement of material into the southern hemisphere; and, in general, by using this enhanced aerosol as a "seed," to study global circulations over the following seasons.

4.2.2 Lidar Measurements

Lidar measurements are made by observing laser backscattering from atmospheric molecules and aerosols as a laser pulse propagates through the atmosphere. The received signal is range resolved and the quantity of aerosol backscattering is dependent on the optical scattering properties and amount of aerosols present. A convenient measure of the aerosol backscatter is the lidar backscatter ratio, defined as the ratio of total backscattering (molecular plus aerosol) to the molecular backscattering. Details of the analysis procedure used in the processing of data are given in Russell et al. (1979). Lidar ratios of 1.1, for example, indicate that aerosol particles are backscattering 10% as much as the local gas molecules. Values of 1.1 for ruby lasers operating at a

wavelength of $0.6943 \mu\text{m}$ are typical of the background conditions before the Mount St. Helens eruption. The normal height range examined for stratospheric aerosols extends from regions near the tropopause to about 30 km, with the peak backscattering values generally occurring about 6 km above the tropopause.

As an example of the long-term time history of the stratospheric aerosol concentrations through the summer of 1980, presented in Fig. 4.5 are the results of lidar observations at Hampton, Virginia (37°N , 76°W), obtained with the NASA Langley Research Center's (NASA-LaRC) 48-inch lidar system. This plot shows the time history of the peak backscatter mixing ratio (total lidar backscatter ratio minus one) in the stratosphere made at a wavelength of $0.6943 \mu\text{m}$. Indicated are a few of the major volcanic eruptions over this time period thought to have injected significant amounts of material into the stratosphere. The details of buildup and decay of stratospheric material following the eruption of de Fuego in October 1974 are described in McCormick et al. (1978). The new stratospheric material from this volcano was shown to have an e-folding time of about 12 months; a similar lifetime can be expected for the Mount St. Helens case.

In order to examine the dispersion of the Mount St. Helens material at different altitudes, Fig. 4.6 shows the value of the lidar peak backscatter ratio obtained with the 48-inch lidar system for two different heights. The solid curve represents the measurements of a high-altitude layer between 20.5 and 23 km while the dashed curve gives the time history of the material between 17 and 19.5 km. The first measurement of the main stratospheric layer at Hampton occurred on 4 June, while the higher altitude layer was first observed on 6 July. This upper layer evidently traveled around the world in about 56 days in a westerly direction from Mount St. Helens.

In addition, measurements were made with a NASA-LaRC airborne lidar system in the 21 May to 27 May time period. The lidar detected various parts of the total volcanic material as it moved eastward across the eastern United States of America. The results indicated very intense layers in the 12 to 16 km region with backscatter ratios ranging from 4 to 100 at the ruby wavelength, $0.6943 \mu\text{m}$. Analyses of these data, together with lidar measurements at $1.060 \mu\text{m}$ (Nd-Yag laser), as well as lidar depolarization measurements, suggest that these initial low stratospheric clouds were probably composed of silicate-type particles; that is, their scattering characteristics indicate they have a higher than normal refractive index and are irregularly shaped (McCormick, 1980).

Other northern hemisphere stratospheric lidar measurements have also been made in the time period following the eruption on 18 May. These locations include observations made from Nagoya, Japan (35°N , 137°E),

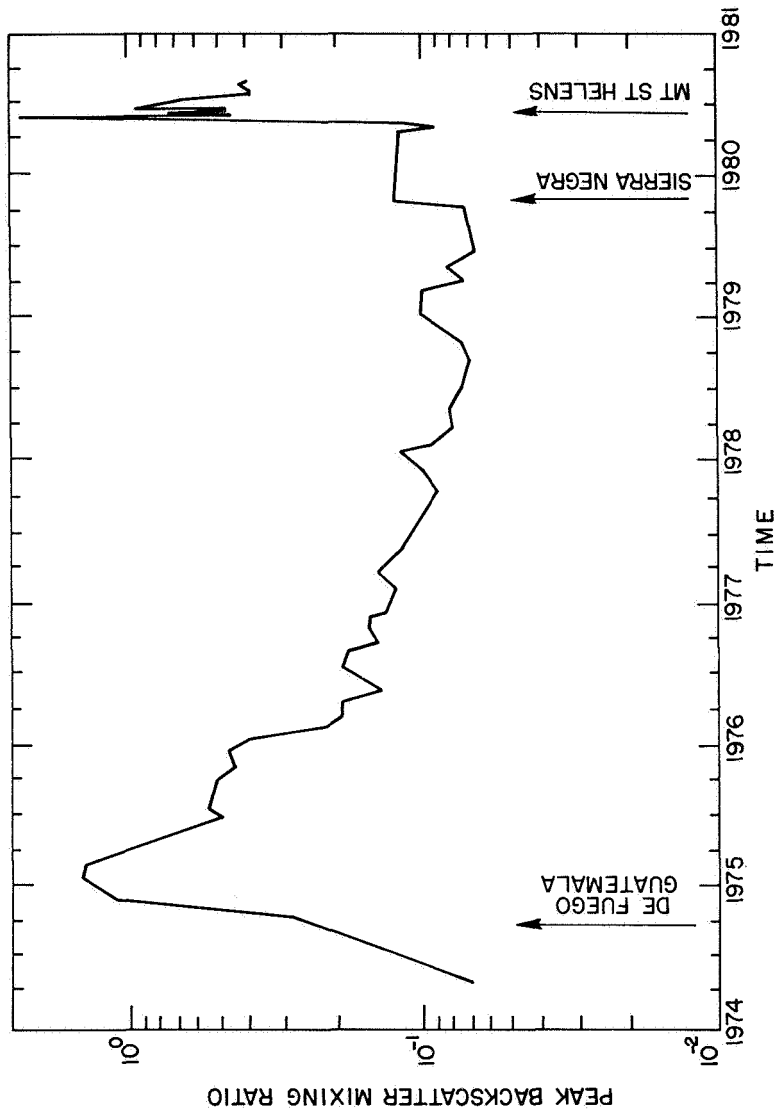


FIGURE 4.5 Variation of the lidar peak backscatter ratio minus one, obtained at Hampton, Virginia (37.9°N , 76.3°E) between 1974 and 1980. The sharp rise and decay following the de Fuego eruption is clearly visible, as is a smaller enhancement following the Sierra Negra eruption and a large enhancement following the Mount St. Helens eruption.

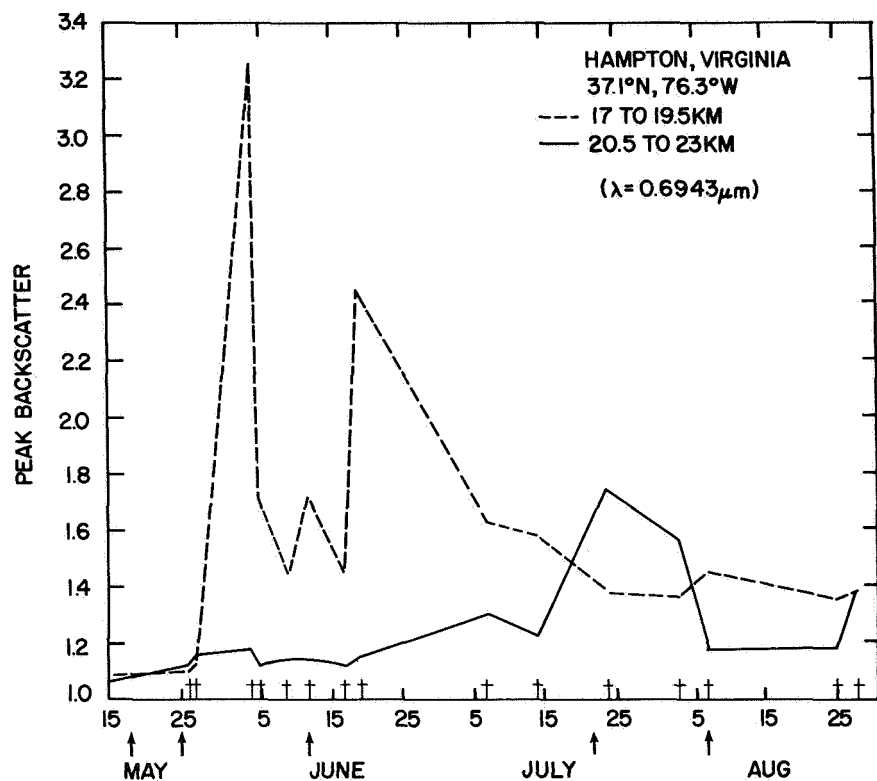


FIGURE 4.6 Variation of the lidar peak backscatter ratio for two altitude ranges obtained at Hampton, Virginia (37.9°N, 76.3°E) following the 18 May 1980 eruption. Note that the ratio for the lower altitudes increased very soon after the eruption but that the ratio for the higher altitudes did not increase until about 2 months after the eruption. The † indicate measurement days and the ↑ indicate the major MSH eruptions

Garmisch-Partenkirchen, West Germany (48°N , 11°E), Haute Provence, France (44°N , 6°E), Laquila, Italy (42°N , 23°E), Madison, Wisconsin (43°N , 89°W), Urbana, Illinois (40°N , 88°W), Boulder, Colorado (40°N , 105°W), and Slough, England (51°N , 1°W). Some of these data are presented in Figs. 4.7 and 4.8. They were kindly provided by each of the laboratories for use in this document. The lines with arrows (in Fig. 4.7) or the shaded area drawn on the graph (in Fig. 4.8) for the specific altitudes, were derived from a zonal wind model compiled by Newell et al., 1972. Figure 4.7 plots data for the first observation of the arrival over the site of layers between 12 and 15 km and Fig. 4.8 for those above 20 km. Also indicated are observations made by the SAGE satellite and by the University of Wyoming's balloon-borne dustsonde instrument. It can be seen that the dates of arrival of these layers at the various stations generally agree with the predictions based on average wind profiles and are consistent with each other. This is particularly true for the layers at altitudes higher than 20 km that moved in a westerly direction more slowly as shown in Fig. 4.8.

Later measurements made by the NASA-LaRC 48-inch and airborne lidar systems suggest that by November 1980 the volcanic layers had become much more homogenized in the northern hemisphere. Typically, this main post-volcanic stratospheric layer extended from slightly above the tropopause through 22 km with a peak ruby lidar backscatter ratio of 1.35 at 17.5 km. The higher altitude layer (20 to 23 km), first observed over Hampton on 6 July, was occasionally present at this time. Its backscatter ratio at $0.6943\text{ }\mu\text{m}$ was as high as 1.2 to 1.3. It is thought that by this time the aerosols contributing to this observed backscattering profile are mostly sulfuric acid particles. Based on this assumption, optical model conversion procedures, as described in section 4.2.1 (Russell et al., 1981), were utilized to derive a volcanic increase to the stratospheric aerosol mass loading of from 0.3 to 0.7×10^6 tonnes, depending on the assumptions of the aerosol size distribution, composition, and geometric extent. This value is very similar to the mass loadings derived from the analysis of the SAGE measurements given in section 4.2.1.

4.2.3 Balloon Photographs

The volcanic material that moved eastward in the lower stratosphere was also detected by photography of the earth's limb at low solar elevation angles from a high-altitude balloon package (Ackerman et al., 1980, see color illustration C.4). The photograph from 5 June 1980, taken at 44°N and 2°E from 35.2 km, shows large enhancements in scattered sunlight from horizontally stratified aerosol layers near 16 km. A photograph taken under similar experimental conditions on 5 May 1980, before the Mount St. Helens eruption, shows the absence of these layers. Densitometric measurements of the film show enhancements in limb radiance of a factor of three at 15 km. Layers are discernible from 100 meters to several kilometers in vertical thickness.

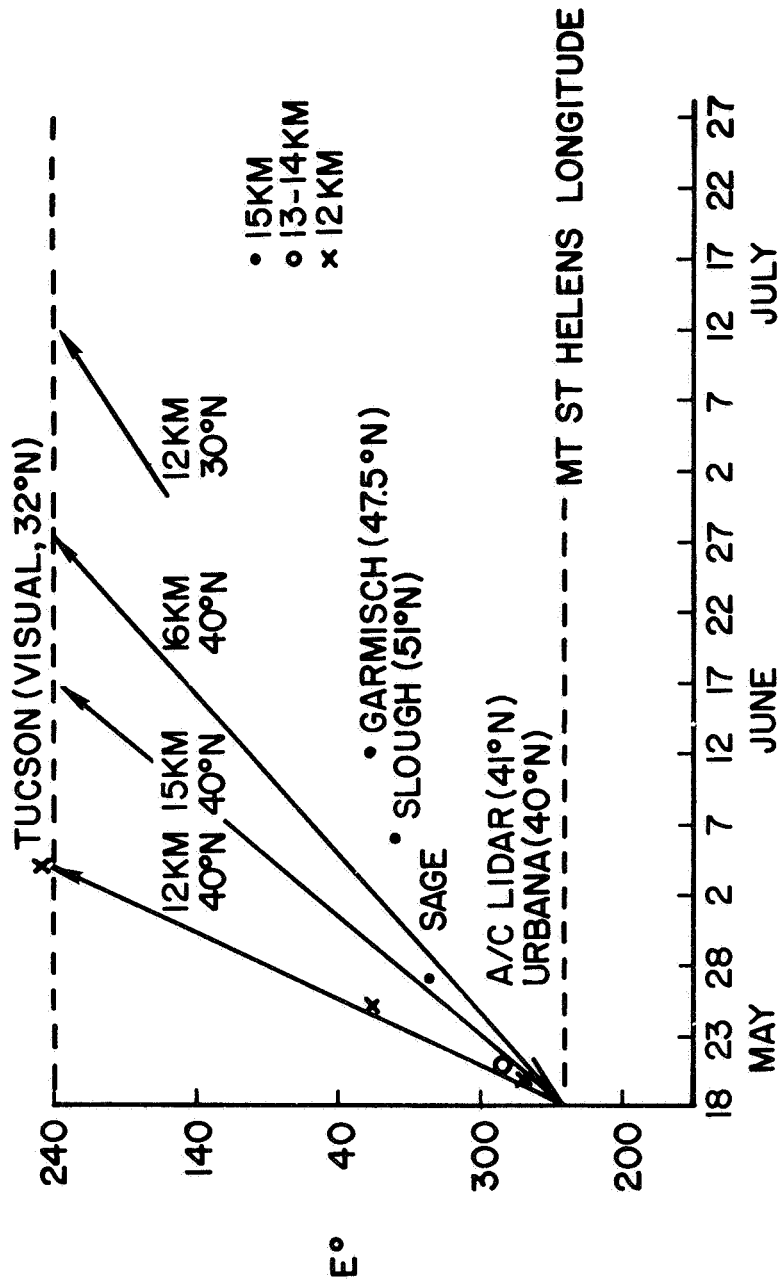


FIGURE 4.7 Times of arrival of aerosol layers between 12 km and 16 km as observed by various lidar stations around the globe. The straight lines show the expected air movements at the latitudes and heights involved (Newell et al., 1972).

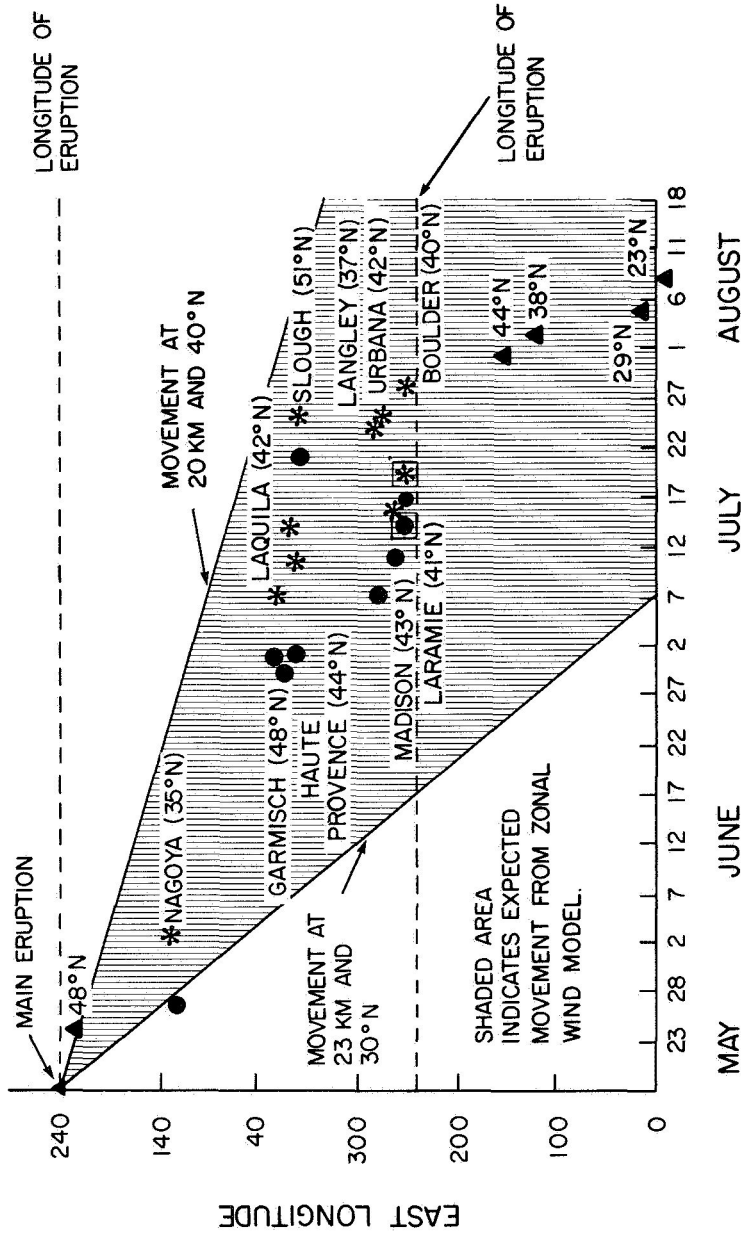


FIGURE 4.8. Times of arrival of aerosol layers above 20 km as observed by various lidar stations around the globe.
 * Layer at 20 to 22 km. • Layer at 22 to 24 km. The cross-hatched area represents the average expected range of stratospheric air movements. Also shown are the dates, latitudes and longitudes of SAGE observations (▲) and of dustsonde observations (■ and □) made at Laramie, Wyoming.

The arrival at this particular time and geographic position of volcanic material is also consistent with all the aforementioned measurements.

4.2.4 Radar Measurements

National Weather Service radar observations were made of the eruptive columns from Portland, Oregon, and Auburn, Washington. Detailed measurements of the column height for the 18 May and later eruptions were taken and are described in Chapter 1. The principal features of these measurements, which corroborate the worldwide remote sensor measurements, are the following:

1. The 18 May eruption showed the greatest column height (greater than 24 km) and duration (ash emission reached above 12 km for about 9 hours).
2. Column heights for the later eruptions did not exceed 15.2 km (eruption of 12 June) and their durations did not exceed 30 minutes (eruption of 26 May).

4.2.5 Ground-Based Passive Optical Measurements

This section describes the ground-based passive optical techniques which appear useful for studying the character of the dust veil from volcanoes. They include the following:

1. *Small field-of-view solar photometry* in which extinction is measured in one or more narrow wavelength bands chosen to avoid gaseous absorption. Total loading of dust can be estimated from a single wavelength and when extinction is measured at several wavelengths, estimates of the size distribution of particles are possible (King et al., 1978).
2. *Solar aureole photometry* in which the angular scattering pattern around the sun is measured. This technique yields information on the diffuse component and can be used to estimate particle size distribution up to about 10- μm radii (Deepak, 1977).
3. *Time-lapse color photography* of the sky, which is largely qualitative but can give important information on dust veil spatial structure and motion, and on optical effects such as halos and coloration, which can be indicative of particle size (Lerfeld, 1980; Ackerman et al., 1980).
4. *Wide bandwidth photometry*, such as recorded by standard pyranometers and normal incidence pyrheliometers. This technique has the drawback that gaseous absorption effects are merged with the effects caused by dust, but they have the distinct advantage of being deployed in observing networks with data taken routinely (Russell and Uthe, 1977).

As an example of the narrow bandwidth photometric results, Fig. 4.9 shows the ratio of extinction measured at Boulder, Colorado, following the 18 May eruption to the “clean atmosphere” extinction [from Valley (1965)]. The

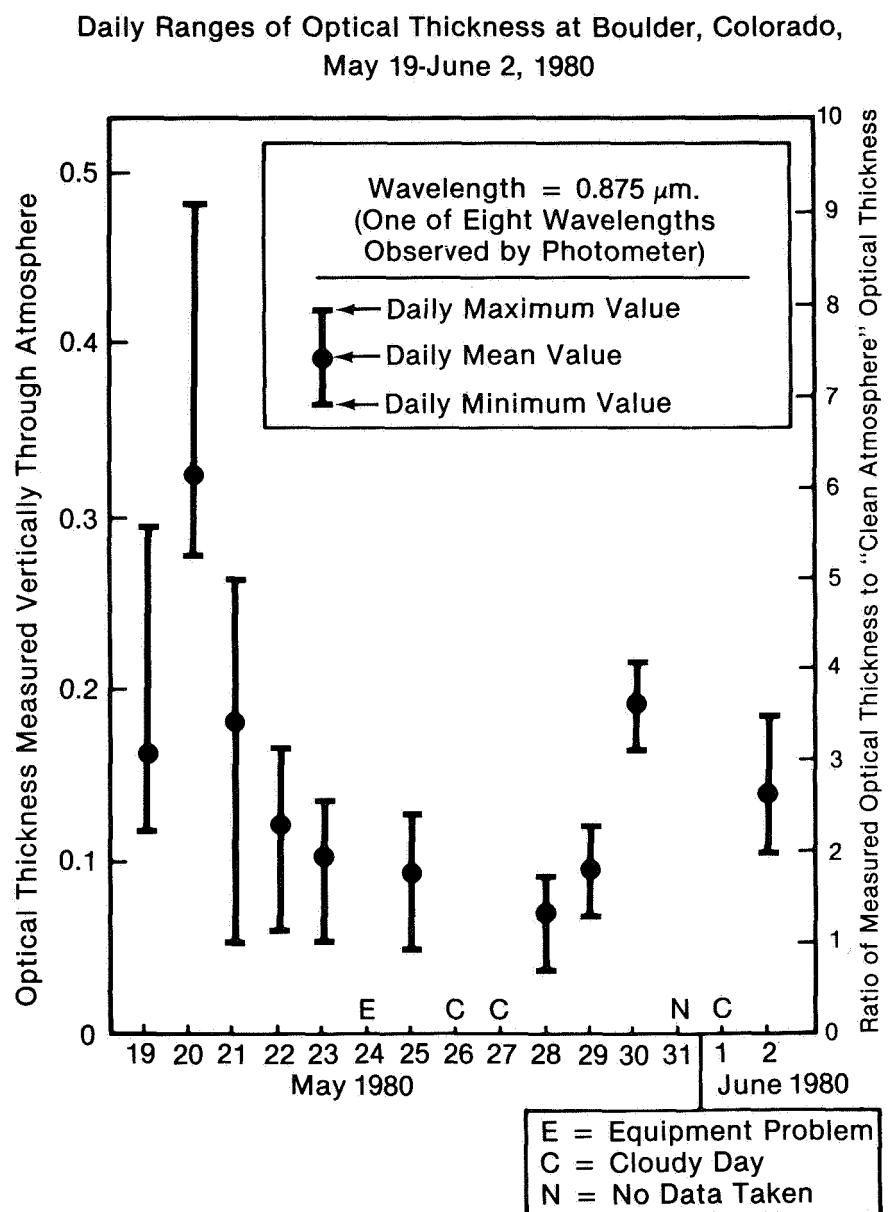


FIGURE 4.9 Daily variation of optical thickness at a wavelength of $0.875 \mu\text{m}$, observed at Boulder, Colorado, during 19 May to 2 June 1980.

maximum, minimum, and mean values of this ratio for each day at the wavelength $0.875 \mu\text{m}$ are shown. Corresponding optical depths are listed on the left ordinate of the figure. The passage of the airborne effluents from the 18 May eruption can be seen on the 19th and on several days thereafter. Values of optical depth as high as 0.48 were recorded. An indication of increased extinction due to the 25 May eruption can also be seen.

An analysis by DeLuisi et al. (1980) of the National Oceanic and Atmospheric Administration (NOAA), Boulder, Colorado, of the ratio of the change in diffuse to direct transmitted solar radiation (in a narrow bandwidth) for 2 days (3-4 June) showed that the volcanic material that passed overhead was weakly absorbing with an imaginary component of the refractive index of less than 0.005 at $0.4915 \mu\text{m}$. The volcanic material observed strongly overhead at Boulder on 3 June was assumed to have circled the globe from the 18 May eruption, being part of the material at jet stream altitudes.

In July the NOAA lidar system at Mauna Loa detected volcanic material overhead. The transmission (total solar spectrum) decreased during this period by less than 0.003 as measured with a pyrheliometer. This technique is explained in Mendonca et al. (1978). A long-term set of these data is shown in Fig. 4.10 where a 6-month running mean of transmission since 1958 is plotted. The effects of the eruptions of Mt. Agung in 1963 and de Fuego in 1974 are easily seen.

4.2.6 Radiative Properties as Inferred by Satellite Measurements

Effects of the Mount St. Helens volcanic cloud on the radiation budget parameters measured by the NOAA-6 Advanced Very High Resolution Radiometer (AVHRR) have been examined by researchers at NOAA's National Environmental Satellite Service, Suitland, Maryland. Based on differences observed in these parameters in the Wyoming-Montana region between 19 May, when the cloud was present, and 21 May, when the cloud had moved east of the region, the following preliminary conclusions have been made:

1. The albedo in this region was greater on 19 May by up to a factor of two with a value of 30% to 35%.
2. The longwave emission to space was lower on 19 May by $20\text{-}80 \text{ W m}^{-2}$ depending on location in the region.
3. The net radiation (difference between absorbed solar and emitted thermal radiation) was lower by $35\text{-}50 \text{ W m}^{-2}$ on the 19th. This latter result is consistent with the findings of Ohring and Clapp (1980) where the albedo effect dominates the "greenhouse" effect for tropospheric clouds.

The issue of whether these changes were entirely due to the volcanic cloud or not is still under examination.

Another study examined the radiative effects of the volcanic plume as measured by the High Resolution Infrared Radiation Sounder (HIRS-2)

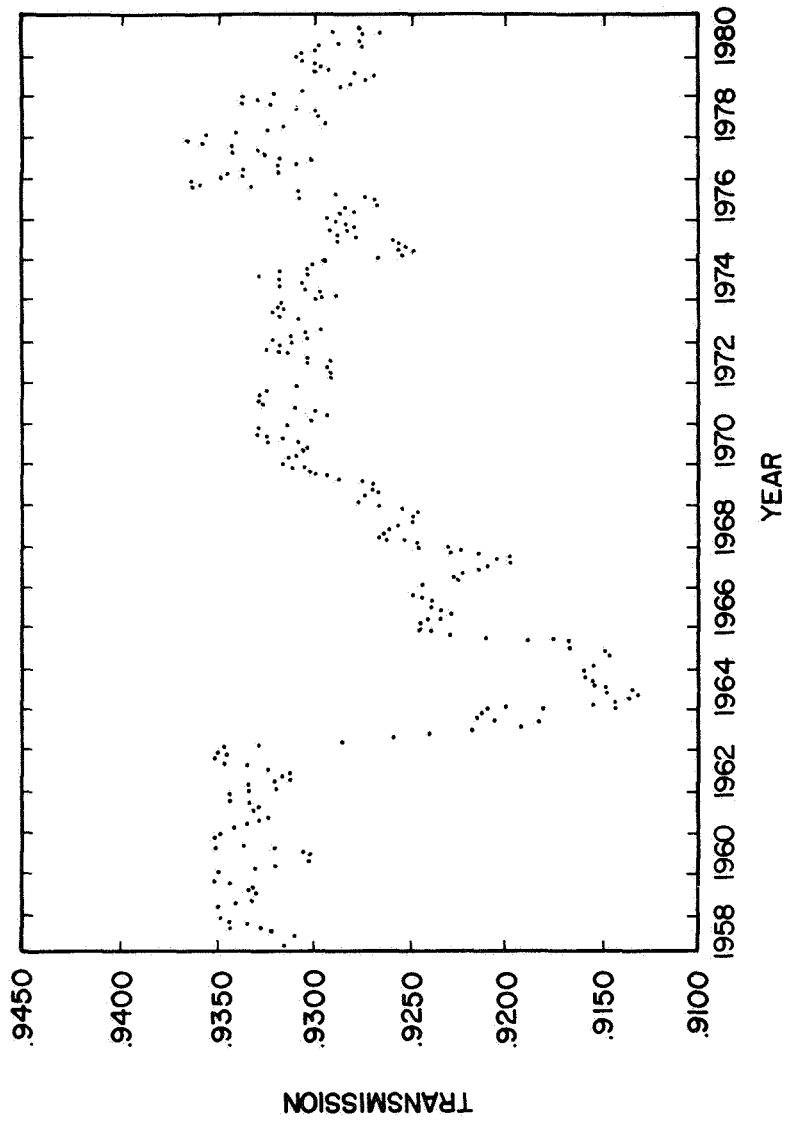


FIGURE 4.10. Six-month running means of atmospheric transmission as measured by a pyrheliometer on Mauna Loa, Hawaii.

instrument on the TIROS-N satellite at about 1500 hours local time on 19 May. Differences in the equivalent blackbody temperatures of the ash cloud from the surrounding clear sky were largest in the 11 μm window, 9.6 μm O₃ absorption channel, and 6.3 μm H₂O absorption channel. These values were about 27 K, 19 K, and 10 K lower in the cloud, respectively.

A computer-enhanced Geosynchronous Operational Environmental Satellite (GOES)-West image, for the 10.5- to 12.5- μm window channel about 10 hours after the 18 May eruption was also evaluated. The equivalent blackbody temperature of the volcanic cloud ranged from 215 K to 230 K. When compared with nearly coincident radiosonde data from Spokane, Washington, and assuming the cloud to be perfectly absorbing, the "effective" cloud altitude for this wavelength is somewhere between 8.5 and 11.5 km. Detailed trajectory analysis using GOES data has been discussed in Chapter 2.

4.2.7 Sulfur Dioxide Measurements

Sulfur dioxide (SO₂) has a strong absorption band in the 0.3 μm wavelength region. The majority of the remote measurements of SO₂ concentrations in the plume were made using correlation spectrometers operating in this wavelength region. Correlation spectrometers use a gas cell containing the compound of interest in one path of an optical system and compare this signal with that through another path using an empty cell. This technique has the advantage that it obtains a signal from all the absorption lines present in the spectrum rather than the single line observed with a conventional spectrometer. Hence, it generally has a greater sensitivity to the species of interest. The source used for all measurements consists of scattered sunlight which contains absorption features due to constituents present in the atmosphere above the instrument.

Correlation spectrometers equipped to measure SO₂ were operated from the ground close to Mount St. Helens from 29 March 1980, and aircraft measurements have been made from 29 March until the present (Harris et al., 1980; Moyers, 1980). In addition, one measurement of the SO₂ content of one of the plumes from the 18 May eruption was obtained from a ground-based measurement by two ozone spectrophotometers (Brewer and Dobson units). They were operated by the Canadian Atmospheric and Environment Service at Downsview, Ontario (Kerr et al., 1980). Since a study of the effects of atmospheric SO₂ on the measurement of ozone by such instruments was in progress, the identification of the anomalous absorption observed on 20 and 21 May as being due to SO₂ associated with the plume from the 18 May eruption was straightforward.

The SO₂ concentration data obtained close to the volcano have been combined with data on the plume size and wind velocity to determine the SO₂ flux from the volcano. The Canadian measurement appears to be associated with that portion of the plume confined to the troposphere. The fluxes obtained by the various groups are summarized in Table 4.2.

TABLE 4.2 SO₂ Flux Measurements

<i>(a) Correlation spectrometry measurements (Harris et al., 1980)</i>	
<i>Date</i>	<i>SO₂ emission rates</i>
<i>29 March-14 May</i>	<i>10-50 tonnes day⁻¹</i>
<i>25 May-10 October</i>	<i>130-3,400 tonnes day⁻¹</i>
<i>5 June-10 October</i> <i>(nونeruptive periods)</i>	<i>Total emission ≈ 150,000</i>
<i>(b) Dobson and Brewer spectrophotometers (Kerr et al., 1980)</i>	
<i>Date</i>	<i>SO₂ column loading</i>
<i>Normal background</i>	<i>0.003-0.005 cm</i>
<i>20-21 May</i>	<i>0.010-0.060 cm</i>

4.3 CONCLUSIONS

A summary of conclusions derived from remote sensing measurements is given as follows.

1. Material reached at least 23 km based on lidar and SAGE data. Local radar showed the eruption column to reach at least 24 km with several lower maxima during the day.
2. Distinct enhancements (layers) at various altitudes and geographic locations to 23 km were produced.
3. Early after the eruption (≤ 2 months) layers at a given altitude had a limited horizontal extent.
4. Layers from 10 to 14 km moved rapidly eastward circuiting the globe in as soon as 16 days. Lidar scattering ratios for the near 14-km material were as large as 100 at 0.694 μm. (Background ratios are approximately 1.1 at this wavelength.) Extinction coefficients as high as 0.01 km⁻¹ were measured at 1.0 μm.
5. The 15- to 16-km layers moved eastward more slowly, crossing the US eastern coast on 23 May, reaching Europe no later than 5 June.
6. The 18-km layer moved in a more complex manner, reaching the eastern US coast on about 4 June.

7. The material above 20 km moved westward with enhancements in lidar backscatter observed at various locations at heights of approximately 23 and 21.5 km with the higher layer occurring earlier indicating a faster global movement. The averages being 8 m/sec and 6 m/sec for the two layers (~ 56 and 70 days to circle the globe, respectively). Immediately after the eruption, extinction coefficients of $\sim 0.01 \text{ km}^{-1}$ at $1.0 \mu\text{m}$ were observed in highly concentrated geographic regions.

8. Stratospheric optical depths for the northern hemisphere in August showed large meridional and zonal variations over scales of 1000 km. Values ranged from 0.001 to greater than 0.005 (at $1.0 \mu\text{m}$).

9. Ground-based optical depths as high as 0.48 at $0.875 \mu\text{m}$ were recorded at Boulder on 20 May. A typical clear atmosphere value is 0.053.

10. Changes in stratospheric optical depth over Mauna Loa in July were less than 0.003.

11. By September the 14- to 20-km material had lost its fine vertical structure and appeared as one broad layer centered at about 18 km. The material above 20 km had more or less merged into one layer which still exhibited a patchy nature.

12. Mass calculations for the stratospheric injection gave 0.3 to 0.7×10^6 tonnes based on US lidar data and 0.3×10^6 tonnes based on SAGE data. Corresponding average mass densities for the northern hemisphere were 0.4 to $0.6 \mu\text{g m}^{-3}$ and $0.3 \mu\text{g m}^{-3}$ (using a 4-km thick layer). This is to be compared with a pre-eruption value of $0.1 \mu\text{g m}^{-3}$ (using a 10-km thick layer).

13. A comparison of the estimates of stratospheric aerosol mass loading for recent volcanic eruptions is given in Table 4.1.

14. The NOAA-6 AVHRR measurements showed that the dust cloud on 19 May increased the albedo in the area covered by the cloud (Montana and Wyoming) by a factor of two.

15. Local (in the vicinity of the volcano) radar measurements gave maximum altitudes for eruptions after 18 May that did not exceed 16 km. These eruptions lasted for less than 30 minutes as compared to the 9 hour 18 May eruption.

4.4 RECOMMENDATIONS

For the first time, the remote sensing community was in the position to rapidly measure volcanic effluents and their dispersion on a global scale. This was possible, primarily, because of the two satellites (SAM II and SAGE), specifically designed to measure global stratospheric aerosols. These were augmented by a number of ground-based lidars spread about the northern hemisphere which provided point measurements of the altitude and time of arrival of various volcanically produced layers. Both provided a capability, through optical modeling, of calculating the enhancement in stratospheric

aerosol mass caused by Mount St. Helens and, in addition, the corroboration of dispersion analyses. This data set, along with the ground-based transmission data set, will be invaluable for assessing any potential climate effect due to this eruption. Complementing these data was the local radar whose data are useful in describing the source as a function of time and the satellite imaging data for its early dispersion. All these remotely sensed data will also assist in various climate and atmospheric studies including determining the microphysics of the gas-to-particle conversion process that occurred in the effluent with time.

Listed below are a number of recommendations, with respect to remote sensing, that would optimize the climate and atmospheric assessment of future volcanic eruptions.

1. The continued use of SAM II and SAGE, and in the future, satellites similar to SAM II and SAGE, should be maintained or deployed in order to establish and continue a global stratospheric aerosol climatology. More wavelengths, and possibly, near forward scattering capabilities should be added to further characterize the aerosol parameters important in radiative calculations.

2. Other satellite techniques should be developed (e.g., limb scattering and shuttle lidar) which would provide more data per spacecraft revolution and more of a tropospheric capability. Shuttle lidar flights of even limited duration would complement the SAGE-type measurements.

3. The continued use of lidar is also strongly recommended. Their establishment in the southern hemisphere and at equatorial and high latitudes are urged. Improvements, such as increased simultaneous wavelength and depolarization measurement capabilities, are encouraged. These would help delineate, for example, ash-like from sulfate-like particles.

4. The use of airborne lidar systems should be continued so that an all-weather capability exists, as well as the capability to underfly satellite sensors and to perform extended regional measurements. An aircraft-mounted lidar can be flown above clouds which would normally prevent ground-based measurements from being made.

5. Early measurements of SO₂ flux within the downwind plume from future eruptions should be made from airborne platforms similar to those used, for example, in the Research on Atmospheric Volcanic Emissions (RAVE) program. A capability to remotely sense stratospheric SO₂ flux is needed also.

6. The study of the feasibility of satellite SO₂ measurements should be encouraged.

7. A carefully planned and calibrated network of ground-based sensors, capable of measuring diffuse and direct solar radiation should be created along with an examination of the feasibility of using other ground-based data for providing more information on the overhead aerosol. Along these lines, a

careful look at the World Meteorological Organization's (WMO) turbidity network and the NOAA Geophysical Monitoring for Climatic Change (GMCC) network should be made.

8. The feasibility of characterizing tropospheric aerosols from satellite platforms should be determined. Shuttle lidar and a properly designed imaging system are potential candidates.

ACKNOWLEDGMENTS

The panel wishes to thank the many researchers who so kindly provided their data, much of which were unpublished, for use in this report. A special thanks goes to the lidar groups listed below and the SAGE science team.

Researchers providing lidar data include: A. D'Altorio, Guido Visconti, and G. Fiocco*, Instituto di Fisica, Universita dell'Aquila (*Universita di Roma); J. J. DeLuisi, V. Derr, R. Fegley, and T. McNice, NOAA-ERL, Boulder, Colorado; E. W. Eloranta, University of Wisconsin, Madison, Wisconsin; C. S. Gardner, C. F. Sechrist, Jr., and J. D. Shelton, University of Illinois, Urbana, Illinois; Y. Iwasaka and S. Hayashida, Nagoya University, Nagoya, Japan; J. Lefrere, J. Pelon, C. Cahen, A. Hauchecorthe, and P. Flamant* (provided by Marie-Lise Chanin, *Laboratoire de Meteorologie Dynamique, Palaiseau, France), Service d'Aeronomie du CNRS, Verrieres-le-Buisson, France; R. Reiter, H. Jager, W. Carnuth, and W. Funk, Fraunhofer Institute for Atmospheric Environmental Research, Garmisch-Partenkirchen, FRG; and L. Thomas, C. P. Chaloner, and S. K. Bhattacharya, Rutherford and Appleton Laboratories, Slough, England.

The SAGE science team includes: D. M. Cunnold and G. W. Grams, Georgia Institute of Technology; B. M. Herman, University of Arizona, Tucson, Arizona; J. D. Laver, NOAA, Washington, DC; M. P. McCormick, NASA Langley Research Center, Hampton, Virginia; D. Miller, British Meteorological Office, Bracknell, England; D. G. Murcray, University of Denver, Colorado; T. J. Pepin, University of Wyoming, Laramie, Wyoming; and P. B. Russell, SRI International, Menlo Park, California.

4.5 REFERENCES

Ackerman, M., C. Lippens, and M. Lechevallier, 1980: Volcanic material from Mount St. Helens in the stratosphere over Europe. *Nature*, 16, 614-615.

Cadle, R. D., C. S. Kiang, and J. F. Louis, 1976: The global scale dispersion of the eruption clouds from major volcanic eruptions. *J. Geophys. Res.* 81(18), 3125-3132.

Cadle, R. D., F. G. Fernald, and C. L. Frush, 1977: Combined use of lidar and numerical diffusion models to estimate the quantity and dispersion of volcanic eruption clouds in the stratosphere: Volcan Fuego, 1974 and Augustine, 1976. *J. Geophys. Res.* 82(12), 1783-1786.

Deepak, A., 1977: Inversion of solar aerosol measurements for determining aerosol characteristics. *Inversion Methods in Atmospheric Remote Sounding* (A. Deepak, ed.). Academic Press, New York.

DeLuisi, J. J., B. G. Mendonca, and K. J. Hanson, 1980: Measurements of stratospheric aerosol over Mauna Loa, Hawaii and Boulder, Colorado. Paper presented at NASA Workshop on Mount St. Helens Eruption: Its Atmospheric Effects and Potential Climatic Impact (Washington, D.C.), November 18-19.

Harris, D. M., T. J. Casadevall, D. A. Johnston, W. I. Rose, T. J. Bornhorst, R. E. Stoiber, L. L. Malinconico, and S. N. Williams, 1980: Contributions of CO₂ and SO₂ to the atmosphere from volcanic activity at Mount St. Helens. Paper presented at NASA Workshop on Mount St. Helens Eruption: Its Atmospheric Effects and Potential Climatic Impact (Washington, D.C.), November 18-19.

Kerr, J. B., W. F. J. Evans, and C. L. Mateer, 1980: Measurements of SO₂ in the Mount St. Helens debris. Paper presented at NASA Workshop on Mount St. Helens Eruption: Its Atmospheric Effects and Potential Climatic Impact (Washington, D.C.), November 18-19.

King, M. D., D. M. Byrne, B. M. Herman, and J. A. Reagan, 1978: Aerosol size distributions obtained by inversion of spectral optical depth measurements. *J. Atmos. Sci.* 35, 2135-2167.

Lazarus, A. L., R. D. Cadle, B. W. Gandrud, J. P. Greenberg, B. J. Huebert, and W. I. Rose, Jr., 1979: Sulfur and halogen chemistry of the stratosphere and of volcanic eruption plumes. *J. Geophys. Res.* 84(C12), 7869-7875.

Lerfeld, G. M., 1980: Volcanic material from Mount St. Helens in the stratosphere over Europe. Paper presented at NASA Workshop on Mount St. Helens Eruption: Its Atmospheric Effects and Potential Climatic Impact (Washington, D.C.), November 18-19.

McCormick, M. P., G. S. Kent, G. K. Yue, and D. M. Cunnold, 1981: *SAGE Measurements of the Stratospheric Aerosol Dispersion Loading from the Soufriere Volcano*, NASA TP-1922.

McCormick, M. P., T. J. Swissler, W. P. Chu, and W. H. Fuller, Jr., 1978: Post-volcanic stratospheric aerosol decay as measured by lidar. *J. Atmos. Sci.*, 35, 1296-1303.

McCormick, M. P., P. Hamill, T. J. Pepin, W. P. Chu, T. J. Swissler, and L. R. McMaster, 1979: Satellite studies of the stratospheric aerosol. *Bull. Am. Met. Soc.*, 9, 1038-1046.

McCormick, M. P., 1980: Lidar measurements of Mount St. Helens Eruption, Paper presented at NASA Workshop on Mount St. Helens Eruption: Its Atmospheric Effects and Potential Climatic Impact (Washington, D.C.), November 18-19.

Mendonca, B. G., K. J. Hanson, and J. J. DeLisi, 1978: Volcanically related secular trends in an atmospheric transmission at Mauna Loa Observatory, Hawaii. *Science*, 202, 513-515.

Moyers, J., 1980: Results of the September 22, 1980, RAVE study of the Mount St. Helens plume. Paper presented at NASA Workshop on Mount St. Helens Eruptions: Its Atmospheric Effects and Potential Climatic Impact (Washington, D.C.), November 18-19.

Newell, R. E., J. W. Kidson, D. G. Vincent, and G. J. Boer, 1972: *The General Circulation of the Tropical Atmosphere, I*. Massachusetts Institute of Technology Press, Cambridge, Massachusetts.

Ohring, G., and P. Clapp, 1980: The effect of changes in cloud amount on the net radiation at the top of the atmosphere. *J. Atmos. Sci.*, 37, 447-454.

Rosen, J. M., and D. J. Hofmann, 1980: Dustsonde measurements of the Mount St. Helens dust cloud over Wyoming. Paper presented at NASA Workshop on Mount St. Helens Eruption: Its Atmospheric Effects and Potential Climatic Impact (Washington, D.C.), November 18-19.

Russell, P. B., T. J. Swissler, and M. P. McCormick, 1979: Methodology for error analysis and simulation of lidar aerosol measurements. *Appl. Opt.*, 18, 3783-3797.

Russell, P. B., T. J. Swissler, M. P. McCormick, W. P. Chu, J. M. Livingston, and T. J. Pepin, 1981: Satellite and correlative measurements of the stratospheric aerosol: I. A flexible optical model for data conversions. *J. Atmos. Sci.* 38(6), 1280-1294.

Russell, P. B., and E. E. Uthe, 1977: Atmospheric albedo changes measured in the Mount Sutro Tower Aerosol and Radiation Study. *Proc. IAMAP Symp. Radiation in the Atmosphere* (H. J. Bolle, ed.) pp. 513-515, Science Press.

Valley, Shea L., ed., 1965: *Handbook of Geophysics and Space Environments*, Air Force Cambridge Research Laboratories, Bedford, Massachusetts.

CHAPTER 5

CHEMISTRY OF THE MOUNT ST. HELENS EFFLUENT

5.1 INTRODUCTION

A rich variety of chemical compounds was injected into the atmosphere by Mount St. Helens, both in its large eruptions and in its continuing emission. In Table 5.1, these compounds are listed within chemical groups. The most abundant gases emitted were H_2O , CO_2 , and SO_2 . Of the reactive gases, SO_2 was predominant. Chapter 3 on *in situ* analysis provides details of composition. For some of the substances listed in Table 5.1, chemical processes that occur in the atmosphere can be specified or inferred on the basis of laboratory and field data. They are:

1. The chemical production of aerosols which affect the earth's radiation budget. The important species are the sulfur containing gases, together with water vapor.
2. The chemical interaction of volcanic gases (and perhaps volcanic aerosol surfaces) with the free-radical ozone chemistry of the stratosphere. The important species are H_2O and SO_2 , and perhaps reactive chlorine compounds, CO , and oxides of nitrogen.
3. The chemical influence of volcanic gases and aerosols on local and regional air quality, weather, and ecosystems. The important species are the sulfur gases and aerosols and perhaps compounds containing nitrogen and chlorine.

A number of compounds of Table 5.1 seem unlikely to produce any significant chemical effects, either as a result of their low chemical reactivities or their small volcanic emission fluxes, or both. These compounds include H_2 , CO_2 , N_2O , HF , CH_3I , CCl_4 , CFCl_3 , CH_3CCl_3 , CH_4 , and substances containing F^- and Br^- .

In each of these areas, SO_2 is the species of major importance because of its relatively large abundance in the volcanic emissions and its high reactivity in the atmosphere.

5.2 EARLY COMPOSITION AND DEVELOPMENT OF THE ERUPTION CLOUDS

As a first step in the preliminary assessment of the atmospheric chemical aspects of the effluents from the Mount St. Helens eruptions, brief summaries are presented of the chemical composition of the fresh material in the atmosphere, based on the detailed sampling and analyses described in Chapter 3.

TABLE 5.1 Chemical Compounds in Emission from Mount St. Helens

<i>Gases:</i>	<i>Oxygen-hydrogen compounds:</i>	$H_2O^{*†}$, H_2
	<i>Carbon oxides:</i>	$CO^{†}$, CO_2^*
	<i>Nitrogen compounds:</i>	NO , N_2O , HNO_3
	<i>Sulfur compounds:</i>	H_2S^* , $CS_2^{†}$, $OCS^{*†}$, $SO_2^{*†}$
	<i>Halogenated compounds:</i>	HF , $HCl^{†}$, $CH_3Cl^{*†}$, CH_3I , CCl_4 , $CFCl_3^*$, CH_3CCl_3
<i>Ions:</i>	<i>Alkanes:</i>	CH_4
	<i>Sulfates:</i>	$SO_4^{=†}$
	<i>Nitrates:</i>	$NO_3^-†$
	<i>Halides:</i>	$Cl^-^{*†}$, Br^- , F^-

* Detected by more than one observer

† Detected in the stratosphere

Specifically, the data used resulted from measurements made in the stabilized clouds in the stratosphere within a few days of the 18 May, 25 May, and 12 June eruptions. These synopses are necessarily mainly qualitative. Quantitative aspects may be attended by large uncertainties because of impossibility of obtaining spatially and temporally representative samples. However, as will be seen, a sensible general picture of the major chemical aspects emerges from such considerations.

5.2.1 Sulfur

On 19 May, 1 day after the most violent eruption of Mount St. Helens, samples of air taken between 13 and 18 km (Inn et al., 1981; Lazarus and Gandrud, 1981) showed high concentrations of SO_2 (\cong 10 to 100 ppbv) and low concentrations of sulfate [\cong 1 to 4 ppb; concentrations of sulfate (SO_4^-) are given as molecular mixing ratios; thus direct comparison can be made to the volumetric mixing ratios given for gases]. On 22 May however, at higher altitudes (18 to 21 km), the situation was reversed. A large quantity of SO_4^- (1 to 80 ppb) and a small quantity of SO_2 (0.1 to 4 ppbv) were found. In subsequent eruptions, this latter pattern was maintained, with measurements made after several days yielding $SO_4^-:SO_2$ ratios greater than unity. However, no single cloud was ever sampled more than once in any week-long period so there are no data suitable for reliably estimating the early-time rates of conversion of SO_2 to SO_4^- . Observed differences could be due in part to initial differences in composition and in part to varying conversion rates.

Reduced sulfur gases (H_2S , OCS , and CS_2) were not found in significant quantities (> 1 ppbv) in any of the Mount St. Helens clouds even 1 day after the eruptions. This was probably because the emissions contained small

amounts of reduced gases compared to SO_2 . However, it is possible that a gas such as H_2S was emitted in relatively large quantities but was oxidized in or removed from the stratospheric clouds within a day. The early tropospheric cloud was found by the University of Washington group (Hobbs et al., 1981) to have had apparently an unusually large relative H_2S content compared to SO_2 . In their samplings of the early stratospheric clouds, the NASA-Ames Research Center (NASA-Ames) group (Inn et al., 1981) were unable to detect any H_2S . Such findings prevent arriving at definitive conclusions concerning the relative importance of H_2S from Mount St. Helens.

5.2.2 Water Vapor

Water vapor is generally the most abundant gaseous effluent in volcanic eruptions. It is likely that this was the case for all the eruption plumes of Mount St. Helens. When the vapor-laden plume becomes mixed with cooler surrounding air, condensation upon wettable ash particles in the plume occurs. The liquid droplet or ice particles so formed would be subject to rainout in the troposphere. Any condensed water reaching or formed in the stratosphere would be subject to gravitational settling, which would provide a mechanism for depletion relative to other gaseous effluents which are essentially non-condensable under atmospheric conditions. The major eruptions of Mount St. Helens which had buoyant plumes extending into the stratosphere could have injected considerable quantities of water. However, after reaching thermal equilibrium, the resulting concentrations of water vapor would have been no greater than about 100 ppmv which is saturation for the prevailing stratospheric conditions. The excess water would have condensed, probably as ice, in the stratosphere and settling would eventually remove it to the troposphere. The findings by Murcray et al. (1981) and Inn et al. (1981) of water vapor concentrations in the range of 20 to 100 ppmv on 22 May between 18 and 20 km altitude are consistent with the above discussion of water vapor injection into the stratosphere by Mount St. Helens.

5.2.3 Chlorine

The principal chlorine-containing molecule in volcanic gases is HCl , which is very soluble in water. While some HCl gas may have been injected into the stratosphere by Mount St. Helens, it is expected that almost all of the emitted HCl would have been dissolved in cloud water and subsequently deposited on the surface in precipitation or as dry particulate chloride (the remaining material after evaporation of cloud water). Although the abundance of HCl in some volcanic gases is thought possibly to approach that of sulfur gases, the preceding discussion leads to the expectation that concentrations of volcanic HCl in the stratosphere should be considerably lower than those for volcanic sulfur. This is consistent with the observations of Lazarus and Gandrud (1981) who found the concentrations of acidic chlorine vapor

(about 1 ppbv probably as HCl) from Mount St. Helens to be of the order of 1% to 10% of the SO₂ concentrations. It is of interest that Inn et al. (1981) found that stratospheric concentrations of methyl chloride (CH₃Cl) in the Mount St. Helens cloud (1 to 5 ppbv) were as high as or higher than the concentrations of HCl. However, in view of the likely large tropospheric scavenging of HCl, it is seen that CH₃Cl is probably not the major volcanic chlorine species. Nonetheless, there is a possibility that the volcanic effluent which may most affect the ozone chemistry of the stratosphere is CH₃Cl.

5.2.4 Nitrogen Oxides

Cryogenic samples taken in the Mount St. Helens clouds by Inn et al. (1981) gave some indication of NO_x injections. Two samples from the 18 May eruption clouds apparently contained 50 to 200 ppbv of soluble nitrogen gas which produced nitrate upon addition of water. On the other hand, filter collections of HNO₃ vapor and particulate nitrate showed roughly background levels in all the clouds (Lazarus and Gandrud, 1981). It is problematical whether significant quantities of NO_x originated within the magma. Violent lightning activity associated with the eruption may have produced small and locally patchy concentrations of NO_x. Another possible nonvolcanic source of the NO_x may have been thermal decomposition of natural nitrosyl compounds of soils in the heated plume. Further study of the ash may allow insight concerning the possible magmatic origin of the oxides of nitrogen. In this regard it is of interest to note the detection in the RAVE study in the steady plume from Mount St. Helens in September 1980 of NO in concentrations of about 0.1 to 0.3 ppbv which was about three orders of magnitude smaller than the SO₂ concentrations (see the paper by Friend et al., 1981). Since the soils from within the crater should have lost all of their bound nitrogen by that time, it seems possible that the detected NO may have been released from the magma. If indeed the magmatic ratio of sulfur to bound nitrogen is of the order of 1000:1, then the NO_x concentrations inferred by Inn et al. in the 18 May samples likely had a predominantly nonvolcanic component (since the sulfur/nitrogen ratios were apparently in the range of 0.1 to 1.0).

5.2.5 Ash

Large quantities of ash and mineral debris were seen in the stratosphere on 19 May (below 18 km). Many large, dry ash particles were apparently present. By 22 May, however, the mass of ash collected above 18 km was lower by a factor of about 10 to 100, and the ash was flooded with H₂SO₄. It may be that less ash was injected at high altitudes, or that the large ash particles at higher altitudes rapidly settled from the cloud.

5.2.6 Other Constituents

Carbon monoxide (CO) was measured in the Mount St. Helens stratospheric clouds by Inn (1981, private communication). In two instances the CO:SO₂ ratio was about 10. On 22 May, at about 19 km, however, the ratio was $> 10^4$. The CO concentration was 2 to 4 ppm. This amount of CO can affect OH concentrations and consequently the SO₂ oxidation rates.

Concentrations of CH₄, N₂O, and fluorocarbons were not found to be enhanced over background in the stratospheric clouds.

5.3. CLIMATE EFFECTS BY CONVERSION OF SULFUR GASES TO PARTICLES

It is probable that the primary means by which volcanic effluents affect the global climate is through the conversion in the stratosphere of sulfur gases to particulate sulfate. Direct stratospheric injections of ash particles and primary sulfate particles may also affect climate. The proportion of sulfur gases to ash in the eruption cloud is the main factor determining the relative importance of each effect. In this regard, it is notable that nonexplosive volcanic eruptions which have very large proportions of gaseous emissions or those which emit strongly over an extended period of time may have impacts upon climate. Shortly after an eruption, conditions in the ash-filled cloud containing much condensed water are likely to be favorable for the so-called heterogeneous oxidation of SO₂. In this process, gaseous SO₂ is absorbed by the particles and subsequently oxidized either on the surface of solid particles or in the body of a liquid droplet. Other environmental factors which are thought to influence the rate of heterogeneous oxidation of SO₂ are concentrations of H₂O₂ (or its precursor O₃), alkaline substances in the ash or ammonia in the air which enhance the absorption of SO₂ by the particles or droplets, and trace metal catalysts that are present in the ash. (See Moller, 1980, for a review of these SO₂ reaction rates.) These heterogeneous reaction rates can be very large (at least under appropriate laboratory conditions) yielding SO₂ lifetimes as low as an hour or so. However, details of the mechanisms for these reactions, which are also important in acid rain formation, remain largely unknown.

The heterogeneous oxidation of SO₂ in stratospheric volcanic clouds can account for early formation of sulfate, particularly in association with ash particles. The principal effect is to enhance the size of existing particles which would, in turn, enhance the gravitational settling rates of the affected particles. Once sufficient dilution of the eruption cloud occurs by mixing with previously clean stratospheric air, the conditions of lower concentrations of reactants and low temperature tend strongly to suppress the rates of heterogeneous chemical processes. Thus, on a large scale basis, the heterogeneous conversion of SO₂ from Mount St. Helens to SO₄²⁻ in the strato-

sphere seems unlikely to have contributed significantly to aerosol formation. Rather, as is discussed later, the favorable process for large-scale long-term SO_2 to SO_4^{2-} conversion involves the homogeneous photochemical oxidation of SO_2 .

On the basis of present knowledge of chemical reactions and composition of the stratosphere, it is reasonably certain that SO_2 placed in the stratosphere is photochemically oxidized, ultimately to what is believed to be sulfuric acid, by the reaction $\text{SO}_2 + \text{OH} + \text{M} \rightarrow \text{HSO}_3 + \text{M}$. The mean lifetime of SO_2 for this reaction is estimated to be of the order of 25 to 100 days depending upon model estimates of OH concentrations. The supposed product of this reaction, HSO_3 , has not been identified either in the atmosphere or in the laboratory. If, indeed, HSO_3 does form from the reaction, its subsequent reactions in the atmosphere and its ultimate end products are uncertain. Friend et al. (1980) and Davis et al. (1979) have discussed possible reactions of sulfur-oxygen radicals and their hydrates to form such species as $\text{H}_2\text{S}_2\text{O}_6$ (dithionic acid) and $\text{H}_2\text{S}_2\text{O}_8$ (peroxodisulfuric acid). Turco et al. (1979) have suggested that HSO_3 may be converted to SO_3 by reaction with OH radicals and the SO_3 may then be converted to H_2SO_4 by reaction with H_2O . Thus, to summarize the above, though the chemical mechanisms are not known in detail, SO_2 in the stratosphere is oxidized via reaction with OH radicals to form intermediate sulfur-oxygen species which in turn form particles commonly thought to consist of H_2SO_4 and H_2O .

The question of the means by which sulfate aerosols are formed from gaseous species in the stratosphere is of particular significance in any assessment of the state of knowledge of the impact of volcanic emissions on global climate. Unfortunately, it is also an open question. The foregoing discussion illustrates the state of knowledge concerning the chemical identity of the product of SO_2 photooxidation. One concept of aerosol formation considers that H_2SO_4 is the principal product of SO_2 photooxidation and that the principal fate of the H_2SO_4 vapor is to condense on the surface of "prior existing nuclei." In this manner, sulfate aerosol is formed while essentially no new particles nucleate (because the homogeneous condensation of H_2SO_4 and H_2O vapor is far too slow). Simulations of aerosol formation by these processes have been made by Turco et al. (1979). Another notion of aerosol formation propounded by Friend et al. (1980) holds that, while the principal sink of gaseous sulfur oxyacids (H_2SO_6 or $\text{H}_2\text{S}_2\text{O}_8$) is scavenging by aerosol surfaces, *new particles* are formed by "activationless" clustering of H_2O and HSO_x molecules. At this juncture, there are no atmospheric data which permit unambiguous resolution to the question of particle formation. However, it does appear likely that the major chemical pathway for the conversion of most of the volcanic SO_2 in the stratosphere is the homogeneous oxidation by OH radicals. The observations of apparent new particle formation by Hofmann

and Rosen (1982) and Rodgers et al. (1980) are in accord with this concept, since the heterogeneous mechanism *per force*, cannot create new particles.

In the light of the foregoing discussion, the expected effects of the emissions from Mount St. Helens on 18 May 1980 on the earth's radiation balance are largely caused by ash particles and sulfur-oxyacid aerosol particles suspended in the stratosphere. Present understanding of atmospheric photochemistry implies that weeks to months are probably required for nearly complete conversion of the emitted sulfur gases to aerosol. Thus, ash particles may have been relatively more responsible for early effects on the radiation balance, but as the ash settled out, the secondary aerosol formed from H_2S and SO_2 oxidation probably played an increasingly important role.

5.4 EFFECTS UPON STRATOSPHERIC OZONE

The ozone content of the stratosphere can affect the earth's climate through the balance of radiation. The HCl and CH_3Cl injected into the stratosphere by a volcanic eruption can, in principle, decrease the ozone concentration. The formation of atomic chlorine by reaction of the HCl with OH is followed by the catalytic decomposition of the ozone by the Cl . However, it appears that insignificant amounts of HCl were injected into the stratosphere by the 18 May eruption (Lazarus, personal communication; see also Cadle, 1980). Methyl chloride (CH_3Cl) is also a source of atomic chlorine in the stratosphere, since the former is both photolytically decomposed and attacked by OH . Both processes release atomic chlorine. Since the concentrations in the early clouds were found to be about 1 to 5 ppbv and background concentrations are of the order of 1 ppbv, it is expected that the CH_3Cl emissions by Mount St. Helens had insignificant global-scale effects upon stratospheric ozone.

Unexpectedly, small amounts of oxides of nitrogen and nitric acid were also found to be present in the Mount St. Helens plume. If injected into the stratosphere, these compounds would have entered into the complicated chemistry of that region. However, fairly elaborate model studies would be required to estimate the effects, which seem likely to be too small to be of importance.

5.5 MOUNT ST. HELENS VOLCANO AND ACID RAIN

Mount St. Helens released large amounts of sulfur dioxide into the lower atmosphere by major explosive eruptions and by continuing fuming from the crater. Sulfur dioxide is a precursor to sulfuric acid, which is largely responsible for acid rain. (Nitric acid also contributes to acid rain in the northeastern USA, but no large enhancement of HNO_3 or NO_x has been attributed to Mount St. Helens.) Almost all of the HCl was probably rained out or absorbed in cloud droplets and moist surfaces near the volcano.

In the case of the eruption of 18 May, most of the SO₂ injected into the stratosphere would have been inaccessible to rainstorms for many months. The residence times of chemically inert trace substances in the lower stratosphere are altitude dependent and range from about 0.5 to 1.5 years. These residence times should apply to volcanic sulfur. The stratospheric sulfuric acid aerosol formed from SO₂ oxidation is released to the troposphere largely at midlatitudes in the region of the jet stream by tropopause folding (Danielsen, 1968). In addition to the great dilution already experienced in the stratosphere, the H₂SO₄ returned via tropopause folding will be further diluted with tropospheric air. The impact of this acid source on the precipitation occurring in the region of the jet stream will therefore be negligible compared to H₂SO₄ derived from industrial pollution sources around the world.

Sulfur dioxide emitted into the troposphere at midlatitudes is estimated to have an average residence time of only 1 day (Moller, 1980). Therefore, the SO₂ emitted into the troposphere during the major eruptions of Mount St. Helens would have only a transient effect spanning several days after each eruption. The sulfate aerosol produced by the SO₂, likewise, has a residence time of 3 to 5 days. Thus, any significantly enhanced acid rains would have had to occur in less than a week after the eruption. The dry volcanic ash in the troposphere was not found to be acidic.

Following the major eruption of 18 May, Mount St. Helens has been continually emitting significant amounts of SO₂ into the stratosphere. The SO₂ daily flux has ranged between 130 to 3400 tonnes. The SO₂ emission rate from a large midwestern power plant (2400 MW) is estimated at 520 tonnes day⁻¹ (Husar et al., 1978). Accordingly, the ongoing noneruptive SO₂ emissions have been similar to those of a large power plant.

A power plant with a stack of 218 meters deposits very little sulfur (50 to 100 km from the plant—Wilson, 1978). The much greater height of the Mount St. Helens crater ensures a much greater horizontal dispersal of the volcanic SO₂. Nevertheless, an isolated SO₂ source of this magnitude could not generate a regional-scale acid rain problem as occurs in the midwest and northeast. It is more probable that local rainstorms which incorporate the Mount St. Helens plume might show occasional enhanced acidity.

5.6 CHEMISTRY AND CLIMATE EFFECTS

Preliminary calculations of the effects of Mount St. Helens gas and particle emissions on stratospheric aerosols and ozone were performed for the Workshop by R. P. Turco, O. B. Toon, R. C. Whitten and R. G. Keesee (private communication, 1980). The model used for this purpose is described by Turco et al. (1979). The major conclusions drawn from the simulation studies are summarized as follows:

1. As noted earlier, there was some experimental evidence that heterogeneous reactions occurred during the early history of the Mount St. Helens eruption clouds. The detailed microphysical simulations suggest that the initial rates of SO_2 oxidation may have been 15%/hr, and that such rates are consistent with the amounts of water and ash injected into the stratosphere by the volcano.

2. The predicted long-term effects of Mount St. Helens SO_2 and H_2O emissions on the optical thickness of the stratospheric aerosol layer are shown in Fig. 5.1. Homogeneous SO_2 oxidation and SO_2 removal by diffusion and washout were accounted for. For an SO_2 injection of 10^6 tonnes, the calculated hemispherical optical depth perturbation is about 1×10^{-2} at 550 nm (the ambient optical depth is about 3×10^{-3}). Dust initially contributes about 3×10^{-3} to the opacity as well, but the dust is quickly removed. The predictions appear to be consistent with subsequent satellite and lidar observations, and independent estimates of the sulfur injection for Mount St. Helens.

3. Total hemispherical ozone reductions calculated for the Mount St. Helens eruptions are $\leq 0.2\%$. This result was obtained using a complete stratospheric photochemical scheme, and including the volcanic injections of SO_2 , H_2O , OCS , CH_3Cl , and HCl .

5.7 OVERVIEW OF CHEMICALLY GENERATED EFFECTS

The effects of the chemistry of volcanic emissions on climate and on stratospheric and tropospheric chemistry cannot be assessed independently of knowledge of the emission fluxes and of the transport of the emissions and their reaction products. These requirements restrict many of the remarks to general statements concerning potential effects. For example, it can be said that the time scale of the effects of volcanic halogens on stratospheric chemistry will be a strong function of the chemical form of whichever species are dominant, but one cannot quantify that time scale without at least relative fluxes for the dominant halogen. Given limitations of this type, the following statements can be made.

The climatic effects of volcanic emissions are controlled by the amount of sulfur transported to the stratosphere, since the generation of sulfate aerosol is potentially important to the earth's radiation budget. The time scale for sulfate formation depends on the mix of emitted sulfur compounds, whose individual conversion rates range from sulfate (fastest) through SO_2 , H_2S , and CS_2 to OCS (slowest).

The addition of water vapor to the stratosphere has the potential to increase the OH content, as H_2O is the precursor of OH . It appears more likely, however, that a decrease in OH concentration will occur following an eruption as a result of the injection of SO_2 (and perhaps CO and other gases). The magnitude and sign of the OH change will depend upon the amounts of H_2O and SO_2 which reach the stratosphere.

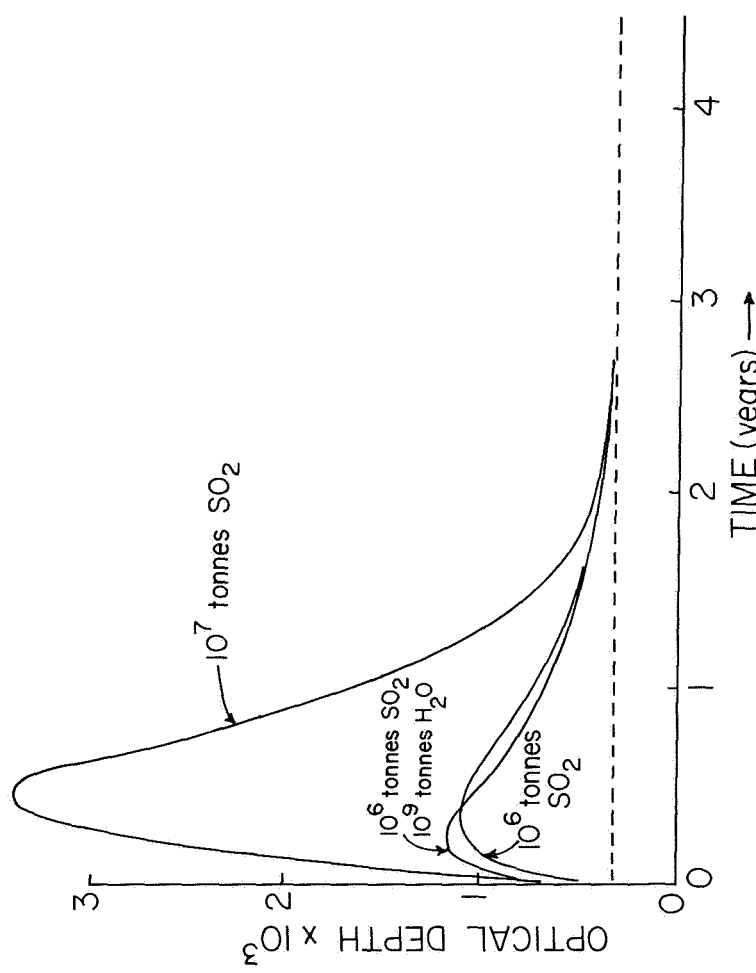


FIGURE 5.1. Calculated stratospheric aerosol optical depths at 550 nm versus time for several volcanic injections of SO_2 and H_2O into the lower stratosphere. The total injections are given in metric tonnes (10^6 g), and are averaged over the northern hemisphere. The SO_2 injections of 10^6 tonnes apply to Mount St. Helens. The SO_2 injection of 10^7 tonnes represents an eruption intermediate in size between Fuego (1974) and Agung (1963).

Volcanic emissions (principally the sulfur-containing species, but also those of nitrogen and chloride) are likely to increase slightly the acidity of precipitation in the region of the volcano, with concomitant effects on lakes, vegetation, etc. Volcanic emissions, such as those of Mount St. Helens, have the potential to influence climate through chemical and physical transformations, and to affect both stratospheric and tropospheric chemistry largely through radical reactions and formation of acidic aerosol constituents. The magnitudes of the effects depend on the composition and quantity of the emitted compounds. A preliminary conclusion is that the volcanic emissions of Mount St. Helens have had no major chemical consequences.

5.8 CONCLUSIONS

The following main conclusions can be drawn from the preceding discussions.

1. Most of the emissions of sulfur compounds from Mount St. Helens injected into the stratosphere will eventually form sulfate aerosols. It appears that the quantity of aerosol generated by the volcano was not large enough to perturb significantly the earth's radiation balance.
2. The apparent increasing dominance in abundance of sulfate particles over ash particles with time in the stratosphere can be explained by (a) early scavenging of ash by the condensation of emitted water vapor to form rapidly settling ice crystals, (b) rapid settling of large ash-containing particles, and (c) continuing production of sulfate by oxidation of sulfur gases.
3. Compounds of sulfur, nitrogen, and chlorine from Mount St. Helens participated in the chemistry of the stratospheric ozone layer, but the emission fluxes apparently were too small to cause a significant change in the chemical processes affecting ozone.
4. The emissions of sulfur compounds (and perhaps those of nitrogen and chlorine) had the potential to increase the acidity of precipitation within a few hundred km of the volcano but not on a larger scale.
5. An interesting new result of the Mount St. Helens studies is the detection of oxidized nitrogen compounds (NO , N_2O , HNO_3). The compounds are potentially capable of perturbing all chemical cycles of interest here, and their presence and concentrations should be investigated in further studies of volcanic emissions at Mount St. Helens and elsewhere.

5.9 RECOMMENDATIONS

The ability to make SO_2 and H_2SO_4 measurements during the next Airstream aircraft flights would yield information about the rates of oxidation of SO_2 and H_2S . However, a number of such Airstream missions during the year following the next large eruption would be especially informative.

Because the finding of H₂S concentrations in excess of SO₂ concentrations in some portions of the 18 May emissions was entirely unexpected, measurements of H₂S/SO₂ ratios in the emissions of other major eruption events is desirable. In the past, eruption clouds (as contrasted with fumerole emissions) have exhibited SO₂/H₂S ratios much larger than unity although these occurred in relatively small eruptions.

The simultaneous measurement of the important gaseous sulfur species and sulfate aerosol concentrations in eruption clouds at various relative positions downwind of the source could provide important information concerning the gas-to-particle conversion processes. Because source composition and atmospheric conditions are highly variable, it may be necessary to conduct studies in many such plumes. The presence and concentrations of the nitrogen compounds, because of their effects upon stratospheric chemistry, should be investigated in further studies of volcanic emissions at Mount St. Helens and elsewhere.

5.10 REFERENCES

Bandy, A. R., P. J. Maroulis, A. L. Torres, and L. A. Wilner, 1981: Estimate of the fluxes of NO, SO₂, H₂S, CS₂ and OCS from Mount St. Helens on project RAVE. [Available from first author, Drexel University, Philadelphia, Pennsylvania.]

Cadle, R. D., 1980: Some effects of the emissions of explosive eruptions in the stratosphere. *J. Geophys. Res.*, 85, 4495-4498.

Calvert, J. G., F. Su, J. W. Bottenheim, and O. P. Strausz, 1978: Mechanism of the homogeneous oxidation of sulfur dioxide in the troposphere. *Atmos. Environ.*, 12, 197-226.

Danielsen, E. F., 1968: Stratospheric tropospheric exchange based on radioactivity, ozone, and potential vorticity. *J. Atmos. Sci.*, 25, 4495-4498.

Davis, D. D., A. R. Ravishankara, and S. Fischer, 1979: SO₂ oxidation via the hydroxyl radical: Atmospheric fate of HSO_x radicals. *Geophys. Res. Lett.*, 6, 113.

Friend, J. P., R. A. Barnes, and R. M. Vasta, 1980: Nucleation by free radicals from the photooxidation of sulfur dioxide in air. *J. Phys. Chem.*, 84, 2423-2436.

Friend, J. P., M. A. Hart, J. L. Moyers, W. H. Zoller, J. M. Phelan, A. L. Torres, R. E. Stoiber, J. Wells, A. R. Bandy, P. J. Maroulis, L. Wilner, M. P. McCormick, D. C. Woods, and W. I. Rose, Jr., 1981: Research on atmospheric volcanic emissions: An overview. [Available from first author, Drexel University, Philadelphia, Pennsylvania.]

Hofmann, D. J., and J. M. Rosen, 1982: Balloon-borne observations of stratospheric aerosols and condensation nuclei during the year following the Mount St. Helens eruptions. [Accepted for publication by *J. Geophys. Res.* Available from J. M. Rosen, University of Wyoming, Laramie, Wyoming.]

Hobbs, P. V., L. F. Radke, M. W. Eltgroth, and D. A. Hegg, 1981: Airborne studies of the emissions from the volcanic eruptions of Mount St. Helens. *Science*, *211*, 816-818.

Husar, R. B., D. E. Patterson, J. D. Husar, N. V. Gillani, and W. E. Wilson, 1978: Sulfur budget of a power plant plume. *Atmos. Environ.*, *12*, 549-568.

Inn, E. C. Y., J. F. Vedder, E. P. Condon, and D. O'Hara, 1981: Gaseous constituents in the plume from eruptions of Mount St. Helens. *Science*, *211*, 821-823.

Lazarus, A. L., and B. W. Gandrud, 1981: Filter measurements of stratospheric sulfate and chloride in the eruption plume of Mount St. Helens. *Science*, *211*, 826-827.

Moller, D., 1980: Kinetic model of atmospheric SO₂ oxidation based on published data. *Atmos. Environ.*, *14*, 1067-1076.

Murcray, D. J., F. J. Murcray, D. B. Barker, and H. J. Mastenbrook, 1981: Changes in stratospheric water vapor associated with the Mount St. Helens eruption. *Science*, *211*, 823-824.

Oliver, R. C., 1976: On the response of hemispheric mean temperature to stratospheric dust: An empirical approach. *J. Appl. Meteorol.*, *15*, 933-950.

Rodgers, C. F., J. G. Hudson, and W. C. Kocmond, 1980: Stratospheric CCN measurements in the vicinity of Mount St. Helens plumes. [Written personal communication.]

Turco, R. P., P. Hamill, O. B. Toon, R. C. Whitten, and C. S. Kiang, 1979: A one-dimensional model describing aerosol formation and evolution in the stratosphere: I. Physical processes and mathematical analogue. *J. Atmos. Sci.*, *36*, 699-717.

Wilson, W. E., 1978: Sulfates in the atmosphere: A progress report on project MISTT. *Atmos. Environ.*, *12*, 537-547.

CHAPTER 6

INFLUENCE OF MOUNT ST. HELENS AND OTHER VOLCANOES ON CLIMATE AND WEATHER

6.1 ROLE OF VOLCANIC AEROSOLS IN RADIATIVE TRANSFER AND ENERGY BUDGET

The earth's climate, particularly the near surface temperature, is strongly a function of the planet's radiative energy budget. Solar radiation impinging on the earth is partly reflected back to space and partly absorbed in the atmosphere and at the surface. Radiation of thermal origin is emitted by the surface-atmosphere system and eventually escapes to space.

The primary mechanism by which volcanic activity influences the climate system is through changes in the aerosol content of the atmosphere. Aerosols of volcanic origin can be divided into two main families according to their composition and mechanism of formation or injection. Ash particles are injected directly into the atmosphere during the eruption, whereas sulfate particles are largely generated *in situ* from the gas phase through imperfectly known mechanisms. In view of competing growth and transport processes, the aerosol population is expected to change as a function of space and time.

Volcanic aerosols scatter solar radiation and thus they modify both the amount of energy reaching the ground and the energy diffused back to space. The aerosols also absorb and reemit infrared radiation, thus modifying the planetary thermal radiation field. The absorption of radiation and the successive collisional heat exchange and reemission lead to *in situ* warming or cooling of the ambient gas. The net effect is generally one of cooling the surface, whereas the net effect in the stratosphere is that of warming, due to absorption of both solar and infrared radiation. The stratospheric heating is also affected by the albedo of the underlying atmosphere and surface.

In order to determine theoretically the effects of volcanic particles on the radiation budget, several aerosol properties must be known (see, e.g., Toon and Pollack, 1976, 1980; Fiocco, Grams, and Mugnai, 1976; Mugnai, Fiocco, and Grams, 1978). First, the quantity of aerosols, as a function of size, needs to be known. Second, their composition must be known, at least insofar as it is reflected in the bulk optical properties of the material, i.e., refractive index and emissivity. The imaginary part of the visible refractive index, which characterizes the absorption properties of the particle, is of particular interest.

The wavelength dependence of the optical properties must be determined to accurately assess the radiative effects of aerosols. This is obtained from the information about size and bulk optical characteristics. For spheres, this is accomplished by means of the Mie theory. Nonsphericity or roughness of the particle modifies the results to some extent. The Mie theory accounts for the angular dependence of the scattered field, which is important in determining the diffuse field distribution.

The effect of the aerosols on the radiation budget is not instantaneously reflected in a change in atmospheric and surface temperatures because of the heat capacity of the atmosphere-surface system. Several weeks are required for the stratospheric temperature to adjust after aerosols are injected. The surface responds over a period of years and, indeed, may never respond completely because the particles are removed within a year or two, which some authors believe to be less than the surface response time. After the eruption of Mount Agung in March 1963 and the appearance of a substantial aerosol layer, the tropical lower stratosphere warmed by several degrees (Newell, 1970, 1971; McInturff et al., 1971), the free air in the tropical troposphere cooled by about one-half a degree (Newell and Weare, 1976; Angell and Korshover, 1977) and the surface also cooled (Angell and Korshover, 1977). These observed temperature changes have been successfully reproduced in models by Fiocco et al. (1977) and Hansen et al. (1978). In the latter model both the amplitude and phase of the temperature changes were close to those observed.

6.2 CLIMATOLOGICAL EVIDENCE FROM PAST VOLCANOES

A number of empirical and statistical studies have revealed evidence of volcanic impact on climate and the atmospheric circulation (Sear and Kelly, 1980). It should be noted, however, that all such analyses are limited by uncertainties in both the volcanic and climatic data sets. Historical chronologies of volcanic activity and/or the dust loading of the stratosphere (Lamb, 1970; Hirschboeck, 1980; Newhall and Self, 1982) can all be criticized on a number of grounds and must be used with caution. In particular, the reliability of the data varies greatly from one period to another and from one area to another, and none of these chronologies provides estimates of the sulfur contribution to the stratosphere. The instrumental climate record is restricted in geographical and temporal extent. Reliable data for the upper atmosphere are only available for recent decades, and surface data, although available for a longer time period, are increasingly restricted in geographical coverage prior to 1920. In some areas, however, the surface record does extend back 200 to 300 years. Indirect information on climate in early periods is available from a variety of sources (documentary, geological, biological, and so on), but the interpretation of such data needs to be approached with care. Most empirical studies of

Volcano-climate links have been hampered by uncertainties in the data bases, by lack of global representativeness due to the restricted geographical coverage of the long-term climate data, and by the difficulties in separating the volcanic effects from other influences on the climate system.

Despite these limitations, which could be reduced in further analyses, volcano-climate links have been convincingly demonstrated on a variety of time-scales. For example, Taylor et al. (1980) have identified a statistically significant short-term volcanic signal in surface temperature data. The signal is of the order of a few tenths of a degree centigrade, and lasts for a year or two after single, large eruptions. Yamamoto et al. (1977) find that this volcanic signal is larger at high latitudes than in the tropics. A number of authors have suggested that the apparently high frequency of explosive volcanic activity during the early 19th century was a factor in causing or prolonging the Little Ice Age (Pollack et al., 1976a, 1976b) and that the general climate warming affecting the northern hemisphere during the early 20th century was a result of the clearance of volcanic aerosols from the stratosphere at that time. Significant correlations between volcanic data and various atmospheric circulation parameters (most notably the strength of midlatitude westerlies) have also been demonstrated on time-scales ranging from years (Lamb, 1970) to decades (Kelly, 1977). There is a need for further studies of the spatial patterns of climate change following large volcanic events.

Greater data availability over the last two to three decades has enabled more detailed observational studies to be made of recent volcanic events. The first large volcanic eruption which was monitored by the global radiosonde network, established after World War II, was that of Mount Agung, Bali (8°S, 115°E) which occurred in February and March 1963, with the largest explosive eruption occurring on 17 March. In the tropical lower stratosphere, temperature increases of more than 5°C were observed within a month or so, which at that time were thought to be due to the absorption of solar radiation by aerosols which had evolved from the sulfur gases injected by the eruption (Newell, 1970). The region of positive temperature anomalies spread polewards somewhat like the radioactive trace substances from tropical nuclear tests that entered the stratosphere. Examination of the various factors that control tropical tropospheric free air temperature showed that the most important was equatorial Pacific sea surface temperature. The free air temperature was characterized by the difference in geopotential height at pressures of 700 and 300 mb (3 and 10 km) for a group of stations selected to represent a zonal mean (a technique initiated by Angell and Korshover, 1975). When a regression analysis was performed between the sea temperature and air temperature two seasons ahead, the residuals, corresponding to the unexplained variations of the air temperature, matched closely with the atmospheric transmission at Mauna Loa, Hawaii (Newell and Weare, 1976). The maximum tropospheric temperature difference from the long-term mean corresponded to a cooling of

about 0.4°C and did not occur until over a year after the eruption, whereas the stratospheric warming occurred almost immediately. More details of this type of study have been given by Angell and Korshover (1973).

6.3 MODELING CLIMATIC EFFECTS OF PAST VOLCANOES

Several model calculations of the effects of volcanic dust on climate have been performed recently. These include use of one-dimensional radiative convective models (Pollack et al., 1976a, b; Hansen et al., 1978), zero-dimensional empirical models (Oliver, 1976), zero-dimensional energy balance models (Schneider and Mass, 1975; Bryson and Dittberner, 1976; Harshvardhan and Cess, 1976), a one-dimensional energy balance model (Robock, 1978, 1979), and a three-dimensional general circulation model (Hunt, 1977). The models all concentrate on surface air temperature as the calculated climate variable, although Hansen et al. (1978) and Pollack et al. (1976a, b) also looked at stratospheric temperatures and Hunt also looked at circulation effects. Other aspects of the climate system are undoubtedly affected by volcanic eruptions but have not been included in modeling studies.

In Chapters 1 and 3, stress is laid on the difference between the ash and sulfate from the eruption. In some of the models these substances are treated separately with different absorptance properties. In addition, in recent work by Bryson and Goodman (1980) ash is considered to fall out rapidly (mean stratospheric residence time about 100 days) while sulfate is considered to evolve with a gas-to-particle conversion time constant of 115 days and a mean residence time of 400 days. More experimental values of these constants are needed and can only be obtained by further direct and remote sampling of volcanic clouds.

Both Hansen and Robock calculated the effect of the Mount St. Helens eruption using their climate models, as reported at the Workshop. They used their best estimates of the dust veil and both found very small effects on surface temperature, for example, much less than 0.1°C for the global or hemispheric mean. Because the natural variability of the temperature is much larger than this, it is considered an insignificant effect and will be impossible to measure.

Although different assumptions about the details of the volcanic forcing of the climate models, and different sets of surface temperature records were used in the studies, all the studies agree on one point: large volcanic eruptions cause a lowering of hemispheric or global average surface temperature for a period of several years and are an important cause of climate change on the interannual to 500-year time scale. More definitive quantitative results await future improvements in volcanic dust chronologies, temperature reconstructions, and climate models.

6.4 RELEVANCE OF MOUNT ST. HELENS TO INTERPRETATION OF VOLCANIC EFFECTS ON CLIMATE

The Mount St. Helens eruption provides two types of information of great importance for understanding the role of other eruptions in affecting climate. First, Mount St. Helens shows that eruptions with great explosive energy, which injected large quantities of ash into the atmosphere, do not necessarily cause large increases in stratospheric optical depth. Second, Mount St. Helens provides the first good observations of many of the optical parameters required to properly assess the importance of volcanic eruptions to climate.

Volcanic eruptions which have had an impact on climate have produced stratospheric optical depths of about 0.1 or more for the year or two following the eruption. The optical depth is the logarithm of the transmission of sunlight, so large eruptions may reduce the amount of light reaching the surface in the direct solar beam by 10% or more. Previously, several large explosive eruptions had occurred which did not cause large optical depth changes, but these were largely ignored. Mount St. Helens was a powerful volcanic explosion, but the optical depth following the eruption was only about 0.01, relegating it to a climatologically insignificant eruption. Apparently neither the mass of tephra nor the explosive energy of the eruption are good indicators of the importance of the eruption. Instead, the total mass of sulfur injected into the stratosphere appears to be the most significant factor, as clearly revealed for the first time by the Mount St. Helens explosion.

Several parameters need to be known to assess the importance of an eruption for climate. These include: the optical depth, the visible single scattering albedo, the angular scattering pattern, and the infrared opacity of the particles. Although volcanic optical depths have previously been measured, the Mount St. Helens eruption is the first for which measurements of the remaining three parameters have been made.

The single scattering albedo was found to be larger than 0.98 following the Mount St. Helens eruption. Since other, larger eruptions are thought to have produced much greater quantities of transparent stratospheric sulfate particles, the debris from other eruptions probably had a greater single scattering albedo than that of Mount St. Helens. Hansen et al. (1980) and Pollack et al. (1981) show that eruptions with single scattering albedos above 0.94 will increase the earth's albedo and albedos above 0.98 will cool the earth's surface. Hence, measurements following Mount St. Helens strongly suggest that volcanic stratospheric particles will generally lead to a cooling of the earth's surface.

The aerosol phase function, and the effect of the aerosols on the infrared radiation are both determined by the particle size distribution. Following the Mount St. Helens eruption, the size distribution of the sulfate particles was

well determined for the first time. Measurements of volcanic ash particle sizes were also obtained which supplement the early work following the Mount Agung eruption of 1963. Those distributions cannot be used directly for other eruptions. However, together with the chemical species measurements made after the Mount St. Helens eruption, the particle size measurements can be used to carefully test aerosol chemical-physical models. Such validated models may now be used for the first time to extrapolate the Mount St. Helens event to larger volcanic eruptions. Hence, the particle size distribution following other volcanic events can now be predicted and utilized for theoretical models of climate. Such predictions will need to be checked after a large eruption.

6.5 PROBLEMS FOR FUTURE RESEARCH

6.5.1 Reconstruction of Volcanic Activity and Climate Change during the Past 500 to 1000 Years

Valuable perspective on the climatic impacts of volcanic eruptions can be gained by reference to the historical records of volcanic events and of climate and the investigation of statistical association between them. Past attempts along such lines have been based largely on the Lamb “Dust Veil Index” (DVI) chronology since 1500 AD and various climatic series available mostly from the European sector. The DVI chronology and other extant volcanic chronologies have, however, been based on necessarily crude historical information that renders them neither homogeneous nor reflective of the quantities and composition (especially sulfate aerosols converted from gases) that are most relevant to climatic effects. The available climatic series, on the other hand, are mainly of local or regional (rather than global-scale) representativeness and, therefore, do not provide a suitably general picture of the potential climatic effects of eruptions, in the sense that they neither clarify their basic physical significance nor clearly distinguish between eruption effects and other sources of climatic variations.

Efforts are required to explore the feasibility of constructing new chronologies of volcanic activity that better reflect the history of changes of stratospheric loading by both silicates and sulfate aerosols. Parallel efforts are required to focus paleoclimatic and historical climatic research on more quantitative reconstruction of global-scale climatic conditions, including, to the extent possible, indices of global-scale energy budget and atmospheric circulation and their variations from year to year. These efforts should be aimed at reconstructions for the past 500 to 1000 years, a period of time that would allow assessment of long-term variations in general volcanic activity levels as a potential cause of “Little Ice Age” events and other major climatic variations known to have occurred during the past millennium, as well as assessment of shorter-term climate anomalies in relation to individual volcanic events or series of events.

A recently proposed method of monitoring sulfate aerosol from the past is to measure the electrical conductivity of ice in cores from glacial regions (Hammer, 1977). Such a measure may depend mainly on sulfate or sulfuric acid components which originate from the stratosphere, although there are, of course, some problems of interpretation when nearby volcanoes erupt; for example, Icelandic eruptions affect cores from the Greenland ice cap. Hammer et al. (1980) have evolved a rapid way of measuring conductivity by running a pair of electrodes along a core cut so that it has a flat face. Depth in the ice core gives an independent measure of the date, either from ice flow calculations or from counting seasonal variations of $\delta(\text{O}^{18})$. The dating accuracy is ± 1 year for the past 900 years and ± 3 years from there back to AD 553 (Hammer et al., 1980). Almost all the peaks of conductivity, interpreted as acidity, correspond to known volcanic activity with some exceptions at 622-23, 1257-58, 1600-01. The technique works back to almost 6000 BC, which is the most distant period at which volcanoes have been identified in this manner. Back to about 1000 AD, there is some agreement between the overall pattern of acidity and several proxy indications of temperature. This experimental approach should certainly be continued and extended to other regions, as it monitors one of the main items (stratospheric sulfuric acid or sulfate) thought to be responsible for climatic fluctuations.

6.5.2 Regional Climatic Effects

The climatic impacts of volcanic eruptions are by no means homogeneous in their spatial distribution. Where soils, vegetation, water bodies, and snow fields are destroyed, local changes in albedo and the water budget may persist for years. On a larger scale, the aerosol may initiate less direct changes in the energy budget and variations in the atmospheric circulation that are expressed as regional anomalies. Thus, it is essential to monitor not only global circulation changes, but also trends in regional climates. In order to establish an adequate data base, it will be necessary to maintain surface and upper level observations. Fortunately, the required networks can serve both climate system modeling and studies of regional impacts on environment and society. The ultimate goal is to improve planning and operational decisions that involve the effects of climate on human affairs.

6.5.3 Water Vapor and Condensation Nuclei

Water Vapor. Fourteen years of stratospheric water vapor measurements made by the Naval Research Laboratory at Washington, DC, provide the longest time series of stratospheric water vapor data available and constitute baseline data for the recognition and assessment of future changes in stratospheric concentration. There is an inference in this data series, which began shortly after the Mount Agung eruption, that the Mount Agung eruption was followed by a substantial reduction in stratospheric water vapor and

may, in fact, have been the cause of the reduction. The lowest concentration of the time series (2.0 ppm) was observed in the first year of measurements (1964). The concentration increased over the next 6 years to 3.0 ppm and thereafter stabilized at about 2.7 ppm. The Meteorological Research Flight measurements (as corrected) which were made prior to the Mount Agung eruption show concentrations close to the 2.7 ppm observed in the later years of the Naval Research Laboratory time series and provide a further indication that the 1964 concentration following the Mount Agung eruption was abnormally low.

A similar reduction in stratospheric water vapor may or may not follow the Mount St. Helens eruption. A continuation of the water vapor measurements at Washington, DC, and the comparison of those measurements with the earlier baseline data for this location would provide the opportunity for detecting and identifying a significant change in stratospheric water vapor concentration following the Mount St. Helens eruption, if it occurs. Such a change, together with the inference of a substantial reduction following the Mount Agung eruption, would provide strong evidence for a cause and effect relationship.

Condensation Nuclei. Gaseous emissions from volcano eruptions lead to the production of large amounts of small volatile aerosol particles which play a significant role in the condensation and freezing processes of clouds. These condensation nuclei in the stratosphere affect formation and structure of high altitude clouds. Although the liquid water content of such clouds, if averaged over the hemisphere, will not be markedly influenced by condensation and ice nuclei, it must be expected that influence on cloud droplet size distribution and phase changes will be significant enough to alter noticeably scattering and absorption properties. Because the distribution of condensation and ice nuclei produced by volcanoes is both of hemispheric scale and relatively long lived, influences on climate and regional weather systems through changes in radiative transfer processes can be expected. It needs to be determined how important such cloud processes are compared to the direct influence of aerosol particles on the radiation budget.

6.6 CONCLUSIONS

A summary of the main conclusions derived from earlier discussions is given as follows:

- I. The physical and optical properties of the Mount St. Helens aerosols were found to be such as to lead to an increase in the planetary albedo and to cause a warming of the lower stratosphere and a cooling of the troposphere (albedo for single scattering > 0.98). The signs of these effects were not certain

previously. The high aerosol albedo is particularly noteworthy because it occurred despite the relatively low sulfur content of Mount St. Helens ejecta, indicating that the conclusions should also hold for other volcanoes.

2. The magnitudes of these radiative effects are expected to be small in comparison to the normal total variability of the atmosphere. (The average aerosol optical thickness produced by Mount St. Helens was not larger than about 10^{-2} . It would need to be several times larger to produce tropospheric temperature changes comparable to the total observed variability.)

3. Findings from Mount St. Helens have provided insight into climatic effects of eruptions of other volcanoes. It can be concluded, on the basis of findings from Mount St. Helens studies and prior research, that past single and multiple eruptions have caused significant climatic effects.

4. The cause of the large-scale weather anomalies that followed the eruption of Mount St. Helens (e.g., the summer heat wave and drought in the United States, and the cold wet summer in parts of Europe) is not obviously related to the eruption. Similar anomalies have been observed in the past in the absence of such eruptions.

5. Climatic effects of volcanic eruptions depend on the concentration and composition of aerosols injected into the stratosphere and, in particular, on the amount of injected sulfur. The climate effects are not a simple function of volume of tephra or the explosive energy of the eruption.

6.7 RECOMMENDATIONS

Following is a summary of recommendations for future research efforts.

1. *Continued measurements of the time development of effluents from Mount St. Helens.* The time constants for development and decay of some of the radiatively active constituents important to climate are of the order of a year or longer. Continued measurements of the Mount St. Helens effluents are needed over the next 2 to 3 years, particularly measurements of the aerosols (composition, size, single scattering albedo) and gases, including the radiatively important constituents, water vapor, and ozone.

2. *Long-term measurements of the stratospheric background.* Knowledge of the "unperturbed" stratosphere is needed to permit modeling and analysis of a volcanic perturbation, to assess the cumulative impact of volcanoes on climate, and to determine whether there is an aerosol source other than volcanoes. The needed measurements include aerosol properties, temperature, and H_2O measurements.

3. *Measurements of future large volcanic eruptions.* There is need for intensive study of the next few large eruptions, because there are major differences among different volcano types and because it is important to study a volcano which produces a sufficiently large stratospheric aerosol optical depth to noticeably impact global-scale climate. It is important that the future

studies include measurements of sulfur content of the eruption, with the objective of associating sulfur content with volcano type. Also, it is desirable to have measurements of the effects of the volcanic aerosols on the radiative fluxes in different spectral regions.

4. *Measurement of comparable climate forcings and continued monitoring of climate variations.* The effect of volcanic eruptions can only be reliably associated with climate change if other variable climate forcings are also measured and if the climate is adequately monitored. Among climate forcings, it is particularly important to monitor the solar luminosity, tropospheric aerosols, and the ground albedo. The key climate parameters are temperature and rainfall; maintenance of the radiosonde network is needed to provide adequate temperature monitoring.

5. *Improved reconstructions of past volcanoes, with emphasis on past 500 to 1000 years.* The past several centuries have been a time of substantial variations of both climate and the level of volcanic activity. Studies of this period could provide an opportunity for determining the influence of volcanic eruptions on long-term climate and for testing and calibration of climate models. However, present knowledge as to both volcanic activity and climate variations is not adequate. The best possibility for improving estimates of historical variations of volcanic aerosol loading appears to lie in ice core studies, including cores from more than one ice sheet to minimize the effects of local weather and circulation. Improved reconstructions of climate during this period, particularly of global-scale surface temperature and precipitation variations, are also required.

6. *Modeling studies (a) regional climate effects, (b) past 500- to 1000-year period, and (c) photochemical modeling of aerosols.* Progress has been made in modeling the effect of volcanic aerosols on global mean climate, but their effects on regional climate may be of greater practical importance. These are ripe for study with three-dimensional models. The past millennium has been a time of substantial variations of both climate and volcanic aerosols, and thus provides the best opportunity for analysis of the long-term climate impact of stratospheric aerosols. Available data on precursor gases and the aerosols created by Mount St. Helens provide input for improved photochemical modeling of aerosol formation, growth, and decay. Such models will be useful for scaling aerosol properties to volcanoes of different sizes.

6.8 REFERENCES

Angell, J. K., and K. Korshover, 1975: Estimate of the global change in tropospheric temperature between 1958 and 1973. *Mon. Wea. Rev.*, 103, 1007-1012.

Angell, J. K., and K. Korshover, 1977: Estimate of the global change in temperature, surface to 100 mb, between 1958 and 1975. *Mon. Wea. Rev.*, 105, 375-385.

Bryson, R. A., and G. J. Dittberner, 1976: A non-equilibrium model of hemispheric mean surface temperature. *J. Atmos. Sci.*, 33, 1094-2106.

Bryson, R. A., and B. T. Goodman, 1980: The climate effect of explosive volcanic activity: Analysis of the historical data. Paper presented at NASA Workshop on Mount St. Helens Eruption: Its Atmospheric Effects and Potential Climatic Impact (Washington, D.C.), November 18-19.

Fiocco, G., G. Grams, and A. Mugnai, 1976: Energy exchange and temperature of aerosols in the earth's atmosphere (0-60 km). *J. Atmos. Sci.*, 33, 2415-2424.

Fiocco, G., G. Grams, and A. Mugnai, 1977: Energy exchange and equilibrium temperature of aerosols in the earth's atmosphere. Proc. Symp. on *Radiation in the Atmosphere*, Ed. H.-J. Bolle, Science Press, Princeton, 74-78.

Hammer, C. U., 1977: Past volcanism revealed by Greenland Ice Sheet impurities. *Nature*, 270, 482-486.

Hammer, C. U., H. B. Clausen, and W. Dansgaard, 1980: Greenland ice sheet evidence of post-glacial volcanism and its climatic imput. *Nature*, 288, 230-235.

Hansen, J. E., A. A. Lacis, P. Lee, and W. C. Wang, 1980: Climatic effects of atmospheric aerosols. *Ann. New York Acad. Soc.*, 338, 575-587.

Hansen, J. E., W. C. Wang, and A. A. Lacis, 1978: Mount Agung eruption provides test of a global climate perturbation. *Science*, 199, 1065-1068.

Harshvardhan, and R. D. Cess, 1976: Stratospheric aerosols: Effect upon atmospheric temperature and global climate. *Tellus*, 28, 1-10.

Hirschboeck, K. K., 1980: A new worldwide chronology of volcanic eruptions. *Palaeogeography, Palaeoclimatology, Palaeoecology*, 29, 223-241.

Hunt, B. G., 1977: A simulation of the possible consequences of a volcanic eruption on the general circulation of the atmosphere. *Mon. Wea. Rev.*, 105, 247-260.

Kelly, P. M., 1977: Volcanic dust veils and North Atlantic climate change. *Nature*, 268, 616-617.

Lamb, H. H., 1970: Volcanic dust in the atmosphere; with a chronology and assessment of its meteorological significance. *Phil. Trans. Roy. Soc. A.*, 266, 425-533.

McInturff, R. M., A. J. Miller, J. K. Angell, and J. Korshover, 1971: Possible effects on the stratosphere of the 1963 Mount Agung volcanic eruption. *J. Atmos. Sci.*, 28, 1304-1307.

Mugnai, A., G. Fiocco, and G. Grams, 1978: Effects of aerosol optical properties and size distribution on heating rates induced by stratospheric aerosols. *Q. J. Roy. Met. Soc.*, 104, 783-796.

Newell, R. E., 1970: Modification of stratospheric properties by trace constituent changes. *Nature*, 227, 697-699.

Newell, R. E., 1971: The global circulation of atmospheric pollutants. *Scientific American*, 244(1), 32-42.

Newell, R. E., and B. C. Weare, 1976: Factors governing tropospheric mean temperature, *Sci.* 194, 1413-1414.

Newhall, C. G., and S. Self, 1982: The volcanic explosivity index (VEI): An estimate of explosive magnitude of volcanic eruptions. *J. Geophys. Res.* 87, 1231-1238.

Oliver, R. C., 1976: Hemispheric mean temperature to stratospheric dust: An empirical approach. *J. Appl. Meteor.* 15, 933-950.

Pollack, J. P., O. B. Toon, C. Sagan, A. Summers, B. Baldwin, and W. Van Camp, 1976a: Volcanic explosives and climate change: A theoretical assessment. *J. Geophys. Res.*, 81, 1071-1083.

Pollack, J. B., O. B. Toon, C. Sagan, A. Summers, B. Baldwin, and W. Van Camp, 1976b: Stratospheric aerosols and climate change. *Nature*, 263, 551-555.

Pollack, J. B., O. B. Toon, and D. Wiedman, 1981: Radiative properties of the background stratospheric aerosols and implications for perturbed conditions. *Geophys. Res. Lett.*, 8, 26-28.

Robock, A., 1978: Internally and externally caused climate change. *J. Atmos. Sci.*, 35, 1111-1122.

Robock, A., 1979: The little ice age northern hemisphere average observations and model calculations. *Science*, 206, 1402-1406.

Schneider, S. H., and C. Mass, 1975: Volcanic dust, sunspots, and temperature trends. *Science*, 190, 741-746.

Sear, C. B., and P. M. Kelly, 1980: Mount St. Helens effects on climate. *Nature*, 285, 533-535.

Taylor, B. L., T. Gal-chen, and S. H. Schneider, 1980: Volcanic eruptions and long-term temperature records: An empirical search for cause and effect. *Q. J. Roy. Met. Soc.*, 106, 195-199.

Toon, O. B., and J. B. Pollack, 1976: A global average model of atmospheric aerosols for radiative transfer calculations. *J. Appl. Meteor.*, 15, 225-246.

Toon, O. B., and J. B. Pollack, 1980: Atmospheric aerosols and climate. *American Scientist*, 68, 268-278.

Yamamoto, R., M. Hoshiari, and T. Iwashima, 1977: Changes of surface air temperature averaged globally during the years 1957-1972. *Archiv. Meteor. Geophys. Bioklim.*, B25, 05-115.

INDEX

A

Absorption coefficient, 50,54
 Accretionary lapilli, 17
 Accretionary particles, 17
 Acid rain, 95
 Advanced Very High Resolution Radiometer (AVHRR), 79
 Aerosol(s),
 absorption of solar radiation by, 105
 burden of stratospheric, 59
 chemical production of, 89
 morphology of, 51,57
 phase function of, 107
 photochemical modeling of, 112
 stratospheric, 66
 volatile, 55,110
 volcanic, xxv
 Aerosol formation, 94
 photochemical modeling of, 112
 Aerosol morphology, 51
 Aircraft,
 B-23, 50
 U-2, 49,52
 WB-57, 49,51
 Airfall deposits (*see deposits*)
 Aitken nuclei, 49
 Albedo,
 single scattering, 107
 Ash, 92
 distribution of airfall, 15
 emission rate of, 6
 fine elutriated, 16
 mass concentration of, 51
 stratigraphy of airfall, 17
 vitric-lithic crystal, 17
 Augustine volcano, Alaska, 24

B

B-23 aircraft, 50,54
 ^7Be , 50
 Br^- , 89
 Balloon, 50,55
 Basaltic compositions, 2
 Brewer spectrometer, 82
 Bulk optical characteristics, 104

C

CCl_4 , 48,89
 CFCl_3 , 89
 CF_2Cl , 56
 CH_4 , 89,93
 CH_3CCl_3 , 89
 CH_3Cl , 56,95
 CH_3I , 89
 Cl , 91
 CO , 53,93
 CO_2 , 26,89
 CS_2 , xxiii,54,56,59
 Carbonyl sulfide, 54
 tropospheric concentrations of, 55
 Cerro Azul volcano, 17
 Chemistry,
 Mount St. Helens effluent, 89
 plume, 47
 Chromatography,
 gas, 49
 ion, 49
 Climate effects, 96
 Cloud inhomogeneity, 56,57
 Coagulation
 aerosols, 56
 process of, 48
 sulfuric acid embryo, 56
 Column heights, 30
 Composition
 aerosol, 111
 dacitic ash, 15
 “Dark Ash,” 16
 “pale ash,” 15
 rhyolitic glass phases, 15
 Condensation nuclei (cn), 109, 110
 concentration of, 50
 size of, 51
 Cooling, earth’s surface, 107
 Correlation spectrometer (COSPEC), 63,81
 Crystal fragments, 10
 Crystals, plagioclase, 11

D

Dactic rock, 4
 Depolarization, 84

Deposits,
 basal lithic pyroclastic surge, 2
 debris avalanche, 2
 mudflow, 2
 pyroclastic avalanche, 2
 pyroclastic flow, 4

Dispersal index, 29,30

Dispersion of stratospheric plume, 46

Dobson spectrometers, 82

Dome, lava, 2

Dust loading, stratospheric, 104

Dust veil index, 108

Dustsonde, 50,55,74

E

Electrical conductivity, core ice, 109

Elemental composition mass concentration, 51

Emissivity, 103

Energy budget, 108

Eruption(s)
 Bezymianny, 7
 explosive energy of, 107
 ignimbrite-producing, 31
 intensity of, 27
 Krakatoa, xxv,20
 lightning activity due to, 92
 magmatic, 1
 magnitude of, 28
 Mount Agung, 54,104,105,109
 Mount Lamington, 7
 multiple, xxiii
 observation of the 18 May, 4
 phreatic, 22
 phreatomagmatic, 1,22,32
 plinian, 22,32
 Shiveluch, 7
 sulfur content of, 112

Eruption cloud,
 shape and structure of, 9
 water in, 26

Eruption column(s), 10,24
 gases and aerosols in, 24
 maximum heights of, 10,28
 vertical plinian, 4

Eruption rate(s), 6,30

Eruptive units, Mount St. Helens, 23

Explosivity, xxii,28

Extinction coefficient, xxiii,59,83

F

F-11, 49

F-12, 49

Fallout, distribution of ash, 17

Flows,
 lava, 2
 mud, 2
 pyroclastic, 2

Fluorocarbons, 93

Fragmentation index, 29,30

Frost point hygrometer, 53

Fuego, Guatemala, 24,71

G

GOES (Geosynchronous Operational Environmental Satellite), 37
 GOES-West image, 81

Gas chromatography, 54

Gas-to-particle conversion(s),
 xxiv,56,59,66,106

Geostrophic winds, 39

Glacial ice, 22

Glass inclusions, volatiles in, 25

Glassy pyroclasts, 13

Ground albedo, 112

H

HIRS-2 (High Resolution Radiation Sounder), 79

HCl, 53,91

H₂, 89

HF, 89

H₂O, 49,89

H₂S, xxiii,54,91

Halide ions, 90

Height, eruption column, 8

Heterogeneous oxidation,
 catalytic, 56

Homogeneous photochemical oxidation, 94

I

Ice cores, xxv

Ice particles, 91

Ignimbrite, 31

Index,
 dispersal, 29,30
 dust veil, 108
 fragmentation, 29,30
 refractive, 103
 volcanic explosivity, 28

Infrared opacity, 107

Infrared spectra, 49

Integrating nephelometer, 50

Intensity, eruption, 27

Intrusive magma, 26

Ions,
 alkalane, 90
 halide, 90
 nitrate, 90
 sulfate, 90

Ion chromatography, 49
Isentropic analysis, 46
Isopach, 28

L
Lava flows, 2
Lidar, xxiv, 63, 70, 83
 backscatter for, 72
Lightning, 92
Lithic fragments, 10
Lithic pyroclasts, 14
Little Ice Age, 108
Lower stratosphere, warming of, xxiii, 110

M
Magma(s), 1
 intrusive, 26
 silicic, 2
 sulfur from, 24
Magmatic eruptions, 1
Mammatus clouds, 45
Measurements,
 B-23 aircraft, 50
 balloon, 46, 50, 55
 balloon-borne dustsonde, 74
 depolarization, 71, 84
 frost point hygrometer, 53
 integrating nephelometer, 50
 lidar, xxiii, 42, 46, 70
 NASA-P3 aircrft, 54
 NOAA-6 satellite, xxii
 opal glass impactor, 49
 opal glass integrating plate, 50
 photographic, 74
 pyroheliometer, 79
 quartz crystal microbalance impactor, 49
 RAVE, 56
 SAGE, 37, 43
 TIROS satellite, 37
 U-2 aircrft, 49, 52
 WB-57 aircrft, 49, 51
 wire impactor, 50
Mie theory, 105
Mineral debris, 92
Model(s),
 one-dimensional radiative-convective, 106
 three-dimensional general circulation, 106
 zero-dimensional empirical, 106
 zero-dimensional energy balance, 106

Morphology, particle, 57
Mount Agung, 54, 104, 105, 109
Mount St. Helens,
 eruption and dormant intervals of, 3
 eruptive activity of, 1
 eruptive units of, 23
 geodetic monitoring at, 4
 prehistoric eruptions of, 2
Mudflows, 2

N
NOAA-6 satellite, xxii
NOAA GMCC (Geophysical Monitoring for Climatic Change), xxv, 85
N₂O, 49, 56, 89, 93
NO_x, 49, 92
 plume, 56
Nitrate ions, 90
Nonsphericity, particle, 104
Nuclear explosions, atmospheric, 46
Nucleation, 56

O
O₃, 49
OCS, xxiii, 53, 59
Observations,
 aircraft, 46
 radar, 6
Opacity, 97
Opal glass impactor, 49
Opal glass integrating plate, 50
Optical properties, effluent, 63

P
P-3 aircraft, 50, 54
Paleoclimate, 108
Passive emissions, 26
Phase function, aerosol, 107
Photochemical modeling,
 aerosols, xxv, 112
Photochemical processes, 48
Photography, time-lapse, color, 77
Photometry, 77
Phreatic eruptions, 1, 4
Phreatomagmatic activity, 31, 32
Phreatoplinian, 30
Planetary albedo, xxiii
Plinian column, 7, 21, 23
 radar measurements of, 7
Plinian eruptions, 1, 32
Primary sink, 48
Pumice, 1, 10, 14
Pumice lapilli, 16
Pyrheliometer, 79
Pyroclastic ash flow(s), 2, 4, 16
Pyroclastic fall deposit, 4
Pyroclastic surge, 4

Q

Quartz crystal microbalance cascade impactor, 49

R

RAVE (Research in Atmospheric Volcanic Emissions), 50,54,92
²²²Rn, 53
 Radar observations, 6,63
 Radar system,
 NWS, 6
 Portland, 6
 Seattle, 6
 Radiation budget, 103
 Radiative climate effects, xxiii,
 59
 Radioactive trace substances,
 105
 Radioactivity, 47
 mass concentrations of, 51
 measurements of ²²²Rn, 53
 Refractive index, 103
 Residual aerosol burden, 58

S

SAGE, xxiii,xxiv,54,63,83
 SAM II, xxiv
 SF₆, 49
 SO₂, xxiii,53,89
 average residence time for, 96
 heterogeneous catalytic oxidation, 56
 homogeneous oxidation of, 56
 measurements of, 81
 plume, 53,56
 reduced, 54,90
 stratospheric, 63
 St. Elmo's fire, 20
 Satellite,
 SAGE, 37,43
 SAM II, xxiv
 TIROS, 37
 Shuttle lidar, 84
 Sierra Negra eruption, 72
 Single scattering albedo, 59,107
 Size distribution, 77
 Solar aureole photometry, 77
 Solar luminosity, 112
 Solar photometry, 77
 Soufriere, St. Vincent, 51
 Spectrometer(s),
 Brewer, 82
 correlation, 63,81
 COSPEC, 63,81
 Dobson, 82

Stratospheric aerosol,
 distribution of, 67
 extinction by, 64
 extinction profiles of, 65
 mass loading of, 70,74
 optical depth of, xxiii,68,83,107
 prevolcanic loading of, 66
 volcanically enhanced, 66

Stratospheric residence,
 (e-folding), xxii

Stratospheric warming, 106

Stratospheric water vapor, 109

Sulfate(s), xxiv
 ion, 90
 mass concentrations of, 51
 particle size distribution of,
 107

Sulfur, 22,90

Sulfur compounds, gaseous,
 xxiv

Sulfur dioxide, 54
 measurements of, 81
 tropospheric concentrations
 of, 55

Sulfuric acid, xxiv,56

T

TIROS satellite, 37
 Taupo, New Zealand, 17
 eruptions of, 17

Tephra, 1,10

Terrestrial magnetism and
 electricity, xxv

Three-dimensional models, xxv

Three-dimensional trajectories,
 xxiv,39

Tropopause folding, 96

Troposphere, cooling of, xxiii,
 110

Tropospheric aerosols, 112

Tropospheric plume, 54

Tsuya's scale, 27

Turbidity network, WMO, 85

U

U-2 aircraft, 49,52

Ultraplinian, 30

Ultraviolet spectra, 49

V

Vesicular glass particles, 11

Volcanic aerosols, xxv,55

Volcanic eruptions, 109
(*see* *volcanoes*)
climatic effects of, 97,107,
109,111
climax of, 28
destructive potential of, 31
dispersive power of, 30
intensity of, 27
lightning activity due to, 92
surge of, 32
violence of, 31
Volcanic explosivity index, 28
Volcanic gases, 89
Volcanic plume(s), xxiii,50
gases and aerosols in, 50
radiation in and below, xxiv
radiative effects of, 79
water in, xxiii
Volcano(es),
activity of, 1
Augustine, 24
Bezymianny, 7
Cerro Azul, 17
composite andesitic-dacitic
strato, 7
Fuego, Guatemala, 24,71
Mount Agung, 54,104,105,109
Mount Lamington, 7
Shiveluch, 7
Sierra Negra, 72
Soufriere, St. Vincent, 51
Taupo, New Zealand, 17
Vortex motions,
drag-induced, 45
shear-induced, 45

W

WB-57 aircraft, 49,51
WMO (World Meteorological
Organization), xxv,85
Water concentration back-
ground, 59
Water vapor, 91,109
atmospheric, 26
hydrothermal, 26
meteoric, 26
Winds,
ageosrophic, 39
geostrophic, 39
Wire impactor, 50

XYZ

X-ray fluorescence analysis, 15